ISSN 1756-1841 VOLUME 29 NUMBER 2 2026

International Journal of Rheumatic Diseases

Official journal of the Asia Pacific League of Associations for Rheumatology (APLAR)

WILEY

International Journal of Rheumatic Diseases

For submission instructions, subscription and all other information visit http://onlinelibrary.wiley.com/journal/10.1111/(ISSN)1756-185X

View this journal online at wileyonlinelibrary.com/journal/apl

International Journal of Rheumatic Diseases

WILEY

International Journal of Rheumatic Diseases

LETTER TO THE EDITOR

DRESSed for Relapse: A Rare Case of Leflunomide-Induced DRESS With Hepatic Complications

Kajal Patel[1] | Pooja Jotwani[2] | Marie-Claire Maroun[2]

[1]Department of Internal Medicine, Rutgers Robert Wood Johnson University Hospital, New Brunswick, New Jersey, USA | [2]Department of Internal Medicine, Division of Rheumatology and Connective Tissue Disease, Rutgers Robert Wood Johnson University Hospital, New Brunswick, New Jersey, USA

Correspondence: Marie-Claire Maroun (mm3530@rwjms.rutgers.edu)

Received: 14 October 2025 | **Revised:** 13 January 2026 | **Accepted:** 17 January 2026

Dear Editor,

Drug Reaction with Eosinophilia and Systemic Symptoms (DRESS) is a rare, potentially life-threatening hypersensitivity reaction characterized by fever, rash, eosinophilia, lymphadenopathy, and multi-organ involvement most commonly affecting the liver. Mortality ranges from 5% to 10%, primarily due to hepatic necrosis [1, 2]. While anticonvulsants, allopurinol, antiretrovirals, and antibiotics are common triggers [3, 4], leflunomide is a rare but emerging culprit [5–7]. Its unique pharmacokinetics, including a prolonged half-life and significant enterohepatic recirculation, pose management challenges [8].

We report a rare case of leflunomide-induced DRESS, one of a limited number of published cases to date. This case also highlights the use of cholestyramine washout, a known but underutilized strategy to enhance leflunomide elimination and facilitate clinical recovery.

Diagnosing DRESS can be challenging as its clinical presentation is variable and can mimic infections, autoimmune diseases, or other drug reactions. The RegiSCAR (Registry of Severe Cutaneous Adverse Reactions) scoring system is the most widely used diagnostic tool. It evaluates clinical features such as fever, hematologic abnormalities, skin rash characteristics, internal organ involvement, and exclusion of alternative causes to categorize cases as "no," "possible," "probable," or "definite" DRESS [2].

Management begins with immediate cessation of the offending drug. For non-severe cases, clinical and laboratory monitoring may suffice. Systemic corticosteroids are the mainstay for moderate-to-severe disease. Steroid-refractory or relapsing cases may require escalation to immunosuppressive agents such as cyclosporine, IVIG, or plasmapheresis [2, 9]. These interventions increase the risk of opportunistic infections including CMV reactivation [3].

We present the case of a 65-year-old woman recently diagnosed with rheumatoid arthritis who was started on leflunomide and hydroxychloroquine. Three weeks later, she developed a diffuse maculopapular rash on her extremities, which progressed to involve her trunk. She was hospitalized for a presumed drug-induced rash and showed moderate improvement with high-dose corticosteroids. However, upon tapering, her symptoms worsened, with the emergence of fever, dysphagia, and new mucosal ulcers, prompting readmission. On examination, she had hemorrhagic crusting of the lips, tongue erosions, and a confluent morbilliform rash.

Laboratory workup revealed eosinophilia (16%), atypical lymphocytosis (4%), elevated AST (75 U/L), ALT (125 U/L), ALP (173 U/L), and a CRP of 6.11 mg/dL. Infectious workup was negative. Anti-nuclear antibody (ANA) was positive at a titer of 1:320 (homogeneous pattern), with negative anti-SSA, SSB, dsDNA, chromatin, and Sm/RNP antibodies. Skin biopsy showed interface dermatitis with eosinophilic infiltration, consistent with DRESS. The RegiSCAR score was 9, confirming a definite diagnosis of DRESS (Figure 1). Leflunomide and hydroxychloroquine were discontinued. Despite intravenous methylprednisolone and cyclosporine, her symptoms persisted. A cholestyramine washout was initiated to accelerate leflunomide elimination, resulting in marked clinical improvement within 48 h (Figure 2). She was discharged on cyclosporine, cholestyramine, and a corticosteroid taper.

Clinical Parameters	Clinical Parameter Present	Patient Score
Fever ≥ 38.6	Yes	1
Enlarged Lymph nodes	No	0
Eosinophils	Yes	1
Atypical Lymphocytes	Yes	1
Skin rash > 50% of body surface area	Yes	1
Skin rash suggesting DRESS	Yes	1
Skin biopsy suggesting DRESS	Yes	1
Liver involvement (or internal organ)	Yes	1
Resolution ≥ 15 days	Yes	1
Alternative diagnosis excluded	Yes	1
Total score		9

FIGURE 1 | RegiSCAR (Registry of Severe Cutaneous Adverse Reactions) is a diagnostic scoring for drug reaction with eosinophilia and systemic symptoms (DRESS) in this case. Criteria included fever, widespread morbilliform rash, hematologic abnormalities (eosinophilia and atypical lymphocytosis), liver involvement, supportive histopathology, prolonged disease course with resolution > 15 days, and exclusion of alternative causes, yielding a RegiSCAR score of 9 and confirming a definite diagnosis of DRESS.

Two weeks after hospital discharge, following cyclosporine reduction to 150 mg/day, the patient re-presented with jaundice, diarrhea, pale stools, and recurrence of the rash. Laboratory studies revealed hepatic cholestasis with coagulopathy: AST 301 U/L, ALT 269 U/L, ALP 454 U/L, total bilirubin 8.0 mg/dL, direct bilirubin 6.3 mg/dL, and INR 2.17. Abdominal imaging was unremarkable. Liver biopsy showed chronic, severely active hepatitis with confluent necrosis, and a plasma cell-rich infiltrate. ANA remained positive and a low-titer anti-smooth muscle antibody was detected. Cytomegalovirus (CMV) viremia was also detected. The patient ultimately responded to high-dose intravenous steroids and was discharged on a prolonged prednisone taper with close outpatient follow-up. Approximately 12 weeks after discharge, her liver function tests normalized following completion of the prednisone taper.

Leflunomide-induced DRESS is rare and presents unique management challenges due to its prolonged half-life and extensive enterohepatic recirculation. Leflunomide is metabolized in the liver to its active metabolite, teriflunomide, which has a prolonged half-life of approximately 2 weeks due to enterohepatic recirculation [8]. In our case, despite initiating high-dose corticosteroids and cyclosporine, clinical improvement was only achieved after a cholestyramine washout [5, 10]. This underscores the importance of considering accelerated drug elimination early in steroid-refractory cases.

Cholestyramine is a non-absorbable bile acid sequestrant that binds teriflunomide in the gastrointestinal tract, preventing its reabsorption and enhancing fecal excretion. The standard washout protocol is 8 g three times daily for 11 days, which significantly accelerates teriflunomide clearance [8, 10]. Although well established in overdose protocols, cholestyramine remains underutilized in DRESS management. Our case reinforces its value in persistent or relapsing presentations [10].

Liver involvement occurs in up to 80% of DRESS cases, ranging from mild transaminitis to fulminant hepatic failure [3]. In our patient, worsening liver function and biopsy findings revealed features of immune-mediated hepatitis and possible autoimmune sequelae.

Determining the precise etiology of liver injury was challenging, with contributing factors including cyclosporine toxicity, CMV reactivation, and DRESS relapse. The timing of symptom recurrence following cyclosporine dose reduction supports DRESS relapse. This underscores the importance of gradual immunosuppressant tapering, close follow-up, and early recognition of evolving complications.

Multidisciplinary management, involving dermatology, hepatology, and infectious disease specialists, was critical for guiding treatment and monitoring complications.

In conclusion, leflunomide-induced DRESS is rare but clinically significant, and this case adds to the limited body of literature. Given leflunomide's prolonged half-life and enterohepatic recirculation, cholestyramine washout should be strongly considered in steroid-refractory or relapsing cases. Liver involvement can be severe and may trigger or unmask underlying autoimmune features. Immunosuppressive therapy increases the risk of opportunistic infections such as CMV reactivation. This case underscores the importance of long-term monitoring and multidisciplinary care to optimize outcomes in severe DRESS presentations.

FIGURE 2 | Clinical photographs of the patient's leg before and after initiation of cholestyramine washout, demonstrating improvement in the morbilliform rash following treatment.

Author Contributions

Kajal Patel drafted the manuscript and was involved in patient care. Pooja Jotwani contributed to literature review and was involved in patient care. Marie-Claire Maroun supervised the project and critically revised the manuscript.

Acknowledgments

The authors thank colleagues in the Rheumatology and Dermatology Departments for their clinical support and multidisciplinary discussions involved in the care of the patient.

Consent

Consent was obtained from the patient for this case report. The patient has been de-identified in the case report.

Conflicts of Interest

The authors declare no conflicts of interest.

Data Availability Statement

The authors have nothing to report.

Kajal Patel
Pooja Jotwani
Marie-Claire Maroun

References

1. Y. C. Chen, H. C. Chiu, and C. Y. Chu, "Drug Reaction With Eosinophilia and Systemic Symptoms: A Retrospective Study of 60 Cases," *Archives of Dermatology* 146, no. 12 (2010): 1373–1379, https://doi.org/10.1001/archdermatol.2010.198.

2. S. H. Kardaun, P. Sekula, L. Valeyrie-Allanore, et al., "Drug Reaction With Eosinophilia and Systemic Symptoms (DRESS): An Original Multisystem Adverse Drug Reaction. Results From the Prospective RegiSCAR Study," *British Journal of Dermatology* 169, no. 5 (2013): 1071–1080, https://doi.org/10.1111/bjd.12501.

3. Z. Husain, B. Y. Reddy, and R. A. Schwartz, "DRESS Syndrome: Part I. Clinical Perspectives," *Journal of the American Academy of Dermatology* 68, no. 5 (2013): 14–693, https://doi.org/10.1016/j.jaad.2013.01.033.

4. P. Cacoub, P. Musette, V. Descamps, et al., "The DRESS Syndrome: A Literature Review," *American Journal of Medicine* 124, no. 7 (2011): 588–597, https://doi.org/10.1016/j.amjmed.2011.01.017.

5. S. Gayfield, J. Busken, and S. Mansur, "Recurrent Leflunomide-Induced Drug Reaction With Eosinophilia and Systemic Symptom

(DRESS) Syndrome Despite Prolonged Steroid Taper: A Case Report," *Cureus* 14, no. 9 (2022): e29319, https://doi.org/10.7759/cureus.29319.

6. S. Rao, A. Sunkara, N. Srivastava, P. Sampat, C. Ramos, and E. Albert, "An Uncommon Presentation of DRESS Syndrome Secondary to Leflunomide Use: A Case Report," *Journal of Investigative Medicine High Impact Case Reports* 9 (2021): 2324709621997282, https://doi.org/10.1177/2324709621997282.

7. A. P. Sebastian, P. K. Tirlangi, K. Saravu, and R. Acharya, "Leflunomide-Induced Drug Reaction Eosinophilia Systemic Symptoms and Haemophagocytic Lymphohistiocytosis Overlap Syndrome With Rheumatoid Arthritis," *BMJ Case Reports* 18, no. 1 (2025): e262809, https://doi.org/10.1136/bcr-2024-262809.

8. I. S. Padda and A. Goyal, "Leflunomide," in *StatPearls [Internet]* (StatPearls Publishing, 2023).

9. K. Tan and A. Testro, "Cyclosporine as an Alternative Immunosuppressant for Steroid-Resistant Drug Reaction With Eosinophilia and Systemic Symptoms (DRESS) Syndrome," *BMJ Case Reports* 16, no. 3 (2023): e250983, https://doi.org/10.1136/bcr-2022-250983.

10. M. Laub, R. Fraser, J. Kurche, A. Lara, T. H. Kiser, and P. M. Reynolds, "Use of a Cholestyramine Washout in a Patient With Septic Shock on Leflunomide Therapy: A Case Report and Review of the Literature," *Journal of Intensive Care Medicine* 31, no. 6 (2016): 412–414, https://doi.org/10.1177/0885066615610108.

International Journal of Rheumatic Diseases

WILEY

International Journal of Rheumatic Diseases

ORIGINAL ARTICLE

Identification of SDC1 as a Key Regulator and Therapeutic Target in Rheumatoid Arthritis via JAK2-STAT3 Pathway

Gan Cao[1] | Zhihui Wu[2] | Yatao Du[1] | Dongxue Dai[1] | Yang Sun[1] | Xi Jia[1] | Huixin Cai[1]

[1]Medical Laboratory Department, Baoding No. 1 Central Hospital, Baoding City, Hebei Province, China | [2]The Pathology Department, Xi'an Chest Hospital, Xi'an City, Shanxi Province, China

Correspondence: Huixin Cai (caihuixin5366@163.com)

Received: 25 August 2025 | **Revised:** 17 October 2025 | **Accepted:** 15 December 2025

Keywords: collagen-induced arthritis | rheumatoid arthritis | Syndecan-1

ABSTRACT

Introduction: Rheumatoid arthritis (RA) is a chronic autoimmune disorder with unclear molecular mechanisms, complicating early diagnosis and treatment. This study aimed to identify hub genes and pathways driving RA pathogenesis and assess their therapeutic potential.

Methods: Gene expression datasets related to RA were retrieved from the Gene Expression Omnibus (GEO) database. Differentially expressed genes (DEGs) were identified and analyzed by functional enrichment and protein–protein interaction network construction. Machine learning approaches, including LASSO regression, random forest, and SVM-RFE, were used to screen hub genes. Pathway associations were explored using Gene Set Enrichment Analysis (GSEA). Experimental validation was performed in collagen-induced arthritis (CIA) rat models and MH7A synovial fibroblast cells through Western blot and functional assays.

Results: A total of 106 DEGs were identified in RA synovial tissues, including 76 upregulated and 30 downregulated genes. Enrichment analyses revealed involvement in cytokine–cytokine receptor interaction, lymphocyte-mediated immunity, and immunoglobulin complexes. SDC1 emerged as a key hub gene across all three machine learning methods. GSEA indicated its significant correlation with the JAK–STAT pathway. In CIA rats, SDC1 expression was markedly elevated alongside p-JAK2 and p-STAT3 levels. Silencing SDC1 in MH7A cells reduced cell proliferation, decreased p-JAK2 and p-STAT3 expression, and promoted apoptosis.

Conclusions: This study identifies SDC1 as a central hub gene in RA pathogenesis through activation of the JAK2–STAT3 signaling pathway. These findings highlight SDC1 as a potential biomarker for early diagnosis and a promising target for therapeutic intervention, providing new insights into RA management.

1 | Background

Rheumatoid arthritis (RA) is a chronic, systemic autoimmune disorder [1] that is primarily characterized by inflammatory responses and structural damage affecting the synovial membranes within the joints [2], which may ultimately result in joint deformities and loss of function [3]. Immune abnormalities, genetic factors, and environment are believed to play important roles in pathogenesis [4]. As the early symptoms of RA are not obvious, early diagnosis mainly depends on clinical manifestations [5], laboratory tests (such as rheumatoid factor), and imaging examinations [6]. However, these methods have certain limitations in the early stage of the disease [7]. Therefore, identifying new molecular markers to improve the accuracy of early diagnosis of RA and identifying new molecular targets are vital for the timely detection and management of RA.

Gan Cao, Zhihui Wu authors contribute equal to this study.

Keypoints

- SDC1 identified as a key hub gene in RA by integrated bioinformatics and machine learning.
- SDC1 promotes RA progression via activation of the JAK2–STAT3 pathway.
- Targeting SDC1 may provide a novel diagnostic and therapeutic strategy for RA.

In recent years, bioinformatic technology has played a more significant role in disease research [8] and drug development [9]. Through the comprehensive analysis of high-throughput sequencing and publicly available gene expression databases, disease-related differentially expressed genes (DEGs) can be systematically screened [10], and machine learning can be used to further mine key genes. Although certain progress has been made in RA research, there remain some limitations, including the lack of multi-omics integration, imperfect key gene screening strategies, and insufficient experimental validation of bioinformatics predictions. To address these gaps, our study combined multiple GEO datasets and advanced machine learning methods (LASSO regression, SVM-RFE, and random forest) to systematically identify key genes and signaling pathways. Importantly, the predicted genes were further validated in both cell (MH7A) and animal (CIA rat) models, providing robust functional evidence. This integrated approach enhances the stability, credibility, and translational relevance of our findings, representing a significant advance over previous studies.

2 | Materials and Methods

2.1 | Data Normalization and Identification of Differentially Expressed Genes

Data were sourced from the GEO database, specifically from the datasets GSE77298 and GSE55235 (both designated as training datasets) as well as GSE1919 and GSE12021 (identified as validation datasets). The microarray data corresponding to GSE77298 and GSE55235 underwent processing, normalization, and batch correction using the "sva" package within R software. Subsequently, we employed the "limma" package for the identification of differential genes, with statistically significant genes defined by an adjusted $p < 0.05$ and a log2 fold change greater than 2. Visualization of differentially expressed genes was achieved through the "ggplot2" package and "pheatmap."

2.2 | Analysis of Functional Enrichment and Construction of PPI Networks

To investigate the functions and pathways associated with DEGs, the "clusterProfiler" R software package was used to conduct enrichment assessments of the Gene Ontology (GO) and Kyoto Encyclopedia of Genes and Genome (KEGG) pathways. Next, the STRING database was used to visualize the PPI network of DEGs, and the resulting network was displayed using Cytoscape software (version 3.9). Using Cytoscape software, an in-depth analysis of the PPI network generated by the STRING website was performed using the CytoNCA plugin to identify key genes, known as HubGenes.

2.3 | Identification and Verification of Core Genes

Three machine learning methods—Random Forest, LASSO regression, and SVM-RFE—were employed to precisely identify important hub genes in RA. For LASSO regression, the regularization parameter λ was determined via 10-fold cross-validation to minimize the mean cross-validated error. In SVM-RFE, a linear kernel function was used, and recursive feature elimination was performed iteratively to rank genes based on their contribution to classification accuracy. For Random Forest, 500 trees were constructed, and the mean decrease in Gini index was used to evaluate feature importance. The results obtained from these three methods were compared using the Venn diagram tool, and the overlap among the three methods suggested potential hub genes for diagnosing RA. The external datasets GSE1919 and GSE12021 were utilized to confirm the hub genes.

2.4 | Analysis of Gene Set Enrichment Focusing on a Single Gene

The Spearman correlation method was used to determine the association between core genes and other genes throughout the entire genome, and the genes were ranked according to the correlation coefficients to generate an ordered gene list. Subsequently, GSEA was conducted using R packages, including clusterProfiler, with the c2.cp.kegg_medicus.v2024.1. Hs.symbols.gmt dataset from the MSigDB database serving as the reference gene set, and significantly enriched pathways were obtained. Visual analysis was performed through the creation of enrichment plots to uncover the potential biological roles and associated signaling pathways of the core genes.

2.5 | Cell Culture and siRNA Transfection

The fibroblast-like synoviocyte cell line MH7A was purchased from Meisen Cell Biological Technology (Hangzhou, China). MH7A cells were cultured in 1640 medium (containing 10% FBS). siSDC1 was transferred to cells for 48 h using Lipofectamine 2000 according to the instructions.

2.6 | RT-qPCR

Total RNA was extracted using TRIzol, followed by reverse transcription into cDNA according to the manufacturer's protocol. Quantitative PCR was conducted using the qPCR detection system. The primer sequences used in this study were as follows:

Homo sapiens SDC1 Forward primer (5′ to 3′): CCACCATGAGACCTCAACCC.

Reverse primer (5′ to 3′): GCCACTACAGCCGTATTCTCC.

Homo sapiens β-actin Forward primer (5′ to 3′): CCTGGCA CCCAGCACAAT.

Reverse primer (5′ to 3′): GGGCCGGACTCGTCATAC.

2.7 | Western Blotting Analysis

Total proteins were extracted from cells or tissues, separated by SDS-PAGE, transferred to PVDF membranes, blocked, and incubated with primary and secondary antibodies. The proteins were visualized using an ECL chemiluminescence detection system.

2.8 | Apoptosis Experiment

The cells that were transfected with siRNA were collected. Apoptosis was assessed using an apoptosis detection kit. 1X Binding Buffer was prepared following the protocol provided in the kit, and the cell concentration was set to 3×10^6/ml. Annexin V-FITC was added and the cells were incubated for 15 min. Once the incubation period was complete, cells were washed with 1X Binding Buffer. Subsequently, 7-AAD Viability Staining Solution was added, and analysis was conducted using flow cytometry.

2.9 | Edu Analysis

After transfecting siRNA into MH7A cells for 48 h, the EdU working solution was added and incubated for 2 h to incorporate it into the DNA of proliferating cells. After incubation, the medium was removed, and the cells were fixed for 15 min and washed three times. 0.3% Triton X-100 was added, incubated for 15 min, the cells were washed three times, the Click reaction system was used to label EdU, and the cells were incubated for 30 min. Flow cytometry was used to detect the EdU-488 fluorescence signal, allowing the assessment of MH7A cell proliferation.

2.10 | Construction of CIA Rat Model

A total of 16 male Sprague–Dawley (SD) rats (6–8 weeks old, 180–200 g) were purchased from Beijing Huafukang Biotechnology Co. Ltd. and adaptively raised for 1 week under standard laboratory conditions (22°C ± 2°C, 12 h light/dark cycle, free access to food and water). To construct the collagen-induced arthritis (CIA) model, a mixture of bovine type II collagen and complete Freund's adjuvant (CFA) was prepared and injected subcutaneously at the base of the tail and the left sole for the primary immunization (day 0). A booster immunization was administered on day 7 into the right paw. Rats were observed every 3 days for clinical symptoms, including joint redness, swelling, stiffness, and limited movement, and the degree of joint swelling was measured regularly using a standardized scoring system. Arthritis severity was assessed every 3 days after the booster immunization according to a standard arthritis index (AI) scoring system ranging from 0 to 4 for each paw (0 = normal, 1 = mild swelling and erythema, 2 = moderate swelling, 3 = pronounced swelling, 4 = severe swelling and deformity), with a maximum total score of 16 per animal.

2.11 | HE Staining

A month after the first immunization, synovial tissue was extracted from the joints and preserved in a 4% paraformaldehyde solution for 24 h. This was followed by embedding in paraffin and cutting into sections. Hematoxylin–eosin (HE) staining was conducted following the manufacturer's protocol, and pathological changes in synovial tissue were examined under an optical microscope to assess the characteristics associated with arthritis pathology.

2.12 | Molecular Docking

Molecular docking was used to analyze the interactions between the key proteins and core targets in the relevant pathways. The three-dimensional structures of the proteins were obtained from the Protein Data Bank, and docking analysis was performed using AutoDock to predict the interaction patterns between the core targets and key pathway proteins, which were visualized using PyMOL software. The docking results clearly showed the amino acid residues involved in the binding between SDC1 and JAK2, including ER-171, SER-919 and GLU-845 et al., Strong hydrogen bonds and hydrophobic interactions were observed between SDC1 and JAK2, indicating a stable and specific binding mode.

2.13 | Statistical Analysis

Quantitative data are presented as mean ± standard deviation (SD). Statistical analyses were conducted using R software (version 4.0) and GraphPad Prism 8, with $p < 0.05$ regarded as indicative of statistical significance.

3 | Results

3.1 | Identification of DEGs Between RA and Normal Controls

We merged datasets GSE55235 and GSE77298 and adjusted for batch effects to obtain a normalized combined matrix. There were some differences in the sample distribution between these two datasets (Figure 1A), which may hinder subsequent analysis. The merged dataset after "sva" package processing showed strong homogeneity, indicating high consistency and uniformity (Figure 1B). Based on the filtering criteria of adj. $p < 0.05$ and $|\log2FC| > 2$, a total of 76 genes were upregulated while 30 genes were downregulated when comparing RA to normal controls Table S1. The DEGs between RA and normal controls were visually illustrated using a volcano plot (Figure 1C) and heatmap (Figure 1D).

3.2 | Enrichment Analysis of DEGs

The GO enrichment analysis results (Figure 2A) show that the DEGs identified between the RA and normal control

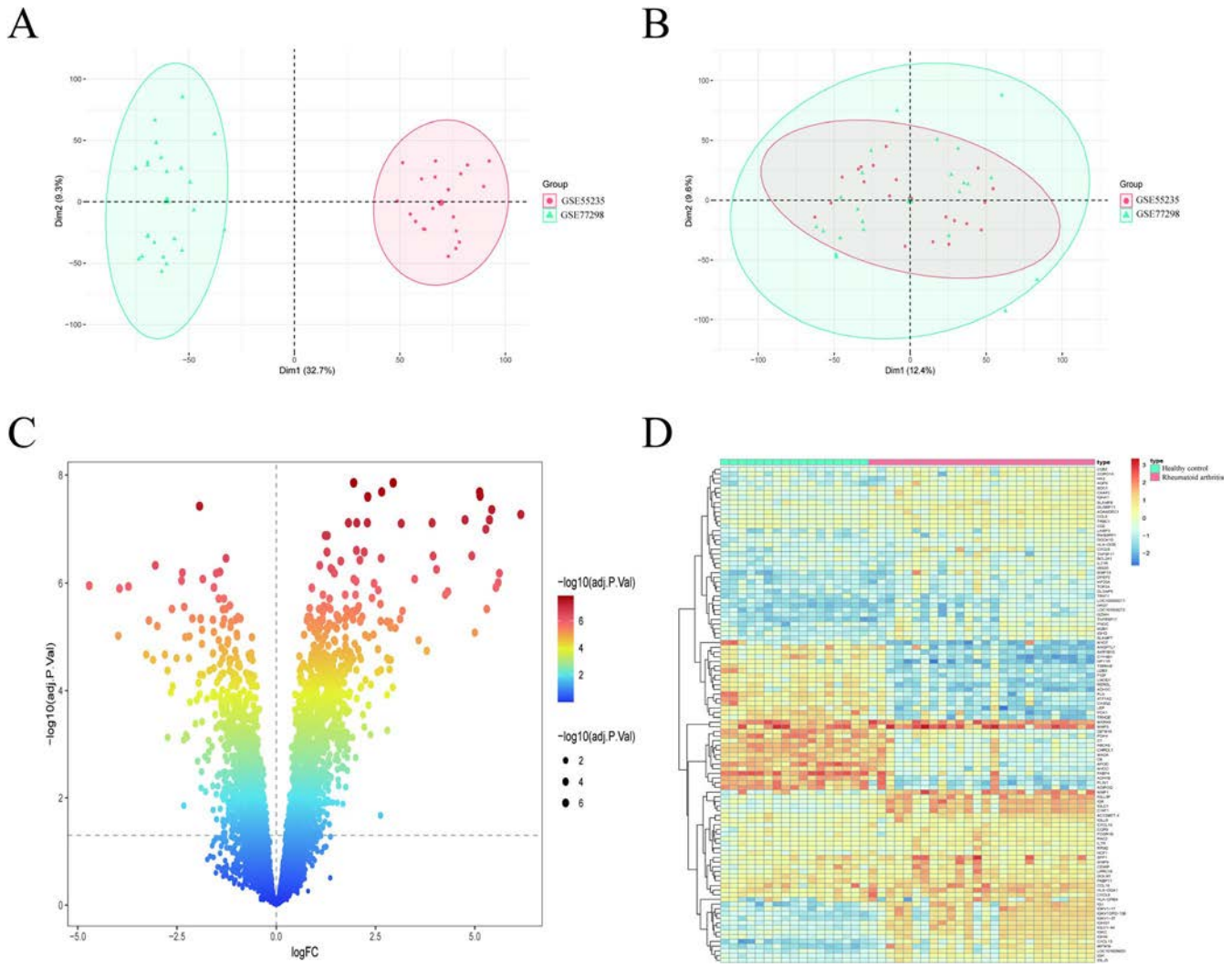

FIGURE 1 | Merging and DEG analysis of GSE datasets. (A) The principal component analysis (PCA) results show the distribution of all samples before normalization. (B) The PCA plot shows the sample distribution after normalization. (C) The volcano plot represents all the normalized mRNA expression data. (D) The heatmap shows the DEGs in the synovial tissue of RA patients.

groups were predominantly associated with pathways including leukocyte-mediated immunity, lymphocyte-mediated immunity, and immunoglobulin complexes, while the KEGG enrichment results (Figure 2B) indicated that the DEGs were primarily enriched in rheumatoid arthritis and chemokine signaling pathway, etc.

3.3 | Identifying Potential Diagnostic Biomarkers for RA Through Machine Learning

Lasso regression was applied to feature gene selection. The plot displays binomial deviance against Log(λ), with the optimal λ identified at the point of minimum deviance (Figure 3A). We then used a random forest algorithm to identify the key genes (Figure 3B). Finally, we employed the SVM-RFE technique (Figure 3C) to identify the essential genes distinguishing RA from normal controls. Venn diagram showing the intersection of core genes of the three different machine learning methods (SVM-RFE, Lasso, and RF). A single characteristic gene, SDC1, was found to be common across all methods (Figure 3D).

3.4 | Construction of PPI Network

PPI analysis was conducted using the STRING database to explore the interactions among all identified DEGs, and a PPI network comprising 262 edges and 75 nodes was generated and visualized using Cytoscape software Figure S1A. The CytoNCA algorithm was used to predict the key DEGs. Finally, 22 DEGs were identified as key genes Figure S1B.

3.5 | Validation of the Hub Gene SDC1 Using External Datasets

To confirm the reliability and significance of the results, two external datasets (GSE12021 and GSE1919) were used to validate

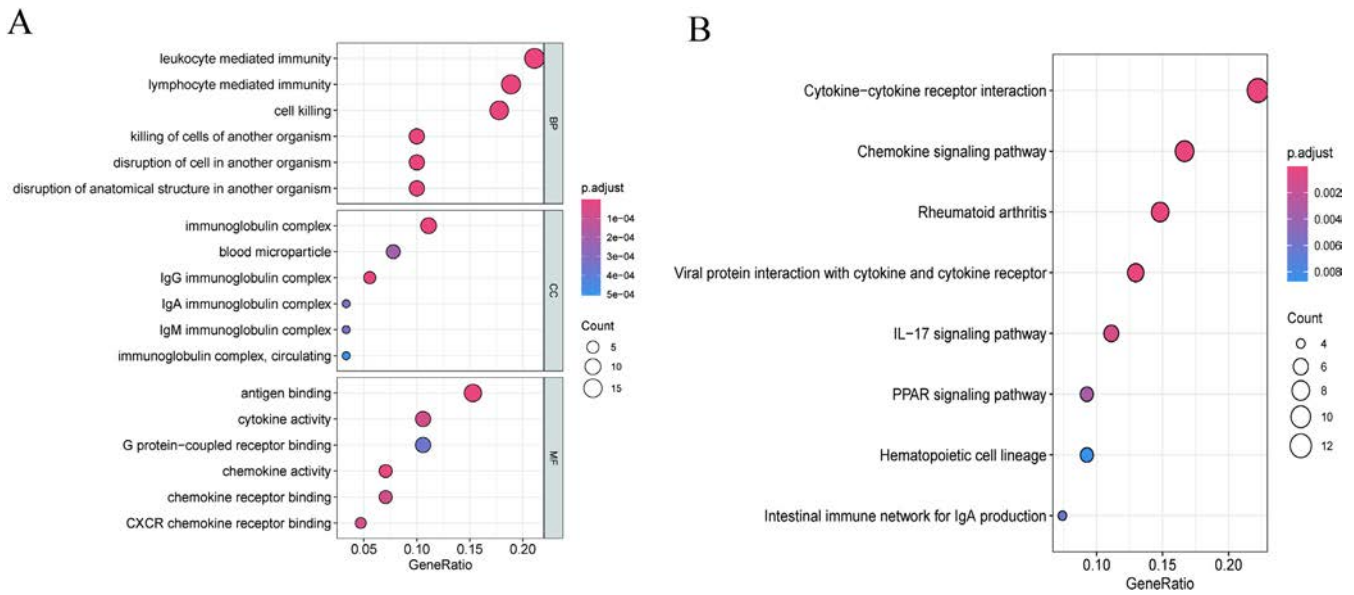

FIGURE 2 | Functional enrichment analysis of differential genes between RA and normal controls. (A) The results of GO pathway enrichment analysis for the differential genes. (B) The results of KEGG pathway enrichment analysis for the differential genes.

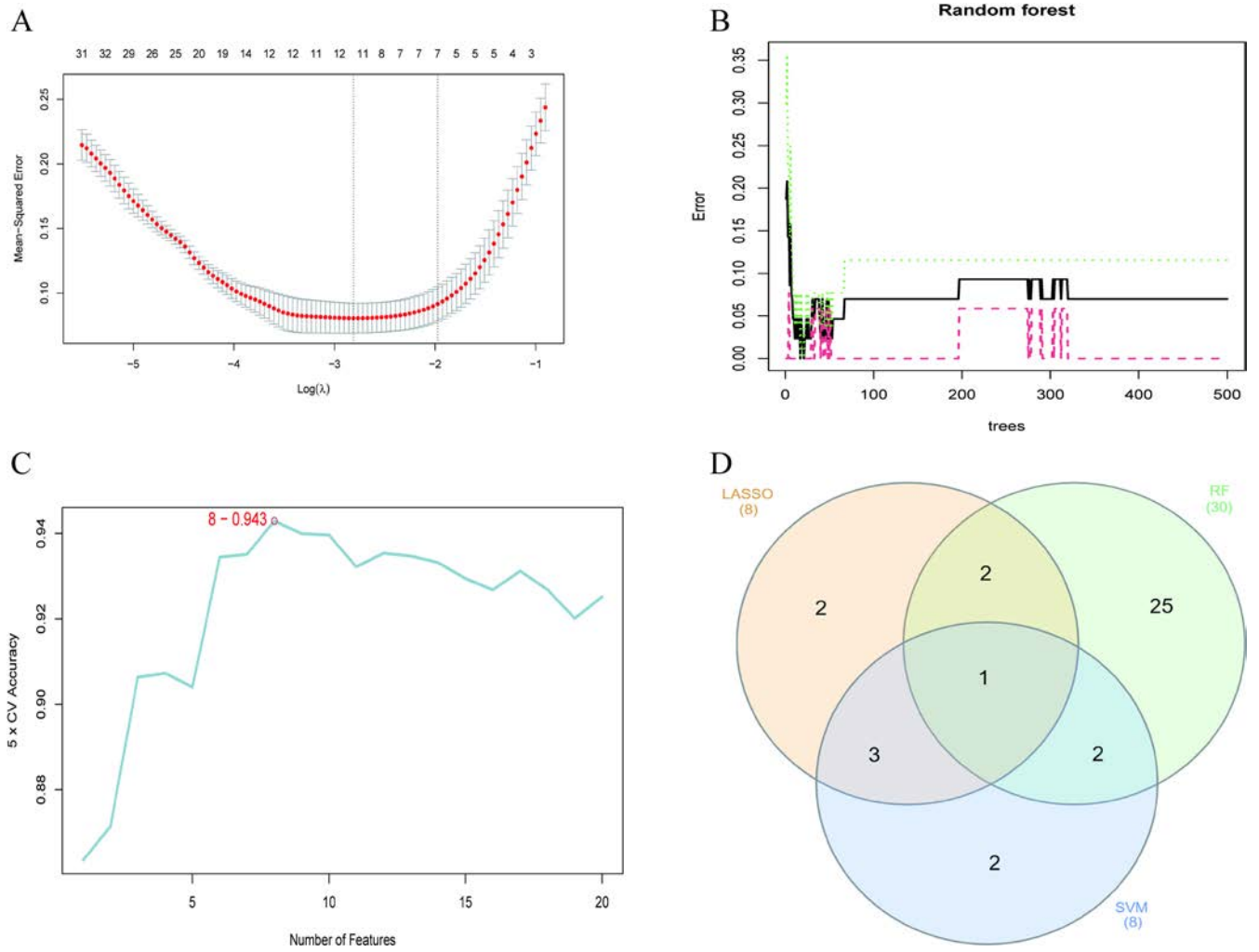

FIGURE 3 | Identifying key genes using machine learning techniques: (A) LASSO regression analysis. (B) RF algorithm application. (C) Feature selection via the SVM-RFE method. (D) Venn diagram illustrating the shared feature genes identified by SVM-RFE, Lasso, and RF methods.

the hub genes. SDC1 was significantly overexpressed in RA synovial tissue (Figure S2).

3.6 | Gene Set Enrichment Analysis

Spearman's correlation analysis was used to calculate the correlation between SDC1 and other genes, and GSEA functional enrichment analysis was performed. The results from GSEA (Figure 4A,B) indicated a significant enrichment of SDC1 in eight KEGG signaling pathways, notably within the CYTOKINE_JAK_STAT_SIGNALING_PATHWAY. Consequently, we hypothesized that SDC1 might be involved in the pathogenesis of RA through the CYTOKINE_JAK_STAT_SIGNALING_PATHWAY.

3.7 | SDC1 Promotes Arthritis in CIA Rats via the JAK2-STAT3 Signaling Pathway

Janus kinase (JAK) consists of four members: JAK1, JAK2, JAK3, and TYK2. Consequently, we conducted molecular docking studies of SDC1 with each of the four JAK family members using AutoDock software. The results of the molecular docking analysis (Figure S3 and Table S2) indicated that SDC1 exhibited the strongest binding affinity with JAK2. We also established a rat model of CIA. After two immunizations, the joints of the CIA rats were significantly swollen (Figure 5A). The HE staining results (Figure 5B) showed synovial hyperplasia and a large amount of inflammatory cell infiltration in the model group, indicating that the model was successfully constructed. The expression of SDC1, pJAK2, pSTAT3, JAK2, and STAT3 was detected by immunoblotting (Figure 5C,D). The results from the WB analysis indicated that in comparison to the normal group, the levels of SDC1, pJAK2, and pSTAT3 in the synovial membrane of joints were markedly elevated in the CIA model group.

3.8 | The Effect of SDC1 Silencing on MH7A Cells

To further verify that SDC1 may be involved in the pathogenesis of RA through the modulation of the JAK2-STAT3 signaling pathway, we used small interfering RNA (si-RNA) technology to interfere with the expression of SDC1 and observed its effects on the expression of pJAK2 and pSTAT3 as well as cell phenotype. Before the experiment, we verified the transfection efficiency of si-RNA. Our results showed that the levels of SDC1 mRNA (Figure 6A) and protein (Figure 6B) significantly decreased after transfection with si-SDC1. Immunoblotting results revealed that the levels of pJAK2 and pSTAT3 in MH7A cells were significantly reduced after transfection with si-SDC1 (Figure 6B). Flow cytometry results demonstrated that transfection of MH7A cells with si-SDC1 significantly reduced their proliferation (Figure 6C) and enhanced their apoptosis (Figure 6D). These results suggest that SDC1 may affect abnormal proliferation of fibroblasts through the JAK2-STAT3 pathway.

4 | Discussion

Rheumatoid arthritis (RA) is a chronic autoimmune disease that results from the combined effects of genetic susceptibility, environmental exposures, and aberrant immune responses [11]. Despite advances in diagnosis and therapy, early detection and targeted treatment remain significant challenges [12]. This study combined bioinformatic analysis with experimental validation and identified SDC1 as a key gene involved in the pathogenesis of RA, indicating that it may play

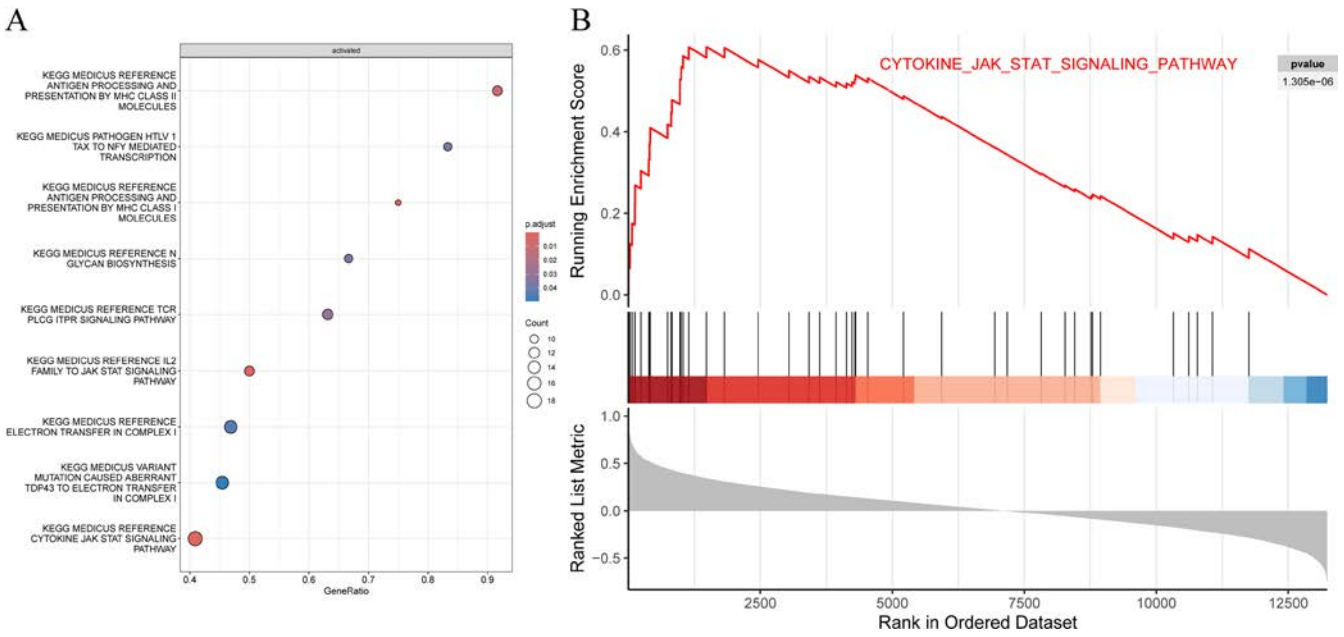

FIGURE 4 | Gene set enrichment analysis. (A) Kyoto Encyclopedia of Genes and Genomes (KEGG) enrichment analysis of SDC1. (B) SDC1 was significantly enriched in CYTOKINE_JAK_STAT_SIGNALING_PATHWAY.

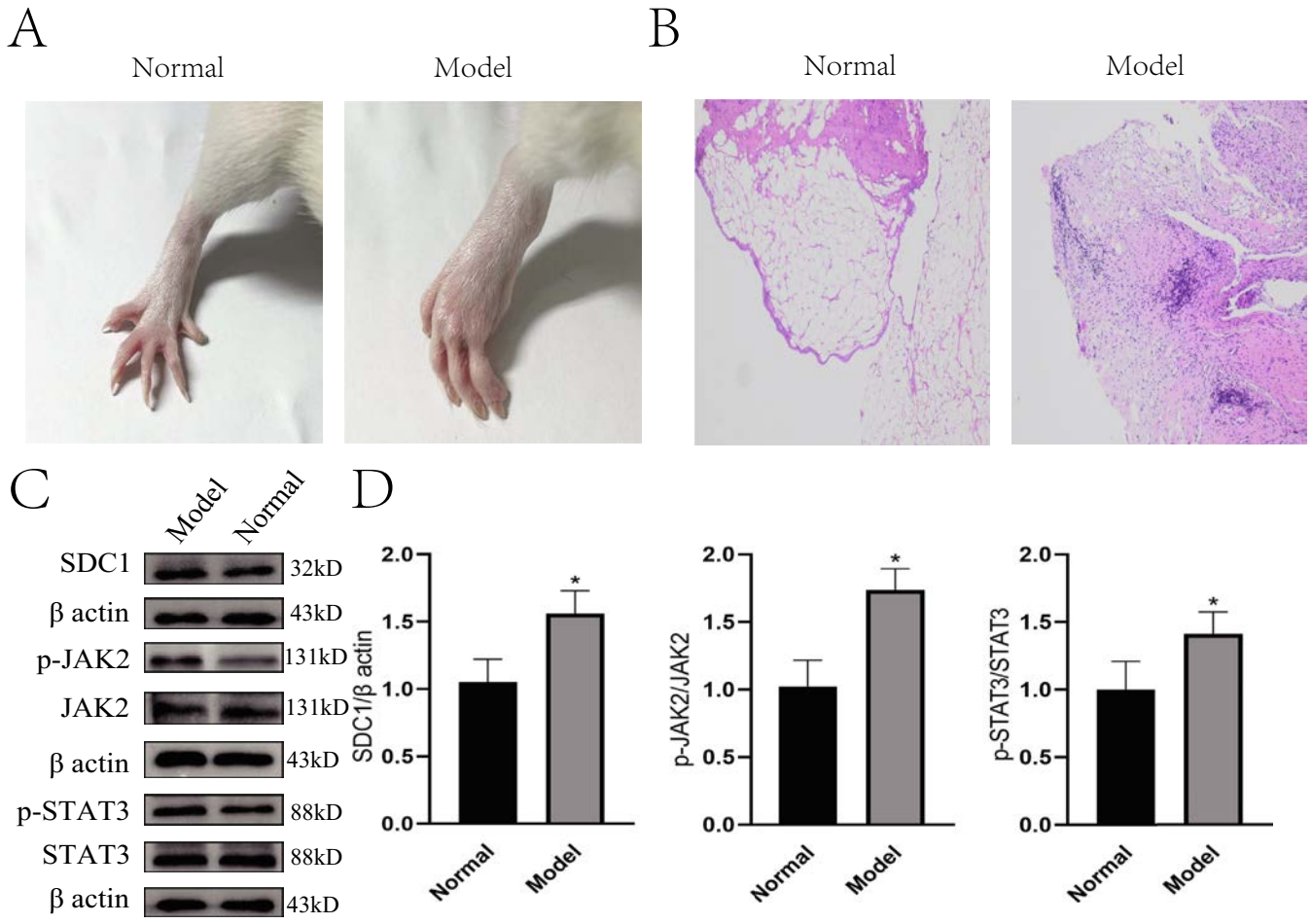

FIGURE 5 | SDC1 and JAK2-STAT3 pathways were significantly activated in CIA rats. (A) Representative images of the hind paw. (B) Pathological images stained with hematoxylin and eosin (H&E) showed significant synovial hyperplasia in the joints of the CIA model group. (C) Representative Western blotting bands of SDC1, pJAK2, pSTAT3, JAK2, STAT3 proteins. (D) Quantitative analysis of SDC1, pJAK2, and pSTAT3 proteins.

a role in disease progression through the JAK2-STAT3 signaling pathway.

4.1 | Syndecan 1 (SDC1)

[13] is widely present on the surface of different types of cells [14] and is crucial for biological processes such as cell signaling [15], cell adhesion [16], proliferation [17] and regulation of immune responses [18]. Research indicates that SDC1 serves a significant regulatory function in autoimmune disorders [19], mainly involving immune cell function [20], inflammatory response [21] and tissue damage. Recent studies highlight the role of Syndecan-1 (SDC-1) in rheumatoid arthritis (RA) pathogenesis [22]. Shahrara et al. demonstrated that the syntenin-1/SDC-1 axis modulates RA progression by regulating the crosstalk between glycolytic macrophages and Th1 cells, linking metabolic reprogramming to inflammatory responses [23]. In contrast, Abdo Jurjus et al. report that SDC-1 deficiency exacerbates experimental RA, with knockout models showing increased TNF-α expression, severe joint erosion, and reduced mast cell activity [24]. These seemingly contradictory findings suggest that SDC-1 may be influenced by the cellular microenvironment, which may serve as both a mediator of inflammatory pathways and a protective factor in joint homeostasis. In SLE, SDC1 regulates B cell activation and participates in immune complex deposition, which is closely linked to the development of SLE [25]. Research indicates that serum SDC-1 levels are elevated in SLE patients experiencing nephritis, suggesting that SDC-1 could serve as a valuable serum biomarker for active lupus nephritis (LN) [26]. The pleiotropic role of SDC1 extends across multiple autoimmune disorders [27]. In inflammatory bowel diseases (IBD), SDC1 maintains the integrity of the intestinal barrier and regulates inflammation, and changes in its expression can impair epithelial repair and immune cell recruitment [28]. Similarly, in multiple sclerosis (MS), SDC1 regulates T cell activation and myelin damage, influencing central nervous system inflammation [29]. Patients with Sjögren syndrome exhibit abnormal SDC1 expression in salivary glands, where they disrupt epithelial function and promote immune cell infiltration, exacerbating tissue damage [30]. These findings collectively suggest that SDC1 is a central regulator of autoimmune pathogenesis across diverse tissues. Our research identified 106 genes that were differentially expressed in RA through an analysis of differentially expressed genes (DEG). SDC1 was identified as a key gene in RA using three machine learning methods: SVM-RFE, LASSO, and random forest. This robust

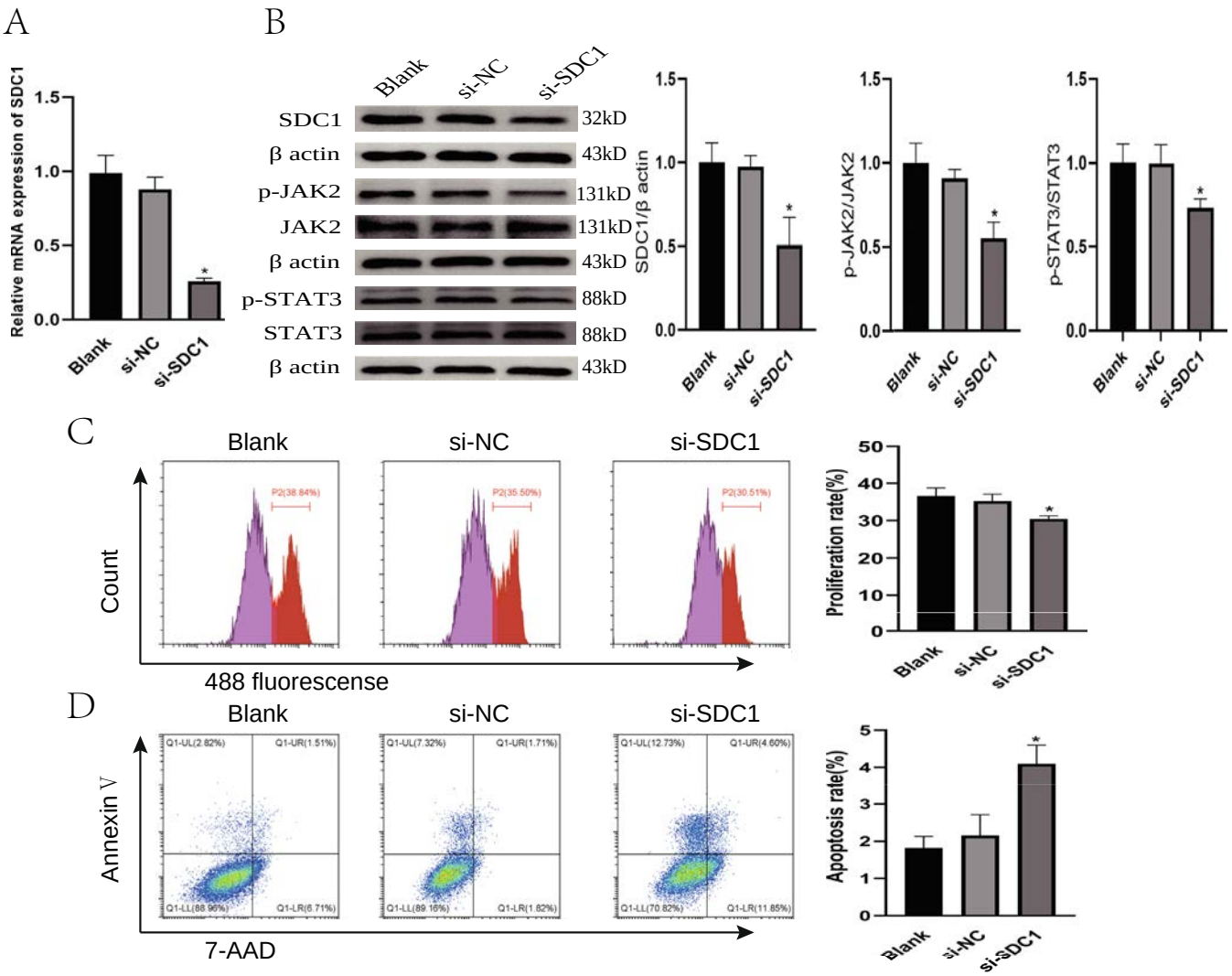

FIGURE 6 | The effect of SDC1 silencing on JAK2-STAT3 signaling pathway, proliferation, and apoptosis in MH7A cells. (A) Validation of si-SDC silencing efficiency. (B) Relative expression of SDC1, pJAK2, pSTAT3, JAK2, and STAT3 proteins after si-SDC1 transfection. (C) MH7A cell proliferation was detected by Edu method after si-SDC1 transfection. (D) MH7A cell apoptosis ratio was detected by flow cytometry after si-SDC1 transfection.

computational prediction strongly implicates SDC1 in the disease's pathological mechanisms, suggesting it may serve as a critical regulator of RA progression. In summary, the role of SDC1 appears to be context-dependent across autoimmune diseases. In systemic lupus erythematosus (SLE), SDC1 has been implicated in modulating B cell differentiation and autoantibody production, while in inflammatory bowel disease (IBD), it participates in epithelial barrier maintenance and regulation of mucosal immune responses. These observations suggest that while SDC1 is broadly involved in immune regulation, the downstream signaling pathways and cellular targets differ by disease context, highlighting a degree of pathway specificity in RA.

Taken together, these insights emphasize the complex and multifaceted roles of SDC1, supporting its potential as a therapeutic target in RA. Targeting SDC1 may need to consider both its protective and pathogenic aspects to achieve precise modulation of synovial inflammation without disrupting homeostatic functions.

Gene set enrichment analysis (GSEA) indicated a strong association between SDC1 and the JAK–STAT signaling pathway. The Janus kinase-signal transducer and activator of transcription (JAK–STAT) pathway plays a crucial role in the transduction of cytokine-mediated signals [31] and is extensively involved in various physiological processes [32]. This pathway is composed of cytokine receptors, JAK kinases, and STAT transcription factors (STAT1-STAT6) [33]. The signal transduction mechanism mainly includes the binding of cytokines to their receptors, thereby regulating the transcription of target genes [34]. Dysregulated activation of the JAK–STAT signaling pathway has been associated with the pathogenesis of numerous disorders, particularly autoimmune diseases [35], cancer [36], etc. [37]. Several studies have shown that the JAK–STAT signaling pathway plays a central role in RA pathogenesis, where it regulates inflammatory responses, drives immune cell activation, and facilitates synovial cell proliferation. Persistent activation of this pathway during the pathogenesis of RA contributes to the progression of joint damage through elevated matrix metalloproteinase gene expression,

chondrocyte apoptosis, and resistance of synovial tissue to apoptosis [38]. Targeted inhibition of the JAK–STAT pathway ameliorates clinical symptoms and slows disease progression in rheumatoid arthritis [39].

Molecular docking analysis revealed that SDC1 exhibited the strongest binding affinity for JAK2. Western blot analysis revealed a significant upregulation of SDC1, p-JAK2, and p-STAT3 in the synovial tissue of rats in the model group, suggesting that SDC1 may contribute to RA pathogenesis by activating the JAK2-STAT3 signaling pathway, thereby promoting synovial cell proliferation and inflammatory responses.

To further investigate the role of SDC1, we reduced SDC1 expression in the MH7A cell line. Our experimental findings revealed that the knockdown of SDC1 notably decreased cell proliferation, lowered the levels of p-JAK2 and p-STAT3, and induced apoptosis in the cells. These results provide additional evidence that SDC1 is critically involved in the pathogenesis of RA through modulation of the JAK2-STAT3 signaling pathway. Therefore, SDC1 may serve as a promising therapeutic target for the management of RA. By inhibiting SDC1 or its related signaling pathways, it may be feasible to effectively curb the abnormal growth and inflammatory response of synovial cells, thereby mitigating the progression of RA.

In addition to its upstream regulatory role in the JAK2–STAT3 signaling pathway, SDC1 has been reported to influence several downstream effectors implicated in RA pathogenesis. Previous studies have shown that SDC1 can modulate the expression of matrix metalloproteinases (MMP-1, MMP-3, MMP-9), contributing to extracellular matrix degradation and cartilage destruction. Moreover, SDC1 has been associated with regulation of pro-inflammatory cytokines, including IL-6, TNF-α, and IL-1β, thereby promoting synovial inflammation and fibroblast activation. These observations suggest that SDC1 may act as a central node linking JAK2–STAT3 signaling to multiple pathogenic effectors in RA, providing a mechanistic framework for understanding its potential as a therapeutic target.

This study underscores the pivotal role of SDC1 in the pathogenesis of rheumatoid arthritis (RA), supported by bioinformatics analysis and experimental validation. It identified how SDC1 regulates the progression of RA through the JAK2-STAT3 signaling pathway.

However, this study had several limitations remain. Although this study confirmed the role of SDC1 in CIA rat models and MH7A cells, its role in rheumatoid arthritis patients still needs further investigation through large-scale clinical studies. The precise regulatory mechanisms of SDC1 in RA are not yet fully understood, and future research should focus on exploring its upstream regulators and downstream effectors.

This study combined bioinformatics, machine learning, and experimental validation to explore the role of SDC1 in rheumatoid arthritis (RA). This suggests that SDC1 may regulate the pathological process of RA through the JAK–STAT signaling pathway. This discovery not only identifies new potential targets for diagnosing and treating RA but also creates new pathways for exploring the function of SDC1 in autoimmune disorders.

5 | Conclusions

This study identified SDC1 as a key gene in the pathogenesis of rheumatoid arthritis. By integrating bioinformatics analysis with experimental validation, we demonstrated that SDC1 promotes disease progression via the JAK2-STAT3 signaling pathway. These findings suggest that SDC1 may serve as a potential biomarker for early diagnosis and a novel target for therapeutic intervention in rheumatoid arthritis.

Author Contributions

Gan Cao: visualization, writing original draft. **Zhihui Wu:** data curation, formal analysis. **Yatao Du:** formal analysis. **Dongxue Dai:** methodology. **Yang Sun:** software. **Xi Jia:** software. **Huixin Cai:** writing, review and editing, conceptualization.

Funding

This study was supported by the Natural Science Foundation of Hebei (H2021104017).

Disclosure

Animal Research: All animal experiments were approved by the Animal Ethics Committee of Ningxia Medical University (approval number: IACUC-NYLAC-2024-008). All procedures were performed in accordance with the Regulations for the Care and Use of Laboratory Animals and the ARRIVE guidelines. Every effort was made to minimize animal suffering and to reduce the number of animals used.

Ethics Statement

The Medical Ethics Committee of Baoding No. 1 Central Hospital reviewed and approved the study protocol (approval no. [2021]008). All participants provided informed consent at the time of enrollment.

Conflicts of Interest

The authors declare no conflicts of interest.

Data Availability Statement

The data that support the findings of this study are available from the corresponding author upon reasonable request.

References

1. A.-F. Radu and S. G. Bungau, "Management of Rheumatoid Arthritis: An Overview," *Cells* 10 (2021): 2857, https://doi.org/10.3390/cells10112857.

2. J. S. Smolen, D. Aletaha, and I. B. McInnes, "Rheumatoid Arthritis," *Lancet* 388 (2016): 2023–2038, https://doi.org/10.1016/S0140-6736(16)30173-8.

3. M. H. Smith and J. R. Berman, "What Is Rheumatoid Arthritis?," *JAMA* 327 (2022): 1194, https://doi.org/10.1001/jama.2022.0786.

4. E. M. Gravallese, G. S. Firestein, N. Koscal, et al., "What Is Rheumatoid Arthritis?," *New England Journal of Medicine* 390 (2024): 332, https://doi.org/10.1056/NEJMp2310178.

5. J. Huang, X. Fu, X. Chen, Z. Li, Y. Huang, and C. Liang, "Promising Therapeutic Targets for Treatment of Rheumatoid Arthritis," *Frontiers*

in Immunology 12 (2021): 686155, https://doi.org/10.3389/fimmu.2021.686155.

6. W. R. Walter and M. Samim, "Imaging Updates in Rheumatoid Arthritis," *Seminars in Musculoskeletal Radiology* 29 (2025): 156–166, https://doi.org/10.1055/s-0045-1802952.

7. J. R. Zech, W. R. Walter, and C. J. Burke, "Sonography of Arthritis: Inflammatory, Infectious, Depositional," *Seminars in Musculoskeletal Radiology* 29 (2025): 145–155, https://doi.org/10.1055/s-0045-1802348.

8. X. Li, X. Zhang, T. Liu, G. Zhang, D. Chen, and S. Lin, "Identification of Immune Characteristic Biomarkers and Therapeutic Targets in Cuproptosis for Rheumatoid Arthritis by Integrated Bioinformatics Analysis and Single-Cell RNA Sequencing Analysis," *Front Med (Lausanne)* 12 (2025): 1520400, https://doi.org/10.3389/fmed.2025.1520400.

9. M. H. Tariq, D. Advani, B. M. Almansoori, et al., "The Identification of Novel Therapeutic Biomarkers in Rheumatoid Arthritis: A Combined Bioinformatics and Integrated Multi-Omics Approach," *International Journal of Molecular Sciences* 26 (2025): 2757, https://doi.org/10.3390/ijms26062757.

10. Y. Hou, Z. Yang, J. Ma, et al., "Identification of PTPRC as a Potential Serum Biomarker in Rheumatoid Arthritis Using Bioinformatics Analysis and Molecular Docking," *International Immunopharmacology* 152 (2025): 114393, https://doi.org/10.1016/j.intimp.2025.114393.

11. L. Yang, F. Cao, J. Lu, et al., "Neutrophil Membrane-Encapsulated Polymerized Salicylic Acid Nanoparticles Effectively Alleviating Rheumatoid Arthritis by Facilitating Sustained Release of Salicylic Acid Into the Articular Cavity From Chondrocytes," *Advanced Healthcare Materials* 14 (2025): 404510, https://doi.org/10.1002/adhm.202404510.

12. Y. K. Wu, L. Zhou, G. Chang, and R. Q. Wang, "Identification and Validation of Fibroblast-Related Biomarkers in Rheumatoid Arthritis by Bulk RNA-Seq and Single-Cell RNA-Seq Analysis," *Clinical and Experimental Rheumatology* 43 (2025): 6am51, https://doi.org/10.55563/clinexprheumatol/x6am51.

13. C. I. McKenzie, A. R. Dvorscek, Z. Ding, et al., "Syndecans and Glycosaminoglycans Influence B-Cell Development and Activation," *EMBO Reports* 26 (2025): 432-6, https://doi.org/10.1038/s44319-025-00432-6.

14. R. Gharbaran, "Advances in the Molecular Functions of Syndecan-1 (SDC1/CD138) in the Pathogenesis of Malignancies," *Critical Reviews in Oncology/Hematology* 94 (2015): 1–17, https://doi.org/10.1016/j.critrevonc.2014.12.003.

15. W. Zheng, Q. Chen, H. Liu, et al., "SDC1-Dependent TGM2 Determines Radiosensitivity in Glioblastoma by Coordinating EPG5-Mediated Fusion of Autophagosomes With Lysosomes," *Autophagy* 19 (2023): 839–857, https://doi.org/10.1080/15548627.2022.2105562.

16. S. Liao, C. Liu, G. Zhu, K. Wang, Y. Yang, and C. Wang, "Relationship Between SDC1 and Cadherin Signalling Activation in Cancer," *Pathology, Research and Practice* 216 (2020): 152756, https://doi.org/10.1016/j.prp.2019.152756.

17. C.-L. Zhang, Q. Shen, F.-D. Liu, et al., "SDC1 and ITGA2 as Novel Prognostic Biomarkers for PDAC Related to IPMN," *Scientific Reports* 13 (2023): 18727, https://doi.org/10.1038/s41598-023-44646-x.

18. Y. Liu, C. Xu, L. Zhang, et al., "Syndecan-1 Inhibition Promotes Antitumor Immune Response and Facilitates the Efficacy of Anti-PD1 Checkpoint Immunotherapy," *Science Advances* 10 (2024): 7764, https://doi.org/10.1126/sciadv.adi7764.

19. S. A. Agere, E. Y. Kim, N. Akhtar, and S. Ahmed, "Syndecans in Chronic Inflammatory and Autoimmune Diseases: Pathological Insights and Therapeutic Opportunities," *Journal of Cellular Physiology* 233 (2018): 6346–6358, https://doi.org/10.1002/jcp.26388.

20. A. K. Jaiswal, M. Sadasivam, and A. R. A. Hamad, "Unexpected Alliance Between Syndecan-1 and Innate-Like T Cells to Protect Host From Autoimmune Effects of Interleukin-17," *World Journal of Diabetes* 9 (2018): 220–225, https://doi.org/10.4239/wjd.v9.i12.220.

21. N. Y. Lee, H. Y. Ture, E. J. Lee, J. A. Jang, G. Kim, and E. J. Nam, "Syndecan-1 Plays a Role in the Pathogenesis of Sjögren's Disease by Inducing B-Cell Chemotaxis Through CXCL13-Heparan Sulfate Interaction-PubMed," *International Journal of Molecular Sciences* 25, no. 17 (2024): 9375, https://pubmed.ncbi.nlm.nih.gov/39273320/.

22. O. Alzoubi, A. Meyer, T. P. Gonzalez, et al., "Significance of IL-34 and SDC-1 in the Pathogenesis of RA Cells and Preclinical Models," *Clinical Immunology* 251 (2023): 109635, https://doi.org/10.1016/j.clim.2023.109635.

23. A. Meyer, R. E. Sienes, W. Nijim, et al., "Syntenin-1-Mediated Arthritogenicity Is Advanced by Reprogramming RA Metabolic Macrophages and Th1 Cells," *Annals of the Rheumatic Diseases* 82 (2023): 483–495, https://doi.org/10.1136/ard-2022-223284.

24. R. Jurjus, L. Dosh, R. Farhat, et al., "Lack of Syndecan-1 Promotes the Pathogenesis of Experimental Rheumatoid Arthritis," *Immunogenetics* 76 (2024): 145–154, https://doi.org/10.1007/s00251-024-01337-9.

25. V. Carnazzo, F. Gulli, V. Basile, et al., "Serum Levels of Free Light Chains and Syndecan-1 in Patients With Rheumatoid Arthritis and Systemic Lupus Erythematosus," *Rheumatology (Oxford, England)* 64 (2024): keae623, https://doi.org/10.1093/rheumatology/keae623.

26. K.-J. Kim, J.-Y. Kim, I.-W. Baek, W. U. Kim, and C. S. Cho, "Elevated Serum Levels of Syndecan-1 Are Associated With Renal Involvement in Patients With Systemic Lupus Erythematosus," *Journal of Rheumatology* 42 (2015): 202–209, https://doi.org/10.3899/jrheum.140568.

27. A. Meyer, S. R. Zack, W. Nijim, et al., "Metabolic Reprogramming by Syntenin-1 Directs RA FLS and Endothelial Cell-Mediated Inflammation and Angiogenesis," *Cellular & Molecular Immunology* 21 (2024): 33–46, https://doi.org/10.1038/s41423-023-01108-8.

28. Y. Zhang, Z. Wang, J. Liu, et al., "Cell Surface-Anchored Syndecan-1 Ameliorates Intestinal Inflammation and Neutrophil Transmigration in Ulcerative Colitis," *Journal of Cellular and Molecular Medicine* 21 (2017): 13–25, https://doi.org/10.1111/jcmm.12934.

29. G. Hinsinger, L. Du Trieu De Terdonck, S. Urbach, et al., "CD138 as a Specific CSF Biomarker of Multiple Sclerosis," *Neurology Neuroimmunology & Neuroinflammation* 11 (2024): e200230, https://doi.org/10.1212/NXI.0000000000200230.

30. N. Y. Lee, N. R. Kim, J. W. Kang, et al., "Increased Salivary Syndecan-1 Level Is Associated With Salivary Gland Function and Inflammation in Patients With Sjögren's Syndrome," *Scandinavian Journal of Rheumatology* 51 (2022): 220–229, https://doi.org/10.1080/03009742.2021.1923162.

31. C. Xue, Q. Yao, X. Gu, et al., "Evolving Cognition of the JAK-STAT Signaling Pathway: Autoimmune Disorders and Cancer," *Signal Transduction and Targeted Therapy* 8 (2023): 204, https://doi.org/10.1038/s41392-023-01468-7.

32. S. Banerjee, A. Biehl, M. Gadina, S. Hasni, and D. M. Schwartz, "JAK-STAT Signaling as a Target for Inflammatory and Autoimmune Diseases: Current and Future Prospects," *Drugs* 77 (2017): 521–546, https://doi.org/10.1007/s40265-017-0701-9.

33. X.-Y. Wei, D.-C. Hu, Z.-P. Gao, and C.-J. Feng, "JAK/STAT Signaling Pathway and Its Regulation on Insect Immunity," *Yi Chuan* 45 (2023): 229–236, https://doi.org/10.16288/j.yczz.22-402.

34. A. Sarapultsev, E. Gusev, M. Komelkova, I. Utepova, S. Luo, and D. Hu, "JAK-STAT Signaling in Inflammation and Stress-Related Diseases: Implications for Therapeutic Interventions," *Molecular Biomedicine* 4 (2023): 40, https://doi.org/10.1186/s43556-023-00151-1.

35. M. Benucci, P. Bernardini, C. Coccia, et al., "JAK Inhibitors and Autoimmune Rheumatic Diseases," *Autoimmunity Reviews* 22 (2023): 103276, https://doi.org/10.1016/j.autrev.2023.103276.

36. A. Valle-Mendiola, A. Gutiérrez-Hoya, and I. Soto-Cruz, "JAK/STAT Signaling and Cervical Cancer: From the Cell Surface to the Nucleus," *Genes* 14 (2023): 1141, https://doi.org/10.3390/genes14061141.

37. J. J. O'Shea, D. M. Schwartz, A. V. Villarino, M. Gadina, I. B. McInnes, and A. Laurence, "The JAK-STAT Pathway: Impact on Human Disease and Therapeutic Intervention," *Annual Review of Medicine* 66 (2015): 311–328, https://doi.org/10.1146/annurev-med-051113-024537.

38. C. J. Malemud, "The Role of the JAK/STAT Signal Pathway in Rheumatoid Arthritis," *Ther Adv Musculoskelet Dis* 10 (2018): 117–127, https://doi.org/10.1177/1759720X18776224.

39. F. Wang, L. Sun, S. Wang, et al., "Efficacy and Safety of Tofacitinib, Baricitinib, and Upadacitinib for Rheumatoid Arthritis: A Systematic Review and Meta-Analysis," *Mayo Clinic Proceedings* 95 (2020): 1404–1419, https://doi.org/10.1016/j.mayocp.2020.01.039.

Supporting Information

Additional supporting information can be found online in the Supporting Information section. **Figure S1:** Construction of protein–protein interaction network and identification of key genes. (a) The PPI network of differentially expressed genes. (b) The prediction results of CytoNCA algorithm, CXCL13, CCL5 and CXCL10 identified as core hub genes. **Figure S2:** Validation of Hub Genes SDC1. Comparison of SDC1 expression in normal and RA synovial tissues using two external datasets (GSE12021 and GSE1919). **Figure S3:** The molecular docking results of SDC1 and JAK2. Predicted SDC1–JAK2 docking model highlighting key interface residues (SER-171, SER-919, GLU-845 et al.) and the main stabilizing forces—hydrogen bonds and hydrophobic interactions. **Table S1:** Complete list of differentially expressed genes (DEGs) identified in the study. **Table S2:** Binding Energy of SDC1 and JAK family.

International Journal of Rheumatic Diseases

WILEY

International Journal of Rheumatic Diseases

ORIGINAL ARTICLE

Clinical and Radiographic Factors Associated With Difficult-to-Manage Axial Spondyloarthritis: A Multicenter Study

Haluk Cinakli[1] | Mete Kara[2] | Gülay Alp[3]

[1]Rheumatology Department, Kırklareli Training and Research Hospital, Kırklareli, Turkey | [2]Rheumatology Department, Izmir City Hospital, Izmir, Turkey | [3]Division of Rheumatology, Department of Internal Medicine, Uşak University School of Medicine, Uşak, Turkey

Correspondence: Gülay Alp (gulay_alp88@hotmail.com)

Received: 21 July 2025 | **Revised:** 16 November 2025 | **Accepted:** 15 January 2026

Keywords: axial spondyloarthritis | biologic therapy | comorbidities | difficult-to-manage | smoking

ABSTRACT

Objective: To evaluate the clinical characteristics, disease burden, and treatment patterns of axial spondyloarthritis (axSpA) using the recently proposed Assessment of Spondyloarthritis International Society (ASAS) definition of difficult-to-manage axSpA (D2M-axSpA).

Methods: A total of 383 patients with axSpA were enrolled. This multicenter cross-sectional study was conducted in three tertiary care centers, enrolling consecutive axSpA patients from outpatient clinics. Patients were classified as D2M-axSpA based on prior use of biologic or targeted synthetic disease-modifying antirheumatic drugs (b/tsDMARDs) and persistent disease activity based on the ASAS definition. Logistic regression analysis identified factors associated with D2M-axSpA.

Results: Among patients, 11.2% met the D2M-axSpA criteria. The cohort was 58.7% male, with a mean age of 43.5 ± 10.5 years. Radiographic axSpA was present in 70.8%, and 69.2% of patients had received biological therapy. D2M-axSpA patients exhibited higher inflammatory markers (ESR, CRP), increased disease activity (BASDAI, ASDAS-CRP), and greater functional impairment (BASFI, ASQoL). Peripheral arthritis ($p = 0.001$), enthesitis ($p = 0.031$), smoking history ($p = 0.037$), and comorbidities ($p = 0.020$) were significantly more frequent in D2M-axSpA. Among D2M-axSpA patients, 22/383 (5.7%) fulfilled the treatment-refractory criteria. Radiographic findings revealed higher rates of sacroiliac ankylosis, lumbar syndesmophytes, symphysitis, and ischial enthesitis, as well as mSASSS scores. Logistic regression identified anterior uveitis (OR: 4.474, $p = 0.007$), peripheral arthritis (OR: 2.684, $p = 0.021$), and comorbidities (OR: 2.878, $p = 0.013$) as independently associated factors.

Conclusion: Findings highlight the clinical and radiographic burden of D2M-axSpA and emphasize the need for optimized treatment strategies, particularly in patients with comorbidities, a history of anterior uveitis or peripheral arthritis, and those with a smoking history.

1 | Introduction

Axial spondyloarthritis (axSpA) is a chronic inflammatory disease primarily affecting the axial skeleton, leading to progressive structural damage and functional impairment [1]. Despite therapeutic advances, a subset of patients remains difficult to manage (D2M), characterized by persistent disease activity and impaired quality of life (QoL). To address this unmet need, the Assessment of SpondyloArthritis International Society (ASAS) recently developed a consensus-based definition of D2M-axSpA, which requires (i) prior failure of ≥2 b/tsDMARDs with different mechanisms of action (MOA), (ii) persistent

Key Messages

- Peripheral arthritis, anterior uveitis, smoking history, and comorbidities have been associated with difficult-to-manage axial spondyloarthritis (D2M-axSpA).
- D2M-axSpA was identified in 11.2% of patients and was strongly associated with higher disease activity and structural damage.
- Early identification of articular, extraarticular manifestations, and comorbidities may help guide treatment strategies to prevent disease progression and optimize therapeutic outcomes.

disease activity (Ankylosing Spondylitis Disease Activity Score using C-reactive protein [ASDAS-CRP]) ≥ 2.1, active peripheral manifestations, or impaired health-related quality of life (HRQoL), and (iii) physician or patient perception of the disease as difficult to manage [2]. Within this framework, the ASAS consensus also describes a treatment-refractory (TR) subgroup, defined as patients showing persistent objective inflammation (elevated CRP and/or magnetic resonance imaging [MRI] activity) despite failure of at least two b/tsDMARDs with different MOA.

Recent studies indicate that approximately 19.6% to 22.9% of axSpA patients receiving biologic therapy meet the criteria for difficult-to-treat (D2T) disease [3, 4]. Several factors have been associated with D2T condition, including female sex, longer disease duration, uveitis, peripheral manifestations, comorbidities such as psoriasis and hypertension, and a higher prevalence of fibromyalgia [3, 5]. Additionally, these patients tend to have higher disease activity scores, increased acute phase reactants, and greater impairment in health-related quality of life measures compared to those with treatment-responsive axSpA [3, 5].

Despite the availability of Tumor Necrosis Factor (TNF) inhibitors, IL-17 inhibitors, and Janus kinase (JAK) inhibitors, a substantial proportion of axSpA patients continue to experience uncontrolled disease activity, highlighting the need for a better understanding of the pathophysiology, predictive factors, and optimal management strategies for D2M-axSpA. Identifying early predictors of D2M disease courses can facilitate timely intervention strategies, guide personalized treatment approaches, and prevent disease progression, disability, and impaired quality of life. Following the publication of the ASAS definition, real-world studies from Europe and Asia confirmed its clinical relevance: Smits et al. (Netherlands) reported 10% prevalence with smoking and psoriasis as independent risk factor [6], and Lee et al. (Korea, KOBIO registry) validated its applicability in Asian populations [7]. These emerging data support the clinical utility of the D2M concept and highlight the importance of early identification of modifiable risk factors such as smoking and comorbidities, which may contribute to poor disease control and treatment refractoriness.

This study applied the ASAS framework in a real-world cohort to identify patients meeting the D2M criteria and to evaluate their demographic, clinical, and radiographic characteristics.

2 | Method

2.1 | Study Design

This multicenter cross-sectional study was conducted between December 2024 and February 2025 at the rheumatology outpatient clinics of three tertiary care centers in Turkey. We consecutively enrolled axSpA patients from our outpatient clinics, ensuring a representative population and incorporating the latest clinical perspectives. The diagnosis of axSpA was established based on the ASAS classification criteria [8]. The treatment decisions, including the initiation and selection of b/tsDMARDs, were made by the treating rheumatologist in accordance with European Alliance of Associations for Rheumatology (EULAR) recommendations, which suggest initiating such therapies in patients with axSpA inadequately controlled on NSAIDs with signs of active inflammation [9].

2.2 | Clinical Evaluation

Disease activity was assessed using the Bath Ankylosing Spondylitis Disease Activity Index (BASDAI) and the ASDAS-CRP [10]; functional status with the Bath Ankylosing Spondylitis Functional Index (BASFI); spinal mobility with the Bath Ankylosing Spondylitis Metrology Index (BASMI); and quality of life with the Ankylosing Spondylitis Quality of Life Questionnaire (ASQoL). Peripheral manifestations were evaluated at the most recent visit using a 66/68 swollen and tender joint count, documentation of dactylitis, and the Leeds Enthesitis Index (LEI), with a score ≥ 1 indicating active enthesitis. In line with the ASAS consensus definition of D2M-axSpA, the second and third criteria were operationalized in this study as follows: impaired health-related QoL was defined as an ASQoL score > 8, a cutoff shown to have good discriminative ability for identifying clinically meaningful QoL impairment in previous Turkish validation studies [11]. Disease perceived as problematic by either the patient or the physician was defined as a patient global assessment (PGA) ≥ 4/10 or a physician global assessment (PhGA) ≥ 4/10, reflecting residual disease burden or dissatisfaction with current disease control despite treatment.

Weight and height were measured, and body mass index (BMI) was calculated. Duration of disease (years), symptom duration, age of diagnosis, acute phase reactants (the erythrocyte sedimentation rate [ESR], CRP mg/dL), and the presence of human leukocyte antigen (HLA)-B27 were recorded. Medication history, including current and previous treatments, was collected through both medical chart review and direct patient interviews. Fibromyalgia was considered present if documented in the patient's medical records based on the treating physician's assessment and/or fulfillment of the 2016 revised American College of Rheumatology (ACR) 2016 Fibromyalgia diagnostic criteria [12], according to this criteria Widespread Pain Index (WPI) and Symptom Severity Scale (SSS) were assessed. Anxiety and depressive symptoms were evaluated using the Hospital Anxiety and Depression Scale (HADS), which consists of two 7-item subscales (HADS-A and HADS-D), each scored from 0 to 21; scores ≥ 11 were considered indicative of clinically relevant symptoms [13]. Comorbidities were assessed using the Rheumatic Disease Comorbidity Index (RDCI) [14] and the Modified Charlson Comorbidity Index (mCCI) [15].

2.3 | Radiological Evaluation

The presence of sacroiliitis, syndesmophytes, ischial enthesitis, and symphysitis was systematically recorded. Sacroiliac ankylosis was defined as complete fusion of the sacroiliac joint observed on standard pelvic radiographs, based on the modified New York grading system (grade 4 sacroiliitis). Hip joint involvement was assessed using the Bath Ankylosing Spondylitis Radiology Hip Index (BASRI-hip), where a score of ≥ 2 was considered indicative of hip involvement [16]. Ischial enthesitis was defined as an irregular appearance at tendon and ligament attachment sites on pelvic radiographs. The modified Stoke Ankylosing Spondylitis Spine Score (mSASSS) was calculated for each patient to quantitatively assess structural damage in the cervical and lumbar spine. The mSASSS was determined by scoring anterior vertebral corners at the C2 to T1 and T12 to S1 levels, with total scores ranging from 0 to 72 [17]. Radiographs used for analysis were not baseline or diagnostic images but the most recent radiographs available within the previous 12 months before study inclusion. When no recent radiographs were available in the medical record, updated images were obtained as part of standard care. These images, obtained during routine clinical follow-up, reflected the patient's current structural status at the time of the cross-sectional evaluation.

All radiographs (cervical and lumbar spine and sacroiliac joint images) were independently evaluated by two rheumatologists (G.A. and H.C.). Both readers had specific training and fellowship experience in spondyloarthritis imaging. The spinal radiographs scored with the mSASSS; the intra-rater ICC values for HC and GA were 0.88 and 0.85, respectively, while the inter-rater reliability was 0.85. These results indicate excellent overall reliability for spinal scoring. The final mSASSS score was determined by calculating the mean of the two readers' scores. In cases of disagreement regarding dichotomous variables, including the presence of enthesitis or radiographic sacroiliitis, the final decision was reached by consensus between the two readers.

2.4 | Statistical Analysis

All statistical analyses were performed using IBM SPSS Statistics for Windows, Version 26.0 (IBM Corp., Armonk, NY, USA). Continuous variables were tested for normality using the Shapiro–Wilk test and presented as mean ± standard deviation (SD) or median (interquartile range [IQR]), as appropriate. Categorical variables were expressed as frequencies and percentages. Between-group comparisons were conducted using the independent samples *t*-test or Mann–Whitney *U* test for continuous variables and the chi-square or Fisher's exact test for categorical variables.

To identify independent factors associated with D2M-axSpA, univariate analyses were first conducted. Variables with a *p*-value <0.10 were selected for multivariable logistic regression analysis using a backward stepwise method. Based on both univariate results and existing literature, the following variables were included in the initial model: history of anterior uveitis, peripheral arthritis, comorbidity presence, ever smoking, sex, Leeds Enthesitis Index (LEI) ≥ 1, ASDAS-CRP score, and mSASSS total score. These variables were chosen for their clinical relevance and prior associations with treatment resistance in axSpA. ASDAS-CRP and mSASSS were included to assess disease activity and structural damage, respectively. Sex and LEI were evaluated as potential confounders or effect modifiers. Odds ratios (ORs) with 95% confidence intervals (CIs) were reported, and a two-sided *p*-value <0.05 was considered statistically significant.

2.5 | Ethics Statement

The study was approved by the local ethics committee (Approval Number: 202400028-05). All participants provided informed consent, and the study was conducted in accordance with the Declaration of Helsinki.

3 | Result

A total of 383 axSpA patients were included, of whom 58.7% were male. The mean age was 43.5 ± 10.5 years, and the median disease duration was 6 (IQR: 8) years. HLA-B27 positivity was observed in 54%, while r-axSpA was diagnosed in 70.8% of cases. The median ESR and CRP levels were 19.5 mm/h (IQR: 22) and 3.78 mg/L (IQR: 6.67), respectively.

The mean BASDAI score was 2.51 ± 2.07, BASFI was 2.37 ± 2.11, and ASDAS-CRP was 2.01 ± 0.95. The mean ASQoL score was 5.11 ± 4.9. Biologic therapy was used by the majority of patients (69.2%), while comorbidities were present in 35% of the cohort. Inflammatory bowel disease (IBD) was reported in 6.3% of patients. Fibromyalgia, assessed in a subgroup of 296 patients using the 2016 ACR criteria, was present in 18.6%. Additionally, symptoms of anxiety and depression were observed in 15.4% and 13.6% of patients, respectively, based on the HADS. A history of enthesitis was observed in 49.4%, while dactylitis, anterior uveitis, and peripheral arthritis were reported in 4.2%, 14.1%, and 32.1%, respectively (Table 1).

Among the cohort, 43 patients (11.2%) were classified as D2M-axSpA. Among D2M-axSpA patients, 22/383 (5.7%) fulfilled the TR criteria. There were no significant differences between the D2M and non-D2M groups in terms of sex, age, current smoking, employment, disease duration, or HLA-B27 positivity. However, a significantly higher proportion of D2M-axSpA patients had a history of smoking compared to non-D2M patients (79.1% vs. 62.9%, $p=0.037$). In addition, the D2M group had significantly higher ESR ($p=0.003$) and CRP ($p=0.016$) levels, as well as a higher prevalence history of enthesitis ($p=0.031$) and peripheral arthritis ($p=0.001$).

BASDAI, BASFI, and ASDAS-CRP were significantly higher in the D2M group. LEI ≥ 1 was similar in D2M-axSpA and non-D2M patients (0.074) (Table 2). D2M-axSpA patients had a significantly higher history of prior treatments. Ever-use of methotrexate and sulfasalazine was significantly more common in the D2T group. Ever-use of adalimumab, etanercept, golimumab, and certolizumab was significantly more frequent in D2M-axSpA patients. JAK inhibitors and IL-17 inhibitors were also more commonly used (Table S1).

TABLE 1 | Demographic, clinical, and disease activity characteristics of axSpA patients.

Variables	*N* = 383	Variables	*N* = 383
Sex, male, *n* (%)	225 (58.7)	SpA family history, *n* (%)	113 (29.5)
Age, years, mean ± SD	43.5 ± 10.5	NSAID, *n* (%)	247 (64.5)
Current smoker, *n* (%)	57 (42.5)	Methotrexate, current, *n* (%)	33 (8.6)
Currently employed, *n* (%)	74 (55.6)	Biological therapy, *n* (%)	265 (69.2)
Symptom duration, years, median (IQR)	7 (8)	ESR mm/h, median (IQR)	19.5 (22)
Disease duration, years, median (IQR)	6 (8)	CRP mg/L, median (IQR)	3.78 (6.67)
AxSpA type, r-axSpA, *n* (%)	271 (70.8)	BASDAI, score, mean ± SD	2.51 ± 2.07
HLA-B27 positive, *n* (%)	135 (54)	BASFI, score, mean ± SD	2.37 ± 2.11
BMI, kg/m^2, mean ± SD	26.6 ± 4.9	ASDAS-CRP, mean ± SD	2.01 ± 0.95
Comorbidity, at least one, *n* (%)	38 (28.4)	ASQoL, mean ± SD	5.11 ± 4.9
Inflammatory bowel disease, *n* (%)	24 (6.3)	LEI ≥ 1, *n* (%)	84 (21.9)
History of enthesitis, *n* (%)	190 (49.4)	BASMI total score, median (IQR)	3.2 (1.8)
History of dactylitis, *n* (%)	16 (4.2)	Fibromyalgia (ACR 2016), *n* (%)[a]	55 (18.6)
History of anterior uveitis, *n* (%)	54 (14.1)	HADS- anxiety, *n* (%)	59 (15.4)
History of peripheral arthritis, *n* (%)	123 (32.1)	HADS -depression, *n* (%)	51 (13.6)
Psoriasis at baseline, *n* (%)	31 (8.1)	D2M-AxSpA	43 (11.2)

Abbreviations: ACR, American College of Rheumatology; AS, Ankylosing Spondylitis; ASDAS-CRP, Ankylosing Spondylitis Disease Activity Score with C-reactive protein; ASQoL, Ankylosing Spondylitis Quality of Life Questionnaire; BASDAI, Bath Ankylosing Spondylitis Disease Activity Index; BASFI, Bath Ankylosing Spondylitis Functional Index; BASMI, Bath Ankylosing Spondylitis Metrology Index; BMI, Body Mass Index; CRP, C-reactive protein; D2M-AxSpA, difficult-to-manage axial spondyloarthritis; ESR, erythrocyte sedimentation rate; HADS, Hospital Anxiety and Depression Scale; HLA, human leukocyte antigen; IQR, interquartile range; LEI, Leeds Enthesitis Index; NSAID, non-steroidal anti-inflammatory drug; r-axSpA, radiographic axial spondyloarthritis.
[a]Fibromyalgia was assessed in a subset of 296 patients using the 2016 ACR criteria.

Patients in the D2M group had significantly longer prior treatment durations. The duration of the first biologic treatment was notably longer in the D2M group compared to non-D2M patients (29.5 [IQR: 29] months vs. 6 [IQR: 30] months, $p = 0.002$). Similarly, the duration of the second biologic treatment was also significantly longer in D2M patients (14 [IQR: 19] months vs. 12 [IQR: 9] months, $p = 0.006$). Treatment discontinuation due to ineffectiveness was more frequent in the D2M group, though the difference was not statistically significant. Similarly, discontinuation due to side effects was similar between groups (Table S2). Consistent with the treatment burden, patients classified as D2M-axSpA had significantly higher exposure to biologic therapies. They were more frequently treated with ≥ 2, ≥ 3, ≥ 4, and ≥ 5 different biologic agents, as well as therapies targeting ≥ 2 different mechanisms of action compared to non-D2M patients (Figure 1). No significant differences were detected in diabetes, hypertension, thyroid disease, hyperlipidemia, fibromyalgia, anxiety, or depression. Likewise, no significant differences were observed in the comorbidity burden measured by the RDCI and mCCI scores. Similarly, fibromyalgia, anxiety, and depression did not differ significantly between the groups (Table 3). However, the presence of at least one comorbidity was significantly higher in D2M-axSpA (52.1% vs. 33.2%, $p = 0.020$).

Radiographic findings showed that sacroiliac ankylosis was more prevalent in D2M-axSpA compared to non-D2M patients. In addition, lumbar syndesmophytes, ischial enthesitis, and symphysitis were also more common in the D2M group. The total and lumbar mSASSS scores were significantly higher in D2M-axSpA. In contrast, the frequency of hip joint involvement was similar between the groups (Table 4).

In the multivariate logistic regression analysis, a history of anterior uveitis was significantly associated with D2M-axSpA (OR: 4.474, 95% CI: 1.519–13.172, $p = 0.007$). Patients with a history of peripheral arthritis had a higher likelihood of being classified as D2M-axSpA (OR: 2.684, 95% CI: 1.157–6.222, $p = 0.021$). The presence of at least one comorbidity was also a significant factor (OR: 2.878, 95% CI: 1.250–6.627, $p = 0.013$). Smoking history showed borderline statistical significance (OR: 2.258, 95% CI: 1.001–6.538, $p = 0.050$) (Table 5).

4 | Discussion

In this multicenter cohort, 11.2% of patients met the ASAS definition for D2M-axSpA. Compared to non-D2M cases, D2M-axSpA patients with a more complex disease course are characterized by higher inflammatory markers, increased structural damage, and increased rates of peripheral arthritis, anterior uveitis, and comorbidities. Our results underscore the multidimensional clinical burden and treatment challenges associated with D2M-axSpA.

TABLE 2 | Demographic and clinical characteristics of patients with and without D2M-axSpA.

Variables	D2M-AxSpA (*N* = 43)	Non-D2M-AxSpA (*N* = 340)	*p*
Sex, male, *n* (%)	23 (53.5)	202 (59.4)	0.457
Age, years, mean ± SD	42.05 ± 9.41	41.98 ± 10.67	0.970
Current smoker, *n* (%)	26 (60.5)	162 (47.6)	0.113
Smoker ever, *n* (%)	34 (79.1)	214 (62.9)	**0.037**
Currently employed, *n* (%)	28 (65.1)	45 (64.0)	0.571
Symptom duration, years, median (IQR)	14.05 (8.64)	14.50 (10.02)	0.975
Disease duration, years, median (IQR)	10.40 (7.29)	9.86 (8.32)	0.390
AxSpA type, r-axSpA, *n* (%)	35 (81.4)	235 (69.4)	0.104
HLA-B27 positive, *n* (%)	19 (55.9)	116 (53.7)	0.813
Spondyloarthritis family history, *n* (%)	14 (32.6)	99 (29.1)	0.641
BMI, kg/m^2, mean ± SD	25.4 ± 6.71	26.60 ± 4.91	0.164
ESR mm/h, median (IQR)	17 (19)	10 (13)	**0.003**
CRP mg/L, median (IQR)	6.5 (8.9)	3.9 (5.9)	**0.016**
History of enthesitis, *n* (%)	28 (65.1)	162 (47.6)	**0.031**
History of dactylitis, *n* (%)	2 (4.7)	14 (4.1)	0.698
History of anterior uveitis, *n* (%)	10 (23.3)	44 (12.9)	0.067
History of peripheral arthritis, *n* (%)	23 (53.5)	100 (29.4)	**0.001**
Psoriasis at baseline, *n* (%)	2 (4.7)	29 (8.6)	0.556
Inflammatory bowel disease, *n* (%)	3 (7)	21 (6.2)	0.742
BASDAI, score, mean ± SD	4.26 ± 1.86	3.58 ± 2.41	**0.036**
BASFI, score, mean ± SD	3.40 ± 1.69	2.75 ± 2.45	**0.003**
ASDAS-CRP, mean ± SD	2.84 ± 0.79	2.35 ± 1.05	**0.001**
ASQoL, mean ± SD	7.88 ± 4.39	6.62 ± 5.40	0.095
PGA, (0–10) median (IQR)	5 (3)	3 (5)	**0.001**
PhGA, (0–10) median (IQR)	3 (3)	2 (3)	**0.004**
LEI ≥ 1, *n* (%)	14 (32.6)	70 (20.6)	0.074
BASMI total score, median (IQR) *N*: 214	2.9 (2.8)	2.75 (2)	0.754

Note: Bold *p*-values indicate statistical significance ($p < 0.05$).

Abbreviations: AS, Ankylosing Spondylitis; ASDAS-CRP, Ankylosing Spondylitis Disease Activity Score with C-reactive protein; ASQoL, Ankylosing Spondylitis Quality of Life Questionnaire; BASDAI, Bath Ankylosing Spondylitis Disease Activity Index; BASFI, Bath Ankylosing Spondylitis Functional Index; BASMI, Bath Ankylosing Spondylitis Metrology Index; BMI, body mass index; CRP, C-reactive protein; D2M-axSpA, difficult-to-manage axial spondyloarthritis; ESR, erythrocyte sedimentation rate; HLA, human leukocyte antigen; IQR, interquartile range; LEI, Leeds Enthesitis Index; PhGA, physician global assessment; PGA, patient global assessment; nr-axSpA, non-radiographic axial spondyloarthritis.

A recent study by Smits et al. was the first to implement the ASAS definition of D2M-axSpA in a real-life clinical registry, reporting a D2M prevalence of approximately 13% [6]. They identified D2M patients as having higher disease activity, poorer functional status, and more frequent switching between treatments. Our findings are largely consistent, with a comparable D2M prevalence of 11.2% and similar clinical characteristics, including significantly elevated ASDAS-CRP and BASDAI scores, greater functional impairment, and extensive prior exposure to biological therapies. However, unlike the Smits cohort, our study incorporated a detailed radiographic assessment, revealing a distinct structural phenotype in D2M-axSpA. Structural damage, including sacroiliac ankylosis, ischial enthesitis, symphysitis, and higher mSASSS scores, were significantly more common in these patients, potentially differentiating them from treatment-responsive cases [6]. Therefore, we thought this structural damage reflects a true D2M phenotype.

In our cohort, a TR subgroup was also identified, comprising 22 patients (5.7%) who fulfilled the ASAS TR criteria. This prevalence is consistent with findings from the Netherlands and Korea, where Smits et al. and Lee et al. reported TR rates of approximately 4%–6% [6, 7]. These results support the external validity of our data and emphasize that, although relatively uncommon, TR-axSpA represents a clinically significant phenotype characterized by persistent inflammation despite multiple b/tsDMARD failures.

While previous studies such as those by Öğüt et al. [4] and Fakih et al. [3] the term "D2T," our study followed the ASAS definition

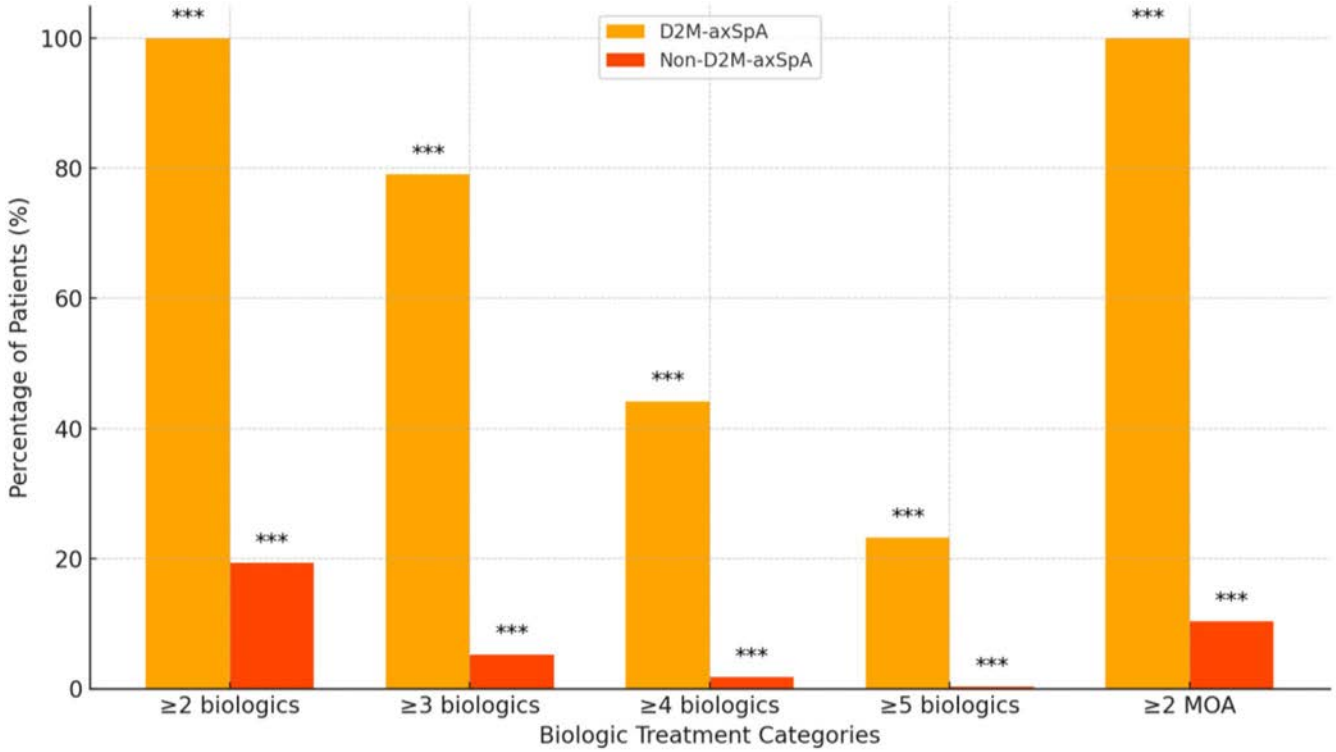

FIGURE 1 | Comparison of biologic therapy burden and treatment switching in D2M and non-D2M axSpA groups. D2M-axSpA, difficult-to-manage axial spondyloarthritis. This figure shows the proportion of axSpA patients treated with multiple biological agents or mechanisms of action, categorized by D2M status. Orange bars represent D2M-axSpA, and red bars represent non-D2M-axSpA patients. Categories include ≥2, ≥3, ≥4, or ≥5 biologic therapies, and ≥2 MOAs. Statistical significance: ***$p < 0.001$ for all comparisons.

of "D2M" axSpA. Although these concepts are similar, D2M-axSpA is a more standardized, consensus-based classification. Therefore, comparisons between studies should be interpreted with this distinction in mind.

The observed prevalence of D2M-axSpA in our cohort (11.2%) was lower than that reported by Fakih et al. (19.59%) [3], potentially due to methodological differences. Notably, their definition of D2T axSpA was based on ICD coding, whereas our study applied clinically detailed criteria to identify D2M cases. Despite this difference, both studies found that D2M-axSpA patients had higher inflammatory markers and greater disease burden. However, more frequent radiographic damage was observed in the current study, a factor not assessed in the analysis by Fakih et al.

Analysis of data from the French National Health System identified psoriasis, peripheral involvement, hypertension, and depression as factors associated with D2T-axSpA [18]. However, in our study, psoriasis, hypertension, and depression did not show a significant association with D2M-axSpA, while comorbidities overall remained an important factor, highlighting potential differences in population characteristics or disease phenotypes. Despite these differences, both studies highlight the importance of comorbidities in the disease burden of D2M-axSpA, with peripheral involvement emerging as a common factor in both cohorts.

Öğüt et al. (2024) found a significantly higher prevalence of fibromyalgia in D2T-axSpA, whereas in our study, fibromyalgia did not differ between groups [4]. However, both studies consistently showed that D2T-axSpA is associated with higher disease activity, increased inflammation, and poorer quality of life, reflecting a greater disease burden. In our study, fibromyalgia was assessed using the 2016 ACR criteria, whereas Öğüt et al. applied the 2010 criteria. The 2016 criteria emphasize symptom severity and may be more specific, potentially accounting for the lower prevalence observed in our cohort.

Furthermore, in our previous work on difficult-to-treat rheumatoid arthritis (D2T RA), fibromyalgia was independently associated with D2T status, even after adjusting for relevant clinical and demographic confounders [19]. In contrast, the present axSpA cohort showed no such association. These findings support the hypothesis that non-inflammatory contributors, such as fibromyalgia, may play a more prominent role in D2T RA, whereas D2M-axSpA is more strongly driven by inflammation and structural damage.

In contrast to previous studies, including Juárez et al. (2024), which reported a gender difference in the prevalence of D2M-axSpA, no such difference was found in our cohort [20]. However, consistent with their findings, smoking was identified as a key associated factor in our study as well. Past smoking (ever smoker) was significantly more common in D2M patients, while current smoking did not show a significant association, suggesting that cumulative exposure may be more relevant. Smoking is a key contributor to disease progression and treatment resistance in axSpA [21]. In our study, ever-smokers were more likely to develop D2M-axSpA. Previous research has demonstrated that smoking

TABLE 3 | Comparison of comorbidities and psychological features between D2M and non-D2M AxSpA patients.

Variables	D2M-AxSpA $N=43$	Non-D2M-AxSpA $N=340$	p
Comorbidity, at least one, *n* (%)	22 (52.1)	113 (33.2)	**0.020**
Diabetes mellitus, *n* (%)	3 (7)	19 (5.6)	0.725
Hypertension, *n* (%)	9 (20.9)	40 (11.8)	0.090
Thyroid disease, *n* (%)	3 (7)	12 (3.5)	0.272
Hyperlipidemia, *n* (%)	3 (7)	8 (2.5)	0.115
Fibromyalgia, *n* (%)[a]	7 (20)	48 (18.4)	0.818
SSS, median (IQR)	5 (3)	3 (4)	0.075
WPI, median (IQR)	4 (3)	3 (5)	0.179
HADS anxiety, *n* (%)	6 (14.0)	53 (15.6)	0.774
Anxiety score, median (IQR)	4 (7)	6 (5)	0.350
HADS depression, *n* (%)	6 (14.0)	45 (13.6)	0.943
Depression score, median (IQR)	5 (8)	6 (5)	0.164
mCCI, median (IQR)	0 (0)	0 (0)	0.539
RDCI, median (IQR)	0 (1)	0 (0)	0.539

Note: Bold *p*-values indicate statistical significance ($p < 0.05$).
Abbreviations: D2M-axSpA, difficult-to-manage axial spondyloarthritis; HADS, Hospital Anxiety and Depression Scale; IQR, interquartile range; mCCI, modified Charlson Comorbidity Index; RDCI, Rheumatic Disease Comorbidity Index; SSS, Symptom Severity Scale; WPI, Widespread Pain Index.
[a]Fibromyalgia was assessed in a subset of 296 patients using the 2016 ACR criteria.

TABLE 4 | Comparison of radiographic evaluation D2M and non-D2M AxSpA patients.

Variables	D2M-AxSpA $N=43$	Non-D2M-AxSpA $N=340$	p
Sarcoiliac ankylosis, *n* (%)[a]	19 (45.2)	98 (29.6)	**0.040**
Presence of cervical syndesmophyte, *n* (%)[b]	10 (24.4)	95 (29.1)	0.533
Presence of lumbar syndesmophyte, *n* (%)[b]	18 (43.9)	93 (28.4)	**0.048**
Presence of symphysitis, *n* (%)	10 (24.4)	27 (8.2)	**0.003**
Ischial enthesitis, *n* (%)	14 (33.3)	55 (16.7)	**0.009**
Presence of hip involvement, *n* (%)	13 (31)	98 (29.6)	0.857
Cervical mSASSS, median (IQR)	0 (11)	0 (3)	0.746
Lumber mSASSS, median (IQR)	11 (21)	0 (4)	**<0.001**
mSASSS total score, median (IQR)	12 (33)	1 (8)	**0.002**

Note: Bold *p*-values indicate statistical significance ($p < 0.05$).
Abbreviations: AxSpA, axial spondyloarthritis; D2M-axSpA, difficult-to-manage axial spondyloarthritis; IQR, interquartile range; mSASSS, modified Stoke Ankylosing Spondylitis Spine Score.
[a]Ankylosis was assessed in patients with available anteroposterior pelvic radiographs ($n=373$).
[b]Cervical and lumbar syndesmophytes were assessed in patients with available lateral spine radiographs ($n=368$).

TABLE 5 | Multivariate logistic regression analysis of factors associated with D2M-AxSpA.

Variables	p	OR	95% CI lower	95% CI upper
Smoker ever (present vs. absent)	0.050	2.258	1.001	6.538
History of anterior uveitis	**0.007**	4.474	1.519	13.172
History of peripheral arthritis	**0.021**	2.684	1.157	6.222
At least one comorbidity	**0.013**	2.878	1.250	6.627

Note: Bold *p*-values indicate statistical significance ($p < 0.05$).
Abbreviations: CI, confidence interval; D2M-AxSpA, difficult-to-manage axial spondyloarthritis; OR, odds ratio.

is associated with higher disease activity, increased MRI detected inflammation, and a greater likelihood of syndesmophyte formation and ankylosis [21]. Additionally, smoking has been linked to radiographic progression and reduced response to TNF inhibitors, which may explain the higher treatment-switching rates observed in our cohort. These findings underscore the detrimental impact of smoking on disease outcomes, further complicating disease management and treatment strategies.

A multicenter retrospective study from Northern France identified peripheral involvement, higher BASDAI, extra-musculoskeletal manifestations, and fibromyalgia as key features of D2T-axSpA; baseline prevalence of inflammatory bowel disease (IBD) was also higher in the subgroup classified as "very D2T" [5]. In contrast, our study did not find fibromyalgia or IBD to be significantly different between D2M and non-D2M patients, though higher disease activity and peripheral arthritis were consistent findings. These discrepancies may be attributable not only to differences in cohort composition, disease phenotypes, and healthcare delivery pathways but also to the use of distinct definitions of disease refractoriness, including the classification of a "very D2T" subgroup, which was not applied in our analysis. Despite these variations, both studies highlight the heterogeneity of D2T-axSpA and reinforce the challenge of managing these patients effectively.

A key strength of this study lies in its direct alignment with the recently proposed ASAS definition of D2M-axSpA, ensuring methodological consistency with current classification standards. Moreover, unlike previous investigations that focused exclusively on bDMARD-exposed populations, our cohort encompassed both biologic-exposed and biologic-naïve patients. This broader inclusion captures a more diverse clinical spectrum and enhances the external validity and generalizability of the findings across real-world axSpA populations.

This study has several limitations. As a cross-sectional analysis, radiographic progression was not assessed longitudinally, limiting insights into structural disease progression over time. Morewer, the causality cannot be established between associated factors and D2M-axSpA status. Additionally, baseline disease characteristics such as initial ASDAS-CRP or MRI findings were not available, as only data from the most recent clinical evaluation were analyzed, which may limit the evaluation of temporal disease dynamics and the identification of early predictive markers for D2M-axSpA development. Differences in national reimbursement policies and limited access to novel agents, such as the late inclusion of JAK inhibitors in reimbursement and the absence of bimekizumab during the study period, may have influenced treatment sequencing, exposure to different MOA, and ultimately the classification of D2M-axSpA. Lastly, only eight patients with nr-axSpA fulfilled the D2M definition, limiting the feasibility of subgroup analysis and interpretation in this specific population.

Its originality lies in presenting a detailed radiographic assessment (mSASSS and pelvic lesions) together with comprehensive clinical profiling within the ASAS D2M framework. By additionally incorporating psychological factors such as anxiety, depression, and fibromyalgia, the study provides a multidimensional view of disease burden in D2M-axSpA across structural, functional, and psychosocial domains.

5 | Conclusion

This study provides novel insights into the clinical characteristics and treatment patterns of patients with D2M-axSpA, identifying higher disease activity, greater structural damage, and increased treatment switching as key features of this subgroup. Peripheral arthritis, anterior uveitis, and the presence of comorbidities were strongly associated with D2M-axSpA. These findings highlight the complexity of treatment resistance in axSpA and emphasize the importance of early identification of high-risk patients to enable more individualized therapeutic strategies. Further prospective studies are required to evaluate long-term outcomes and to optimize management approaches for this challenging patient population.

Author Contributions

All authors contributed to the study conception and design. Mete Kara, Gülay Alp, and Haluk Cinakli were responsible for material preparation, data collection, and analysis. The first draft of the manuscript was written by Mete Kara, Gülay Alp, and Haluk Cinakli, and all authors commented on previous versions of the manuscript. All authors read and approved the final version.

Acknowledgments

The authors have nothing to report.

Conflicts of Interest

The authors declare no conflicts of interest.

Data Availability Statement

The data that support the findings of this study are available on request from the corresponding author. The data are not publicly available due to privacy or ethical restrictions.

References

1. F. Fattorini, S. Gentileschi, C. Cigolini, et al., "Axial Spondyloarthritis: One Year in Review 2023," *Clinical and Experimental Rheumatology* 41, no. 11 (2023): 2142–2150, https://doi.org/10.55563/CLINEXPRHEUMATOL/9FHZ98.

2. D. Poddubnyy, V. Navarro-Compán, M. Torgutalp, et al., "The Assessment of SpondyloArthritis International Society (ASAS) Consensus-Based Expert Definition of Difficult-to-Manage, Including Treatment-Refractory, Axial Spondyloarthritis," *Annals of the Rheumatic Diseases* 84 (2025): 538–546, https://doi.org/10.1016/J.ARD.2025.01.035.

3. O. Fakih, M. Desmarets, B. Martin, et al., "Difficult-to-Treat Axial Spondyloarthritis is Associated With Psoriasis, Peripheral Involvement and Comorbidities: Results of an Observational Nationwide Study," *RMD Open* 9, no. 4 (2023): e003461, https://doi.org/10.1136/RMDOPEN-2023-003461.

4. T. S. Öğüt, F. Erbasan, M. F. Şahiner, et al., "Difficult-to-Treat Axial Spondyloarthritis Patients," *Archives of Rheumatology* 39, no. 3 (2024): 419–428, https://doi.org/10.46497/ARCHRHEUMATOL.2024.10567.

5. C. Philippoteaux, T. Delepine, E. Cailliau, et al., "Characteristics of Difficult-to-Treat Axial Spondyloarthritis: Results of a Real-World Multicentric Study," *Joint, Bone, Spine* 91, no. 2 (2024): 105670, https://doi.org/10.1016/J.JBSPIN.2023.105670.

6. M. L. Smits, C. Webers, H. E. Vonkeman, and A. van Tubergen, "Exploring Difficult-to-Manage Axial Spondyloarthritis: Results From a Dutch Clinical Practice Registry," *Rheumatology* 64 (2025): 3816–3825, https://doi.org/10.1093/RHEUMATOLOGY/KEAF120.

7. K. A. Lee, H. Lee, and H. S. Kim, "Prevalence and Predictive Factors of Difficult-to-Manage Axial Spondyloarthritis: Results From the KOBIO Registry," *International Journal of Rheumatic Diseases* 28, no. 5 (2025): e70242, https://doi.org/10.1111/1756-185X.70242.

8. M. Rudwaleit, D. Van Der Heijde, R. Landewé, et al., "The Development of Assessment of SpondyloArthritis International Society Classification Criteria for Axial Spondyloarthritis (Part II): Validation and Final Selection," *Annals of the Rheumatic Diseases* 68, no. 6 (2009): 777–783, https://doi.org/10.1136/ARD.2009.108233.

9. S. Ramiro, E. Nikiphorou, A. Sepriano, et al., "ASAS-EULAR Recommendations for the Management of Axial Spondyloarthritis: 2022 Update," *Annals of the Rheumatic Diseases* 82, no. 1 (2023): 19–34, https://doi.org/10.1136/ARD-2022-223296.

10. C. Lukas, R. Landewé, J. Sieper, et al., "Development of an ASAS-Endorsed Disease Activity Score (ASDAS) in Patients With Ankylosing Spondylitis," *Annals of the Rheumatic Diseases* 68, no. 1 (2009): 18–24, https://doi.org/10.1136/ARD.2008.094870.

11. H. Alkan, N. Yildiz, and F. Ardiç, "The Correlations Between Disease Specific Quality of Life, Short Form-36 and Clinical Variables in Patients With Ankylosing Spondylitis," *Archives of Rheumatology* 35, no. 4 (2020): 468–476, https://doi.org/10.46497/ARCHRHEUMATOL.2020.7750.

12. F. Wolfe, D. J. Clauw, M. A. Fitzcharles, et al., "2016 Revisions to the 2010/2011 Fibromyalgia Diagnostic Criteria," *Seminars in Arthritis and Rheumatism* 46, no. 3 (2016): 319–329, https://doi.org/10.1016/J.SEMARTHRIT.2016.08.012.

13. A. S. Zigmond and R. P. Snaith, "The Hospital Anxiety and Depression Scale," *Acta Psychiatrica Scandinavica* 67, no. 6 (1983): 361–370, https://doi.org/10.1111/J.1600-0447.1983.TB09716.X.

14. B. R. England, H. Sayles, T. R. Mikuls, D. S. Johnson, and K. Michaud, "Validation of the Rheumatic Disease Comorbidity Index," *Arthritis Care & Research* 67, no. 6 (2015): 865–872, https://doi.org/10.1002/ACR.22456.

15. M. Charlson, T. P. Szatrowski, J. Peterson, and J. Gold, "Validation of a Combined Comorbidity Index," *Journal of Clinical Epidemiology* 47, no. 11 (1994): 1245–1251, https://doi.org/10.1016/0895-4356(94)90129-5.

16. "The Development and Validation of a Radiographic Grading System for the Hip in Ankylosing Spondylitis: The Bath Ankylosing Spondylitis Radiology Hip Index," December 16, 2023, https://pubmed.ncbi.nlm.nih.gov/11128678/.

17. D. Van Der Heijde, J. Braun, A. Deodhar, et al., "Modified Stoke Ankylosing Spondylitis Spinal Score as an Outcome Measure to Assess the Impact of Treatment on Structural Progression in Ankylosing Spondylitis," *Rheumatology* 58, no. 3 (2019): 388–400, https://doi.org/10.1093/RHEUMATOLOGY/KEY128.

18. "Difficult-to-Treat Axial Spondyloarthritis is Associated With Psoriasis, Peripheral Involvement and Comorbidities: Results of an Observational Nationwide Study," February 23, 2025, https://pubmed.ncbi.nlm.nih.gov/37996127/.

19. G. Alp, H. Cinakli, İ. K. Aysin, D. Solmaz, and S. Akar, "Challenges and Insights in Managing Difficult-to-Treat Rheumatoid Arthritis: Real-World Clinical Perspectives," *Clinical and Experimental Rheumatology* 42, no. 7 (2024): 1398–1406, https://doi.org/10.55563/CLINEXPRHEUMATOL/NYU9ER.

20. M. Juárez, D. Benavent, V. Navarro-Compán, et al., "AB0897 Predictive Models to Forecast Difficult-to-Manage Axial Spondyloarthritis," *Annals of the Rheumatic Diseases* 83, no. S1 (2024): 1753–1754, https://doi.org/10.1136/ANNRHEUMDIS-2024-EULAR.6232.

21. H. Y. Chung, P. Machado, D. Van Der Heijde, M. A. D'Agostino, and M. Dougados, "Smokers in Early Axial Spondyloarthritis Have Earlier Disease Onset, More Disease Activity, Inflammation and Damage, and Poorer Function and Health-Related Quality of Life: Results From the DESIR Cohort," *Annals of the Rheumatic Diseases* 71, no. 6 (2012): 809–816, https://doi.org/10.1136/ANNRHEUMDIS-2011-200180.

Supporting Information

Additional supporting information can be found online in the Supporting Information section. **Tables S1–S2:** apl70558-sup-0001-TableS1-S2.docx.

International Journal of Rheumatic Diseases

WILEY

International Journal of Rheumatic Diseases

LETTER TO THE EDITOR

Letter to the Editor: Short-Term Effectiveness of Sulfasalazine and Tofacitinib in NSAID-Refractory Reactive Arthritis

Garzeen Ghaffar[1] | Ahmad Furqan Anjum[2]

[1]Fatima Jinnah Medical University, Lahore, Punjab, Pakistan | [2]Shaikh Khalifa Bin Zayed Al-Nahyan Medical College, Shaikh Zayed Postgraduate Medical Institute (SZPGMI), Lahore, Punjab, Pakistan

Correspondence: Garzeen Ghaffar (garzeen.ghaffar@gmail.com)

Received: 29 August 2025 | **Revised:** 29 August 2025 | **Accepted:** 28 January 2026

To the Editor,

We read with great interest the article by Mruthyunjaya et al. [1], titled "Short-Term Effectiveness of Sulfasalazine and Tofacitinib in NSAID-Refractory Reactive Arthritis", published in the *International Journal of Rheumatic Diseases*. The authors should be acknowledged for addressing this clinically essential but understudied topic and providing vital data on therapy options in individuals with NSAID-refractory reactive arthritis. Their efforts to carefully evaluate the short-term effects of sulfasalazine and tofacitinib in a real-world population are timely and valuable. However, despite the significant insights this study gives, we believe it has the following limitations that deserve consideration.

First, only 46 patients completed the study, all from a single hospital in India. This reduces the ability to generalize results to other populations. Results might not represent broader, more diverse patient groups. Rare adverse effects or subgroup responses may have been missed. A study found a significant difference in treatment effect estimates between single- and multi-center trials, suggesting that the evidence from single-center trials tends to exaggerate treatment effects [2]. Future research should be multi-center and recruit larger, more diverse cohorts.

Second, the study uses a short follow-up duration of 12 weeks. However, reactive arthritis can become chronic; short follow-up may miss long-term relapse or side effects. Although estimates vary greatly, it is believed that 30%–50% of all instances of ReA become chronic, and the remainder recover autonomously within weeks to months [3]. Therefore, future studies should include follow-up of at least 6–12 months to determine the sustained benefits and better long-term safety of each drug.

Third, while the authors acknowledge not ruling out Chlamydia-induced arthritis, they do not address the lack of stratification by other identified or suspected pathogens. Because different infections can trigger arthritis through different pathways, they may also respond differently to treatment. By grouping all patients together without analyzing them separately (enteric vs. genitourinary triggers or culture-positive vs. culture-negative), the study may have blurred the true effectiveness of the drugs. A study suggests that a 6-month course of combination antibiotics appears to be a successful therapy for persistent Chlamydia-induced ReA [4]. Future research should go beyond simply excluding Chlamydia and should actively identify the specific organisms involved.

Fourth, allocation to SSZ (sulfasalazine) or TOF (tofacitinib) was observational, not randomized. Lack of blinding may influence subjective measures like pain, etc., influencing the reported outcomes. A systemic review and meta-analysis report that the trials without patient blinding may slightly exaggerate the desirable effects of treatment [5]. Future studies should use a randomized controlled design with blinded assessors to reduce the bias.

In conclusion, while this study adds useful evidence to the limited literature on the management of reactive arthritis, concerns about sample size, short follow-up, lack of stratification by causative organisms, and lack of blinding should be considered

when interpreting the results. We expect that future research will address these concerns through larger, multi-center randomized controlled trials with longer follow-up and pathogen-specific analyses, ultimately offering more reliable guidance for physicians.

Author Contributions

Ahmed Furqan Anjum conceived the idea and reviewed the original article. Garzeen Ghaffar performed the literature search, drafted the manuscript, and reviewed and approved the final version of the article.

Acknowledgments

The authors have nothing to report.

Funding

The authors have nothing to report.

Conflicts of Interest

The authors declare no conflicts of interest.

Data Availability Statement

The authors have nothing to report.

Garzeen Ghaffar
Ahmad Furqan Anjum

References

1. P. Mruthyunjaya, D. Maikap, S. Ahmed, R. Misra, and P. Padhan, "Short-Term Effectiveness of Sulfasalazine and Tofacitinib in NSAID-Refractory Reactive Arthritis: An Observational Study," *International Journal of Rheumatic Diseases* 28, no. 7 (2025): e70370.

2. S. Unverzagt, R. Prondzinsky, and F. Peinemann, "Single-Center Trials Tend to Provide Larger Treatment Effects Than Multicenter Trials: A Systematic Review," *Journal of Clinical Epidemiology* 66, no. 11 (2013): 1271–1280.

3. J. D. Carter, "Treating Reactive Arthritis: Insights for the Clinician," *Therapeutic Advances in Musculoskeletal Disease* 2, no. 1 (2010): 45–54.

4. J. D. Carter, L. R. Espinoza, R. D. Inman, et al., "Combination Antibiotics as a Treatment for Chronic Chlamydia-Induced Reactive Arthritis: A Double-Blind, Placebo-Controlled, Prospective Trial," *Arthritis and Rheumatism* 62, no. 5 (2010): 1298–1307.

5. T. Pitre, S. Kirsh, T. Jassal, et al., "The Impact of Blinding on Trial Results: A Systematic Review and Meta-Analysis," *Cochrane Evidence Synthesis and Methods* 1, no. 4 (2023): e12015.

International Journal of Rheumatic Diseases

WILEY

International Journal of Rheumatic Diseases

ORIGINAL ARTICLE

Effects of Immune Cells and Plasma Metabolites on Osteoarthritis: A Mediation Mendelian Randomization Study

Changfa Huang[1] | Hao Fan[2] | Zhifa Zheng[2,3] | Wenjing Ma[2] | Ze Wei[2] | Huitian Han[1] | Annan Liang[1] | Xuemeng Mu[1] | Wei Zou[1] | Jing Hao[2] | Fei Liu[2] | Lijin Liu[2] | Su Liu[2] | Lina Zhao[2,3] | Zhihong Wu[2,3]

[1]Department of Orthopedic Surgery, Peking Union Medical College Hospital, Peking Union Medical College and Chinese Academy of Medical Sciences, Beijing, China | [2]Stem Cell Facility, Institute of Clinical Medicine, Peking Union Medical College Hospital, Peking Union Medical College and Chinese Academy of Medical Sciences, Beijing, China | [3]State Key Laboratory of Complex Severe and Rare Diseases, Peking Union Medical College Hospital, Peking Union Medical College and Chinese Academy of Medical Sciences, Beijing, China

Correspondence: Lina Zhao (zhaolina19921125@163.com) | Zhihong Wu (wuzh3000@126.com)

Received: 21 December 2024 | **Revised:** 7 March 2025 | **Accepted:** 4 October 2025

Keywords: causal relationships | immune cells | Mendelian randomization | osteoarthritis | plasma metabolites

ABSTRACT

Objective: Recent studies suggest that immune cells and plasma metabolites may play significant roles in osteoarthritis pathogenesis. However, the causal relationships between these factors and osteoarthritis are unclear.

Methods: Based on the genome-wide association study (GWAS) database, 731 immune cell phenotypes and 1400 metabolites were evaluated for their possible mediating effects on osteoarthritis via two-step Mendelian randomization (MR). Sensitivity analyses were conducted to assess the robustness of our findings.

Results: Our findings revealed that 17 immune cell phenotypes were positively associated with osteoarthritis, suggesting their potential as risk factors. Conversely, 23 immune cell phenotypes exhibited a negative association, indicating possible protective roles against osteoarthritis. Furthermore, we identified 51 metabolites as potential risk factors for osteoarthritis. Conversely, 34 metabolites were deemed protective factors. Notably, 49 plasma metabolites partially mediated the relationship between 35 immune cell phenotypes and osteoarthritis, with leucine levels showing the highest mediation proportion (19.3%) between HLA DR+ CD4+ %lymphocytes and osteoarthritis.

Conclusion: Our study revealed a substantial impact of specific immune cell phenotypes and plasma metabolites on the progression of osteoarthritis, enhancing the understanding of the complex interplay between immunity and metabolism in osteoarthritis pathogenesis. Further research is necessary to clarify the underlying mechanisms driving these associations.

1 | Introduction

Osteoarthritis is a prevalent and debilitating musculoskeletal disease characterized by the degeneration of joint cartilage and the underlying bone, leading to significant discomfort and functional impairment [1]. It is a significant contributor to pain and disability among older adults worldwide, affecting their quality of life and daily activities [2]. According to recent estimates, osteoarthritis affects more than 240 million people globally, with the knee joint being the most frequently

Abbreviations: GWAS, genome-wide association study; IVW, inverse variance weighted; MMP, matrix-degrading metalloproteinase; MR, Mendelian randomization; SNP, single-nucleotide polymorphism.

Changfa Huang, Hao Fan, and Zhifa Zheng contributed equally to this work and shared first authorship.

affected area [2–4]. The incidence of osteoarthritis tends to increase with increasing age, and it is notably more prevalent in women, highlighting a sex disparity in its occurrence [5, 6]. Given its high prevalence and the substantial burden it places on individuals and health care systems, current treatment options for osteoarthritis focus primarily on managing pain and enhancing joint function [4, 7]. This focus on symptomatic relief emphasizes the pressing need for innovative therapeutic strategies to more effectively address the underlying causes of osteoarthritis and improve the overall management of this chronic condition.

Recent studies have suggested that immune cells may play a pivotal role in the complex pathogenesis of osteoarthritis [8–11]. Synovial inflammation, characterized by the infiltration of various immune cells, including macrophages and T cells, has been observed in joints affected by osteoarthritis [12–14]. These findings suggest that immune cells could serve as potential therapeutic targets for the treatment and management of osteoarthritis. However, despite the promising implications of these studies, the specific types of immune cells involved and their precise roles in the multifaceted process of osteoarthritis pathogenesis remain unclear and warrant further investigation to fully understand their contributions to the disease.

Emerging evidence indicates that, in addition to immune cells, various metabolic factors may play a significant role in the development of osteoarthritis [15–17]. Plasma metabolites, which are small molecules that participate in numerous metabolic processes within the body, have been implicated in various diseases, including osteoarthritis [18]. A particular study conducted on a cohort of middle-aged and elderly individuals in China revealed that several plasma metabolites were correlated with the severity of knee osteoarthritis, suggesting that these metabolites might serve as biomarkers for disease progression [19]. These metabolites could influence the pathogenesis of osteoarthritis by modulating the function of immune cells or exerting direct effects on the tissues within the joints themselves. Nevertheless, the causal relationships among immune cells, plasma metabolites, and the development of osteoarthritis have yet to be fully explored, leaving a significant gap in our understanding of how these factors interact and contribute to the disease process.

Traditional observational studies, while valuable in many respects, are often hampered by the presence of confounding factors and the issue of reverse causation, which together create significant challenges in establishing clear and definitive causal relationships between various exposures and their corresponding outcomes. In contrast, Mendelian randomization (MR) has emerged as a powerful and innovative analytical approach that leverages genetic variants as instrumental variables, thereby allowing researchers to explore causality between exposures and outcomes with greater clarity and precision [20]. This methodology effectively mitigates the biases associated with confounding and reverse causation, making it a robust tool for causal inference. MR has been successfully employed in a variety of contexts to investigate the causal relationships among numerous risk factors and diseases, including osteoarthritis [21]. By utilizing genetic data, MR can furnish more substantial and reliable evidence for causal inference, which is crucial for identifying potential therapeutic targets that could lead to improved treatment strategies.

In this study, we aimed to rigorously evaluate the causal effects of immune cells on the development and progression of osteoarthritis while also investigating the mediating role that plasma metabolites may play in this intricate relationship. By employing MR methodology, we intend to uncover new and promising treatment targets for osteoarthritis, thereby enhancing our overall comprehension of its complex pathogenesis and facilitating the development of more efficacious treatment strategies.

2 | Materials and Methods

2.1 | Study Design

We comprehensively evaluated the overall impact of 731 immune cells on osteoarthritis via MR. Reverse Mendelian randomization was used to exclude the reverse causal relationship, whereas the inverse variance weighted (IVW) method was employed to filter immune cells as the outcome factor. Employing two-step MR, we explored the substantial mediatory impact of 1400 plasma metabolites on the causative relationship between immune cells and osteoarthritis (Figure 1).

2.2 | Data Sources

Genetic information related to osteoarthritis was downloaded from the GWAS database (https://gwas.mrcieu.ac.uk/). The selected dataset, ukb-b-14486, contains 462 933 samples of European ancestry, including 38 472 osteoarthritis cases and 424 461 control samples. We obtained additional genetic data on 731 immune cell phenotypes from a cohort study involving 3757 Europeans [22]. In addition, genetic data associated with 1400 plasma metabolites from a cohort study involving 8299 Europeans were used [23].

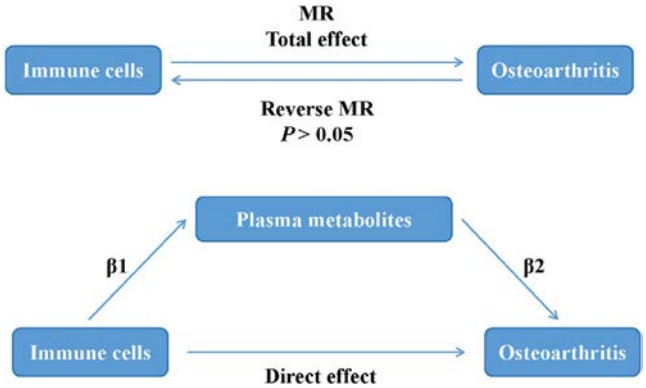

FIGURE 1 | Flowchart. The flowchart illustrates the study design using Mendelian randomization (MR) to evaluate the role of plasma metabolites as mediators in the causal relationship between immune cells and osteoarthritis (OA). It outlines the total effects of immune cells, the mediation analysis through metabolites, and the assessment of direct effects on OA. Reverse MR analysis is included to exclude reverse causation.

2.3 | Selection of Instrumental Variables

First, we applied a strict threshold of $p < 1 \times 10^{-5}$ to obtain single-nucleotide polymorphisms (SNPs) to ensure the reliability of our results. We subsequently refined our selection by screening for linkage disequilibrium with a strict $R^2 < 0.001$ and Kb = 10000. In addition, we calculated F statistics, excluding SNPs with F statistics less than 10 to mitigate the effect of weak instrumental variables on the results.

2.4 | Statistical Analysis

MR analysis was conducted via five methods: IVW, MR–Egger regression, the weighted model, the weighted median, and the simple model. To guarantee the precision and reliability of our findings, we used IVW as the primary approach, and the directions of the odds ratios (ORs) derived from all five MR methods were required to be consistent. The variability among instrumental variables was assessed using Cochran's Q statistic. To evaluate the presence of horizontal pleiotropy, the MR pleiotropic test was employed for MR–Egger regression, with the intercept value being calculated accordingly [24]. Additionally, we evaluated the overall impact of immune cells on osteoarthritis (β0) and their influence on certain metabolites (β1) and investigated how these metabolites may further facilitate osteoarthritis pathogenesis (β2). In this way, we calculated the mediating effect (β1 × β2) and the mediating proportion as the percentage of the mediating effect (β1 × β2) over the total effect (β0). $p < 0.05$ was considered statistically significant. All statistical calculations were performed using R version 4.4.1 and the TwoSampleMR package version 0.5.7.

3 | Results

3.1 | Causal Effects of Immune Cells on Osteoarthritis

We identified 41 immune cell phenotypes associated with osteoarthritis, including IgD+ CD24+ %B cells, activated and resting Treg %CD4+ T cells, CD45RA− CD4+ %T cells, and lymphocyte %leukocytes (Figure 2; Table 1; Table S1). In addition, we performed tests for pleiotropy and heterogeneity (Table 1; Tables S2 and S3). Forest plots, funnel plots, scatter plots, and leave-one-out plots visually confirmed the consistency and reliability of the causal relationships (Figures S1–S4).

In the subsequent reverse MR analysis, we included osteoarthritis as the exposure condition and 41 immune cell phenotypes as the outcome. The analysis revealed that osteoarthritis was significantly associated with CD40 expression on CD14− CD16+ monocytes ($p < 0.05$). No evidence of reverse causality was found between osteoarthritis and the other 40 immune cell phenotypes ($p > 0.05$) (Table S4). Among them, 17 immune cell phenotypes were positively correlated with osteoarthritis, suggesting that they may be potential risk factors for osteoarthritis. Twenty-three immune cell phenotypes were negatively correlated with osteoarthritis, suggesting a potential protective effect against osteoarthritis.

3.2 | Causal Effects of Metabolites on Osteoarthritis

Through rigorous analysis, we initially identified 85 osteoarthritis-associated plasma metabolites, including 12 previously uncharacterized metabolites (Figure 3; Table S5). Among the known metabolites, 51 were potential risk factors for osteoarthritis, including but not limited to 3-hydroxypyridine sulfate levels, argininate levels, *N*-acetylneuraminate levels, the phosphate-to-tryptophan ratio, heptenedioate (C7:1-DC) levels, and the glutamate-to-alanine ratio. In contrast, 34 metabolites were potential protective factors for osteoarthritis, including suberate (C8-DC) levels, 3-phenylpropionate hydrocinnamate levels, 3-hydroxymyristate levels, gamma-glutamylthreonine levels, and cysteine-glutathione disulfide levels. The stability of causal associations was further confirmed by pleiotropic and heterogeneous effect testing (Table 2; Tables S6 and S7). The visualization of forest plots, funnel plots, scatter plots, and leave-one-out plots provided additional evidence for the consistency of the observed causal effects (Figures S5–S8).

3.3 | Mendelian Randomization Analysis of Mediators

After careful screening, we identified 40 immune cell phenotypes as exposure factors and 85 plasma metabolites as outcome variables. We subsequently performed a rigorous MR analysis to investigate the effects of the immune cell phenotype on metabolites. The results demonstrated the effect size of immune cell phenotypes on metabolites (β1), which provided strong support for our further understanding of their associations. We defined 85 plasma metabolites as exposure factors and osteoarthritis as the outcome variable. Based on this framework, we performed MR analysis and obtained robust results that validated the specific effect size of metabolites on osteoarthritis (β2). We subsequently calculated the overall effect of immune cells on osteoarthritis (Table S8).

3.4 | Analysis of Mediation

The mediation analysis identified 49 plasma metabolites that partially mediated the relationships between 35 immune cell phenotypes and osteoarthritis (Table 3). The full mediation analyses are provided in Table S8. Among these pathways, leucine demonstrated the highest mediation (19.3%) between HLA DR+ CD4+ %lymphocytes and osteoarthritis, with the most significant negative mediation effect. Similarly, the taurine-to-glutamate ratio showed strong mediation across multiple pathways, contributing an 18.8% mediation proportion between CD20 on IgD-CD38br lymphocytes and osteoarthritis and an 18.5% mediation proportion between SSC-A on monocytes and osteoarthritis. Overall, these findings provide robust evidence for the mediating role of plasma metabolites in linking immune cell phenotypes to osteoarthritis pathogenesis.

exposure	outcome	nsnp	method	pval	OR(95% CI)
Xanthurenate levels	osteoarthritis	25	Inverse variance weighted	**0.021**	1.004 (1.001 to 1.008)
Suberate (C8-DC) levels	osteoarthritis	22	Inverse variance weighted	**0.030**	0.996 (0.993 to 1.000)
3-phenylpropionate hydrocinnamate levels	osteoarthritis	22	Inverse variance weighted	**<0.001**	0.995 (0.991 to 0.998)
3-hydroxymyristate levels	osteoarthritis	19	Inverse variance weighted	**0.023**	0.995 (0.991 to 0.999)
Butyrylglycine levels	osteoarthritis	20	Inverse variance weighted	**0.002**	1.003 (1.001 to 1.005)
Stearoylcarnitine levels	osteoarthritis	21	Inverse variance weighted	**0.031**	1.003 (1.000 to 1.006)
Gamma-glutamylthreonine levels	osteoarthritis	35	Inverse variance weighted	**0.042**	0.997 (0.994 to 1.000)
1-stearoyl-GPG (18:0) levels	osteoarthritis	24	Inverse variance weighted	**0.017**	1.003 (1.001 to 1.006)
Cysteine-glutathione disulfide levels	osteoarthritis	26	Inverse variance weighted	**0.038**	0.997 (0.995 to 1.000)
1-linoleoyl-GPE (18:2) levels	osteoarthritis	33	Inverse variance weighted	**0.019**	0.997 (0.995 to 1.000)
Octadecanedioate levels	osteoarthritis	25	Inverse variance weighted	**0.045**	1.003 (1.000 to 1.006)
Androstenediol (3beta,17beta) disulfate (1) levels	osteoarthritis	30	Inverse variance weighted	**0.006**	0.997 (0.994 to 0.999)
Cysteinylglycine disulfide levels	osteoarthritis	17	Inverse variance weighted	**0.018**	0.996 (0.992 to 0.999)
Argininate levels	osteoarthritis	23	Inverse variance weighted	**0.020**	1.006 (1.001 to 1.012)
Ferulic acid 4-sulfate levels	osteoarthritis	33	Inverse variance weighted	**0.007**	1.003 (1.001 to 1.006)
3-(3-hydroxyphenyl)propionate sulfate levels	osteoarthritis	19	Inverse variance weighted	**0.035**	0.997 (0.994 to 1.000)
4-hydroxychlorothalonil levels	osteoarthritis	22	Inverse variance weighted	**0.002**	0.995 (0.993 to 0.998)
3-hydroxypyridine sulfate levels	osteoarthritis	22	Inverse variance weighted	**0.007**	1.007 (1.002 to 1.011)
Octadecanedioylcarnitine (C18-DC) levels	osteoarthritis	25	Inverse variance weighted	**0.033**	1.002 (1.000 to 1.005)
Ethylparaben sulfate levels	osteoarthritis	15	Inverse variance weighted	**0.019**	1.004 (1.001 to 1.008)
Sphingomyelin (d18:1/20:0, d16:1/22:0) levels	osteoarthritis	23	Inverse variance weighted	**0.016**	1.004 (1.001 to 1.007)
Sphingomyelin (d18:1/22:1, d18:2/22:0, d16:1/24:1) levels	osteoarthritis	20	Inverse variance weighted	**0.023**	1.004 (1.001 to 1.007)
N-acetylglucosamine/n-acetylgalactosamine levels	osteoarthritis	17	Inverse variance weighted	**0.024**	0.997 (0.994 to 1.000)
5-hydroxyindole sulfate levels	osteoarthritis	17	Inverse variance weighted	**0.010**	0.996 (0.992 to 0.999)
Sphingomyelin (d18:1/19:0, d19:1/18:0) levels	osteoarthritis	23	Inverse variance weighted	**<0.001**	1.005 (1.003 to 1.008)
Linolenoylcarnitine (C18:3) levels	osteoarthritis	22	Inverse variance weighted	**0.022**	1.004 (1.001 to 1.007)
Cerotoylcarnitine (C26) levels	osteoarthritis	28	Inverse variance weighted	**0.026**	1.003 (1.000 to 1.005)
Docosahexaenoylcarnitine (C22:6) levels	osteoarthritis	26	Inverse variance weighted	**0.023**	1.004 (1.001 to 1.007)
Arachidonoylcarnitine (C20:4) levels	osteoarthritis	34	Inverse variance weighted	**0.001**	1.003 (1.001 to 1.005)
5-dodecenoylcarnitine (C12:1) levels	osteoarthritis	24	Inverse variance weighted	**0.019**	0.996 (0.993 to 0.999)
(N(1) + N(8))-acetylspermidine levels	osteoarthritis	36	Inverse variance weighted	**0.022**	1.002 (1.000 to 1.005)
Heptenedioate (C7:1-DC) levels	osteoarthritis	16	Inverse variance weighted	**0.024**	1.006 (1.001 to 1.010)
Gamma-glutamylcitrulline levels	osteoarthritis	26	Inverse variance weighted	**0.046**	0.997 (0.994 to 1.000)
N-lactoyl isoleucine levels	osteoarthritis	15	Inverse variance weighted	**0.028**	1.005 (1.001 to 1.009)
5-hydroxymethyl-2-furoylcarnitine levels	osteoarthritis	22	Inverse variance weighted	**0.044**	0.997 (0.994 to 1.000)
3-bromo-5-chloro-2,6-dihydroxybenzoic acid levels	osteoarthritis	27	Inverse variance weighted	**0.016**	0.996 (0.993 to 0.999)
Bilirubin degradation product, C16H18N2O5 (4) levels	osteoarthritis	16	Inverse variance weighted	**0.030**	1.002 (1.000 to 1.004)
2-methoxyhydroquinone sulfate (2) levels	osteoarthritis	19	Inverse variance weighted	**0.024**	1.003 (1.000 to 1.007)
N-acetylvaline levels	osteoarthritis	19	Inverse variance weighted	**0.014**	0.995 (0.991 to 0.999)
Methyl indole-3-acetate levels	osteoarthritis	22	Inverse variance weighted	**0.003**	1.005 (1.002 to 1.008)
N-acetylneuraminate levels	osteoarthritis	30	Inverse variance weighted	**<0.001**	1.006 (1.003 to 1.009)
Cysteinylglycine levels	osteoarthritis	20	Inverse variance weighted	**0.029**	0.996 (0.993 to 1.000)
Leucine levels	osteoarthritis	20	Inverse variance weighted	**0.005**	0.995 (0.991 to 0.998)
Serine levels	osteoarthritis	33	Inverse variance weighted	**0.021**	1.003 (1.000 to 1.005)
Plasma free asparagine levels	osteoarthritis	22	Inverse variance weighted	**0.030**	0.998 (0.996 to 1.000)
X-11858 levels	osteoarthritis	28	Inverse variance weighted	**0.005**	1.004 (1.001 to 1.006)
X-12283 levels	osteoarthritis	25	Inverse variance weighted	**0.042**	0.997 (0.994 to 1.000)
X-12104 levels	osteoarthritis	12	Inverse variance weighted	**0.005**	1.006 (1.002 to 1.010)
X-12707 levels	osteoarthritis	28	Inverse variance weighted	**0.042**	0.997 (0.993 to 1.000)
X-12906 levels	osteoarthritis	18	Inverse variance weighted	**0.013**	0.995 (0.992 to 0.999)
X-12839 levels	osteoarthritis	29	Inverse variance weighted	**0.004**	1.004 (1.001 to 1.006)
X-18886 levels	osteoarthritis	16	Inverse variance weighted	**0.037**	1.005 (1.000 to 1.010)
X-21467 levels	osteoarthritis	31	Inverse variance weighted	**0.045**	1.002 (1.000 to 1.005)
X-22162 levels	osteoarthritis	25	Inverse variance weighted	**0.041**	1.002 (1.000 to 1.004)
X-24757 levels	osteoarthritis	22	Inverse variance weighted	**0.023**	1.003 (1.000 to 1.006)
X-24949 levels	osteoarthritis	18	Inverse variance weighted	**0.004**	1.004 (1.001 to 1.007)
N-acetyl-L-glutamine levels	osteoarthritis	21	Inverse variance weighted	**0.047**	1.002 (1.000 to 1.004)
N-acetylarginine levels	osteoarthritis	24	Inverse variance weighted	**0.030**	1.002 (1.000 to 1.003)
3-methylcytidine levels	osteoarthritis	18	Inverse variance weighted	**0.026**	1.002 (1.000 to 1.004)
N-acetylcitrulline levels	osteoarthritis	19	Inverse variance weighted	**0.036**	1.002 (1.000 to 1.004)
N-acetyl-1-methylhistidine levels	osteoarthritis	31	Inverse variance weighted	**0.027**	1.002 (1.000 to 1.003)
N-delta-acetylornithine levels	osteoarthritis	24	Inverse variance weighted	**0.038**	0.998 (0.997 to 1.000)
Glycine levels	osteoarthritis	22	Inverse variance weighted	**0.014**	1.002 (1.000 to 1.004)
X-13431 levels	osteoarthritis	27	Inverse variance weighted	**0.044**	1.002 (1.000 to 1.004)
Glycine to alanine ratio	osteoarthritis	19	Inverse variance weighted	**0.012**	1.003 (1.001 to 1.005)
Glycine to serine ratio	osteoarthritis	25	Inverse variance weighted	**0.019**	1.002 (1.000 to 1.004)
Methionine to methionine sulfoxide ratio	osteoarthritis	24	Inverse variance weighted	**0.019**	0.996 (0.993 to 0.999)
Phosphate to glucose ratio	osteoarthritis	17	Inverse variance weighted	**0.049**	0.996 (0.992 to 1.000)
Alpha-tocopherol to sulfate ratio	osteoarthritis	18	Inverse variance weighted	**0.016**	0.996 (0.992 to 0.999)
Carnitine to ergothioneine ratio	osteoarthritis	21	Inverse variance weighted	**<0.001**	1.005 (1.002 to 1.008)
Glutamate to kynurenine ratio	osteoarthritis	23	Inverse variance weighted	**0.007**	1.004 (1.001 to 1.008)
Ornithine to glutamate ratio	osteoarthritis	18	Inverse variance weighted	**0.023**	0.996 (0.992 to 0.999)
Glycine to phosphate ratio	osteoarthritis	27	Inverse variance weighted	**0.036**	1.002 (1.000 to 1.004)
Adenosine 5'-monophosphate (AMP) to flavin adenine dinucleotide (FAD) ratio	osteoarthritis	17	Inverse variance weighted	**0.020**	1.004 (1.001 to 1.008)
Phosphate to tryptophan ratio	osteoarthritis	20	Inverse variance weighted	**0.007**	1.006 (1.002 to 1.010)
Adenosine 5'-monophosphate (AMP) to serine ratio	osteoarthritis	13	Inverse variance weighted	**0.011**	0.993 (0.988 to 0.998)
Cortisol to 4-cholesten-3-one ratio	osteoarthritis	19	Inverse variance weighted	**0.007**	1.005 (1.001 to 1.008)
Taurine to glutamate ratio	osteoarthritis	18	Inverse variance weighted	**0.001**	0.993 (0.989 to 0.997)
Hypotaurine to cysteine ratio	osteoarthritis	32	Inverse variance weighted	**0.041**	0.995 (0.991 to 1.000)
Tyrosine to pyruvate ratio	osteoarthritis	23	Inverse variance weighted	**0.010**	1.004 (1.001 to 1.008)
N-palmitoyl-sphingosine (d18:1 to 16:0) to N-stearoyl-sphingosine (d18:1 to 18:0) ratio	osteoarthritis	20	Inverse variance weighted	**0.046**	0.997 (0.993 to 1.000)
Glutamate to pyruvate ratio	osteoarthritis	25	Inverse variance weighted	**0.040**	1.004 (1.000 to 1.008)
Glutamate to alanine ratio	osteoarthritis	19	Inverse variance weighted	**0.004**	1.005 (1.002 to 1.009)
Histidine to alanine ratio	osteoarthritis	30	Inverse variance weighted	**0.012**	0.996 (0.994 to 0.999)
Alpha-ketobutyrate to 3-methyl-2-oxovalerate ratio	osteoarthritis	15	Inverse variance weighted	**0.034**	0.996 (0.992 to 1.000)

FIGURE 2 | Legend on next page.

FIGURE 2 | Forest plot of causality between 41 immune cells and osteoarthritis. This figure illustrates the causal associations between 41 immune cell phenotypes and osteoarthritis (OA), as identified through Mendelian randomization (MR) analysis. Each immune cell phenotype is represented along with its odds ratio (OR) and 95% confidence interval (CI), providing insights into whether it acts as a risk factor or protective factor for OA. The significant results ($p < 0.05$) highlight potential key immune cell phenotypes influencing OA pathogenesis. The inverse variance weighted (IVW) method was used for robust causal inference.

TABLE 1 | Partial MR analysis of immune cells and OA.

Exposure	Method	N_{snp}	Beta	SE	*p*	Pleiotropy	Heterogeneity
IgD+ CD24+ %B cells	IVW	19	−0.002	0.001	0.027	0.602	0.783
IgD+ CD24− %B cells	IVW	19	0.002	0.001	0.022	0.113	0.999
Activated and resting Treg %CD4+ T cells	IVW	26	0.001	0.001	0.029	0.332	0.453
CD45RA− CD4+ %T cells	IVW	24	−0.001	0.001	0.045	0.198	0.198
EM CD4+ activated T cells	IVW	22	0.001	0.000	0.047	0.919	0.687
CM DN (CD4−CD8−) %DN T cells	IVW	16	0.002	0.001	0.043	0.607	0.197
Lymphocyte %leukocytes	IVW	21	−0.001	0.001	0.042	0.515	0.273
DP (CD4+ CD8+) %leukocytes	IVW	20	0.002	0.001	0.044	0.505	0.837
HLA DR+ CD4+ %T cells	IVW	24	−0.002	0.001	0.012	0.447	0.908
HLA DR+ CD4+ %lymphocytes	IVW	18	−0.002	0.001	0.023	0.324	0.826

Note: This table summarizes the partial MR analysis results, showing causal links between immune cell phenotypes and osteoarthritis (OA). Significant associations ($p < 0.05$) revealed immune cells as potential risk factors or protective agents, with robust findings supported by minimal pleiotropy and heterogeneity.

4 | Discussion

This study aimed to evaluate the causal relationship between immune cells and osteoarthritis and to investigate the mediating role of plasma metabolites in this process. The findings revealed a significant impact of immune cells on osteoarthritis and identified specific plasma metabolites that mediate this effect. These results highlight potential therapeutic targets for osteoarthritis through the modulation of immune cell activity and associated metabolic pathways.

Our findings are consistent with those of previous studies emphasizing the critical role of immune cells in the pathogenesis of osteoarthritis. Zhang et al. [25], for example, identified macrophages, mast cells, memory CD4+ T cells, and B cells as the predominant immune cell populations in osteoarthritic synovial tissue, highlighting substantial immune infiltration in osteoarthritis. Similarly, Liu et al. [26] demonstrated the involvement of natural killer cells, CD4+ T cells, macrophages, and dendritic cells in the immune processes underlying osteoarthritis. Our study builds upon these findings by identifying immune cell phenotypes that are either positively or negatively correlated with OA, suggesting that some immune cells may act as risk factors, whereas others may serve as protective factors. For example, Teng et al. [27] identified specific immune cell phenotypes associated with osteoarthritis. These findings revealed a positive association between CD64 expression on CD14−CD16+ monocytes and hip osteoarthritis, with an odds ratio (OR) of 1.0593. In line with these findings, our study demonstrated a statistically significant positive association between CD64 expression on CD14−CD16+ monocytes and osteoarthritis ($p = 0.008$). In support of these observations, Teunissen van Manen et al. conducted synovial biopsies on numerous end-stage osteoarthritis patients and revealed that CD64 expression in synovial tissue is closely linked to the expression of various proinflammatory cytokines, matrix-degrading metalloproteinases (MMPs), and alarmins. Specifically, CD64 is associated with elevated levels of MMP1, MMP3, MMP9, and MMP13, as well as the proinflammatory cytokines IL-1β and IL-6 and the alarmin S100A9 [28]. This finding aligns with findings from rheumatoid arthritis, where CD64 is markedly upregulated on inflammatory macrophages, contributing to joint inflammation through similar inflammatory and tissue-degrading mechanisms [29]. Together, these studies suggest that targeting CD64+ immune cells may help attenuate the inflammation and tissue degradation associated with OA, potentially offering a novel therapeutic approach.

Our study also revealed a unique reverse causal relationship between CD40 expression on CD14−CD16+ monocytes and osteoarthritis, suggesting that the process of osteoarthritis itself may influence immune cell phenotypes rather than immune activation solely to drive disease progression. This finding highlights the dynamic interplay between joint degeneration and systemic inflammation, where osteoarthritis may modulate CD40 expression as part of a feedback mechanism, potentially impacting monocyte function. CD40 is implicated in the pathogenesis of rheumatoid arthritis, a condition with similarities to osteoarthritis, through the CD40–CD40L axis, which influences T-cell responses, B-cell autoantibody production, and cytokine secretion [30]. Understanding this bidirectional interaction could open new avenues for therapeutic strategies targeting the CD40 signaling axis, with implications for both osteoarthritis and its systemic effects.

exposure	outcome	nsnp	method	pval	OR(95% CI)
IgD+ CD24+ %B cell	osteoarthritis	19	Inverse variance weighted	**0.027**	0.998 (0.996 to 1.000)
IgD+ CD24− %B cell	osteoarthritis	19	Inverse variance weighted	**0.022**	1.002 (1.000 to 1.003)
Activated & resting Treg %CD4+	osteoarthritis	26	Inverse variance weighted	**0.029**	1.001 (1.000 to 1.002)
CD45RA− CD4+ %T cell	osteoarthritis	24	Inverse variance weighted	**0.045**	0.999 (0.998 to 1.000)
EM CD4+ AC	osteoarthritis	22	Inverse variance weighted	**0.047**	1.001 (1.000 to 1.002)
CM DN (CD4−CD8−) %DN	osteoarthritis	16	Inverse variance weighted	**0.043**	1.002 (1.000 to 1.004)
Lymphocyte %leukocyte	osteoarthritis	21	Inverse variance weighted	**0.042**	0.999 (0.997 to 1.000)
DP (CD4+CD8+) %leukocyte	osteoarthritis	20	Inverse variance weighted	**0.044**	1.002 (1.000 to 1.004)
HLA DR+ CD4+ %T cell	osteoarthritis	24	Inverse variance weighted	**0.012**	0.998 (0.996 to 1.000)
HLA DR+ CD4+ %lymphocyte	osteoarthritis	18	Inverse variance weighted	**0.023**	0.998 (0.996 to 1.000)
CD28− DN (CD4−CD8−) %DN	osteoarthritis	26	Inverse variance weighted	**0.022**	1.002 (1.000 to 1.003)
CD28+ DN (CD4−CD8−) %DN	osteoarthritis	26	Inverse variance weighted	**0.022**	0.998 (0.997 to 1.000)
BAFF−R on memory B cell	osteoarthritis	15	Inverse variance weighted	**0.043**	0.999 (0.998 to 1.000)
CD19 on CD20− CD38−	osteoarthritis	20	Inverse variance weighted	**0.043**	1.002 (1.000 to 1.003)
CD20 on IgD+ CD24+	osteoarthritis	23	Inverse variance weighted	**0.044**	0.998 (0.996 to 1.000)
CD20 on IgD+ CD24−	osteoarthritis	23	Inverse variance weighted	**0.013**	0.999 (0.998 to 1.000)
CD20 on IgD+ CD38dim	osteoarthritis	28	Inverse variance weighted	**0.003**	0.998 (0.997 to 0.999)
CD20 on IgD− CD38br	osteoarthritis	14	Inverse variance weighted	0.050	1.001 (1.000 to 1.002)
CD20 on IgD+	osteoarthritis	19	Inverse variance weighted	**0.010**	0.998 (0.996 to 0.999)
CD20 on transitional	osteoarthritis	24	Inverse variance weighted	**0.008**	0.998 (0.997 to 0.999)
CD25 on IgD− CD38−	osteoarthritis	21	Inverse variance weighted	**0.048**	1.001 (1.000 to 1.002)
CD27 on CD20−	osteoarthritis	15	Inverse variance weighted	**0.045**	1.002 (1.000 to 1.003)
CD38 on IgD+	osteoarthritis	14	Inverse variance weighted	**0.022**	1.003 (1.000 to 1.006)
IgD on unsw mem	osteoarthritis	19	Inverse variance weighted	**0.018**	1.002 (1.000 to 1.004)
IgD on IgD+	osteoarthritis	19	Inverse variance weighted	**0.037**	1.002 (1.000 to 1.003)
CD3 on NKT	osteoarthritis	16	Inverse variance weighted	**0.024**	0.998 (0.996 to 1.000)
HVEM on CD8br	osteoarthritis	16	Inverse variance weighted	**0.006**	0.998 (0.997 to 0.999)
CD127 on CD28− CD8br	osteoarthritis	18	Inverse variance weighted	**0.012**	1.002 (1.001 to 1.004)
CD25 on activated Treg	osteoarthritis	16	Inverse variance weighted	**0.028**	0.998 (0.995 to 1.000)
CD25 on secreting Treg	osteoarthritis	13	Inverse variance weighted	**0.031**	0.999 (0.997 to 1.000)
CD33 on CD33br HLA DR+ CD14−	osteoarthritis	21	Inverse variance weighted	**0.037**	0.999 (0.998 to 1.000)
CD4 on monocyte	osteoarthritis	15	Inverse variance weighted	**0.007**	0.998 (0.996 to 0.999)
FSC−A on myeloid DC	osteoarthritis	19	Inverse variance weighted	**0.023**	0.999 (0.998 to 1.000)
CD40 on CD14− CD16+ monocyte	osteoarthritis	24	Inverse variance weighted	**0.017**	1.001 (1.000 to 1.002)
CD64 on CD14− CD16+ monocyte	osteoarthritis	19	Inverse variance weighted	**0.008**	1.003 (1.001 to 1.005)
CD4 on CD45RA+ CD4+	osteoarthritis	26	Inverse variance weighted	**0.039**	0.999 (0.997 to 1.000)
CD45 on CD33dim HLA DR+ CD11b−	osteoarthritis	8	Inverse variance weighted	**0.008**	0.997 (0.994 to 0.999)
CD4 on CD39+ activated Treg	osteoarthritis	22	Inverse variance weighted	**0.035**	0.999 (0.998 to 1.000)
SSC−A on monocyte	osteoarthritis	21	Inverse variance weighted	**0.007**	0.998 (0.997 to 1.000)
SSC−A on HLA DR+ T cell	osteoarthritis	21	Inverse variance weighted	**0.045**	1.002 (1.000 to 1.004)
CD11b on CD14+ monocyte	osteoarthritis	20	Inverse variance weighted	**0.025**	1.001 (1.000 to 1.002)

FIGURE 3 | Forest plot of causality between 85 plasma metabolites and osteoarthritis. This figure depicts the causal relationships between 85 plasma metabolites and osteoarthritis (OA) identified through Mendelian randomization (MR) analysis. Each metabolite is displayed with its corresponding odds ratio (OR) and 95% confidence interval (CI), indicating its role as a potential risk factor or protective factor for OA. Statistically significant associations ($p < 0.05$) are emphasized, providing insights into the metabolic pathways contributing to OA pathogenesis. The analysis was performed using the inverse variance weighted (IVW) method for robust causal estimation.

Additionally, research into the blood plasma metabolites of osteoarthritis patients has garnered considerable attention because of its potential to identify novel biomarkers and shed light on the pathophysiology of this disease. A systematic review and meta-analysis [31] identified 132 small-molecule metabolites that were differentially expressed in osteoarthritis patients compared with healthy controls. Notably, amino acids and their derivatives, including tryptophan, lysine, and proline, have been highlighted as promising biomarkers for osteoarthritis diagnosis and progression monitoring [32]. In line with these findings, our study demonstrated a statistically significant positive correlation between *N*-acetylarginine levels and osteoarthritis ($p = 0.03$), reinforcing its relevance as a potential biomarker. Further investigations by Fu et al. [33] elucidated the role of *N*-acetylarginine in the pathogenesis of hip osteoarthritis. This study identified four critical metabolic pathways, including ethanol degradation, amino sugar metabolism, fatty acid biosynthesis, and aspartate metabolism, which are regulated by acetylarginine. These findings not only support our results but also provide a deeper understanding of how metabolic dysregulation contributes to the development of osteoarthritis. Importantly, *N*-acetylarginine has been identified as a key factor in the protective roles of CD25+ regulatory T cells, highlighting the potential for targeting metabolites in immune-modulatory therapies. Our analysis revealed that *N*-acetylarginine contributes to 4.8% of the documented protective effect, suggesting

TABLE 2 | Partial MR analysis of metabolites and OA.

Exposure	Method	N_{snp}	Beta	SE	*p*	Pleiotropy	Heterogeneity
Xanthurenate levels	IVW	25	0.004	0.002	0.021	0.941	0.020
Suberate (C8-DC) levels	IVW	22	−0.004	0.002	0.030	0.844	0.329
3-Phenylpropionate hydrocinnamate levels	IVW	22	−0.006	0.002	0.001	0.654	0.550
3-Hydroxymyristate levels	IVW	19	−0.005	0.002	0.023	0.705	0.149
Butyrylglycine levels	IVW	20	0.003	0.001	0.002	0.343	0.177
Stearoylcarnitine levels	IVW	21	0.003	0.002	0.031	0.668	0.325
Gamma-glutamylthreonine levels	IVW	35	−0.003	0.001	0.042	0.610	0.151
1-Stearoyl-GPG (18:0) levels	IVW	24	0.003	0.001	0.017	0.925	0.477
Cysteine-glutathione disulfide levels	IVW	26	−0.003	0.001	0.038	0.306	0.900
1-Linoleoyl-GPE (18:2) levels	IVW	33	−0.003	0.001	0.019	0.974	0.384

Note: This table summarizes the partial MR analysis results, showing causal links between metabolites and osteoarthritis (OA). Significant associations ($p < 0.05$) reveal metabolites as potential risk factors or protective agents, with robust findings supported by minimal pleiotropy and heterogeneity.

TABLE 3 | The top 10 mediated proportions in causal relationships.

Exposure	Metabolite	Outcome	Mediated effect	Mediated proportion (%)
HLA DR+ CD4+ %lymphocytes	Leucine levels	Osteoarthritis	−0.000417	19.30
CD20 on IgDCD38br lymphocytes	Taurine-to-glutamate ratio	Osteoarthritis	0.000186	18.80
SSC-A on monocytes	Taurine-to-glutamate ratio	Osteoarthritis	−0.000302	18.50
HLA DR+ CD4+ %T cells	Leucine levels	Osteoarthritis	−0.000377	18.20
IgD+ CD24− %B cells	Ethylparaben sulfate levels	Osteoarthritis	0.000268	17.60
CD25 on IgD− CD38−	5-Hydroxyindole sulfate levels	Osteoarthritis	0.000202	16.80
SSC-A on HLA DR+ T cells	*N*-acetylneuraminate levels	Osteoarthritis	0.00032	16.60
IgD+ CD24+ %B cells	Hypotaurine-to-cysteine ratio	Osteoarthritis	−0.00038	16.40
CM DN (CD4−CD8−) %DN	X-12839 levels	Osteoarthritis	0.000297	16.20
EM CD4+ AC	3-Phenylpropionate hydrocinnamate levels	Osteoarthritis	0.000154	16.10

Note: This table lists the top 10 mediation pathways between immune cell phenotypes and osteoarthritis (OA). Each pathway includes an immune cell (exposure), a metabolite mediator, and OA as the outcome. The mediated proportion represents the percentage of the immune cell's effect on OA explained by the metabolite, with leucine levels showing the highest mediation proportion (19.3%).

that targeting specific metabolites could enhance the efficacy of immune-modulatory strategies for osteoarthritis. The identification of *N*-acetylarginine as a crucial mediator of immune modulation underscores the need to incorporate metabolic pathways into osteoarthritis research. These findings extend beyond the activity of immune cells, offering a more integrative perspective of the disease, which is characterized by both immune and metabolic dysregulation. The robust correlation between *N*-acetylarginine and osteoarthritis progression, along with its mediating influence, indicates that targeting specific metabolic pathways could lead to new therapeutic opportunities. Through the lens of metabolites such as *N*-acetylarginine, we have an opportunity to increase the effectiveness of therapies aimed at balancing immune responses, potentially slowing disease progression and improving patient outcomes. This multidimensional approach, which integrates both immune and metabolic modulation, holds promise for developing a more comprehensive strategy for osteoarthritis management and aligns with current trends in personalized medicine and precision therapies.

Our findings revealed that leucine levels were associated with the highest mediation proportion (19.3%) between HLA DR+ CD4+ %lymphocytes and osteoarthritis. This discovery is supported by multiple experimental studies. Akhtar et al. [34] demonstrated that leucine inhibits inflammatory mediators in osteoarthritic chondrocytes while promoting cartilage repair genes, suggesting a chondroprotective role. Kim et al. [35] reported that leucine is essential for normal chondrocyte development, as its restriction inhibits proliferation and differentiation through both mTOR-dependent and mTOR-independent pathways. In support of the importance of leucine, Moon et al. [36] reported that a leucine zipper protein (SMILE) reduces cartilage

damage and OA biomarkers by modulating inflammatory signaling. Additionally, Tanaka et al. [37] reported that small leucine-rich proteoglycans (SLRPs) play a critical role in maintaining proper collagen fibril formation, with their reduced expression in OA cartilage contributing to matrix degradation. Together, these studies provide strong experimental evidence for the critical role of leucine in cartilage homeostasis and osteoarthritis pathophysiology. Importantly, clinical evidence supports the relevance of leucine in OA pathogenesis through multiple mechanisms. Satis et al. [38] conducted a clinical study revealing that serum leucine levels are the highest in healthy individuals and lowest in patients with severe OA, suggesting a negative correlation between leucine levels and OA severity. These findings indicate that leucine is potentially directly involved in cartilage metabolism and protection. Additionally, Park et al. [39] demonstrated the role of leucine in the musculoskeletal aspect of OA, showing that leucine-enriched amino acid supplementation improves muscle density and quality of life in patients with OA in the knee. These clinical findings align with our genetic data, supporting the multifaceted protective role of leucine in OA. Our study is the first to reveal the mediating role of leucine in the relationship between immune cells and osteoarthritis from a genetic perspective, providing new insights into how metabolites influence both immune regulation and musculoskeletal function in osteoarthritis pathogenesis.

In light of the limitations of this study, several factors should be considered. First, the analysis was conducted without integrating lab experiments, which could have provided additional biological validation and insights into the mechanisms underlying the observed associations. To address this limitation, we plan to investigate the regulatory role of leucine in inflammation using human chondrocyte and immune cell cocultures and validate the effects of leucine on osteoarthritis development in animal models. Second, the genetic data used in this study were derived mainly from populations of European ancestry, which may limit the applicability of these findings to more diverse ethnic groups. This limitation is unavoidable, as comprehensive datasets for 731 immune cell phenotypes and 1400 metabolites are currently available only for European populations. To maintain consistency and reduce potential confounding factors, we focused on osteoarthritis data from populations of individuals with the same European ancestry. Future research should develop immune cell and metabolite datasets for diverse ethnic populations and validate these associations in multiethnic cohorts to ensure broader applicability. Third, the absence of clinical validation analyses means that the practical implications of these findings in a clinical setting remain uncertain. To address this gap, we intend to evaluate the clinical relationship between leucine levels and OA severity across disease stages, which could help translate our genetic findings into practical clinical applications.

5 | Conclusion

In summary, this study highlights the significant impact of immune cells on osteoarthritis and identifies specific plasma metabolites that mediate this relationship. The use of Mendelian randomization methods has strengthened the causal inference of these associations. These findings may facilitate the development of innovative treatment strategies targeting immune cells and metabolic pathways involved in osteoarthritis. Further research, including larger sample sizes, clinical validation, and integration with experimental data, will be essential to fully understand the potential of these targets for the treatment and management of osteoarthritis.

Author Contributions

Changfa Huang: investigation, methodology, visualization, writing – original draft, writing – review and editing. **Hao Fan:** methodology, software, visualization, writing – original draft, writing – review and editing. **Wenjing Ma:** methodology, visualization, writing – review and editing. **Ze Wei:** methodology, visualization, writing – review and editing. **Huitian Han:** methodology, visualization, writing – review and editing. **Annan Liang:** methodology, visualization, writing – review and editing. **Xuemeng Mu:** methodology, visualization, writing – review and editing. **Wei Zou:** methodology, visualization, writing – review and editing. **Jing Hao:** methodology, visualization, writing – review and editing. **Fei Liu:** data curation, methodology, writing – review and editing. **Lijin Liu:** data curation, methodology, writing – review and editing. **Su Liu:** data curation, methodology, writing – review and editing. **Zhifa Zheng:** data curation, methodology, writing – review and editing. **Lina Zhao:** conceptualization, methodology, writing – review and editing, supervision. **Zhihong Wu:** conceptualization, methodology, writing – review and editing, supervision.

Acknowledgments

The authors express their profound appreciation to the researchers who kindly provided the original dataset for this study.

Funding

This research was funded in part by the Beijing Natural Science Foundation (7244389 to L.Z.); National Key Research and Development Program of China (2022YFC2703901 to Z.W.); National Natural Science Foundation of China (82172525, 82402760 to L.Z.); National High Level Hospital Clinical Research Funding (2022-PUMCH-D-002 to Z.W.); CAMS Innovation Fund for Medical Sciences (CIFMS, 2021-I2M-1-052 to Z.W.).

Ethics Statement

All analyses conducted were firmly grounded in publicly accessible data and did not necessitate the procurement of ethical approval or consent.

Conflicts of Interest

The authors declare no conflicts of interest.

Data Availability Statement

We used data from publicly available GWASs and summary statistics. The specific sources of the GWAS dataset and summary statistics are listed in Section 2.

References

1. M. C. Hochberg, A. Guermazi, H. Guehring, et al., "Effect of Intra-Articular Sprifermin vs Placebo on Femorotibial Joint Cartilage Thickness in Patients With Osteoarthritis: The FORWARD Randomized Clinical Trial," *Journal of the American Medical Association* 322, no. 14 (2019): 1360–1370.

2. L. A. Deveza, S. R. Robbins, V. Duong, et al., "Efficacy of a Combination of Conservative Therapies vs an Education Comparator on Clinical Outcomes in Thumb Base Osteoarthritis: A Randomized Clinical Trial," *JAMA Internal Medicine* 181, no. 4 (2021): 429–438.

3. C. A. Gusho and M. Jenson, "Demographic Tendencies and Hospitalization Outcomes Among Inpatient Admissions of Osteoarthritis in the Midwest: A 2016 State Inpatient Database Study," *Cureus* 12, no. 5 (2020): e7959.

4. J. N. Katz, K. R. Arant, and R. F. Loeser, "Diagnosis and Treatment of Hip and Knee Osteoarthritis: A Review," *Journal of the American Medical Association* 325, no. 6 (2021): 568–578.

5. E. Eti, H. B. Kouakou, J. C. Daboiko, et al., "Epidemiology and Features of Knee Osteoarthritis in the Ivory Coast," *Revue du Rhumatisme (English Ed.)* 65, no. 12 (1998): 766–770.

6. A. Aravinthan, M. A. Hossain, B. Kim, et al., "Ginsenoside Rb(1) Inhibits Monoiodoacetate-Induced Osteoarthritis in Postmenopausal Rats Through Prevention of Cartilage Degradation," *Journal of Ginseng Research* 45, no. 2 (2021): 287–294.

7. Y. Zhang, Y. Wang, J. Xu, Z. Wang, W. Zhao, and C. Zhao, "Visceral Adipose Tissue and Osteoarthritis, a Two-Sample Mendelian Randomized Study," *Frontiers in Medicine* 10 (2023): 1324449.

8. P. Cheng, S. Gong, C. Guo, et al., "Exploration of Effective Biomarkers and Infiltrating Immune Cells in Osteoarthritis Based on Bioinformatics Analysis," *Artificial Cells, Nanomedicine, and Biotechnology* 51, no. 1 (2023): 242–254.

9. B. Wen, M. Liu, X. Qin, Z. Mao, and X. Chen, "Identifying Immune Cell Infiltration and Diagnostic Biomarkers in Heart Failure and Osteoarthritis by Bioinformatics Analysis," *Medicine (Baltimore)* 102, no. 26 (2023): e34166.

10. F. Ponchel, A. N. Burska, E. M. Hensor, et al., "Changes in Peripheral Blood Immune Cell Composition in Osteoarthritis," *Osteoarthritis and Cartilage* 23, no. 11 (2015): 1870–1878.

11. Y. Yu, G. Dong, and Y. Niu, "Construction of Ferroptosis-Related Gene Signatures for Identifying Potential Biomarkers and Immune Cell Infiltration in Osteoarthritis," *Artificial Cells, Nanomedicine, and Biotechnology* 52, no. 1 (2024): 449–461.

12. T. O. Smith, E. Higson, M. Pearson, and M. Mansfield, "Is There an Increased Risk of Falls and Fractures in People With Early Diagnosed Hip and Knee Osteoarthritis? Data From the Osteoarthritis Initiative," *International Journal of Rheumatic Diseases* 21, no. 6 (2018): 1193–1201.

13. E. Sanchez-Lopez, R. Coras, A. Torres, N. E. Lane, and M. Guma, "Synovial Inflammation in Osteoarthritis Progression," *Nature Reviews Rheumatology* 18, no. 5 (2022): 258–275.

14. M. Kloppenburg, "Synovial Inflammation in Osteoarthritis. A Treatable Target?," *Seminars in Arthritis and Rheumatism* 64 (2024): 152326.

15. H. Xue, L. Zhang, J. Xu, et al., "Association of the Visceral Fat Metabolic Score With Osteoarthritis Risk: A Cross-Sectional Study From NHANES 2009–2018," *BMC Public Health* 24, no. 1 (2024): 2269.

16. M. S. Adam, H. Zhuang, X. Ren, Y. Zhang, and P. Zhou, "The Metabolic Characteristics and Changes of Chondrocytes In Vivo and In Vitro in Osteoarthritis," *Frontiers in Endocrinology* 15 (2024): 1393550.

17. E. V. Tchetina, K. E. Glemba, G. A. Markova, S. I. Glukhova, M. A. Makarov, and A. M. Lila, "Metabolic Dysregulation and Its Role in Postoperative Pain Among Knee Osteoarthritis Patients," *International Journal of Molecular Sciences* 25, no. 7 (2024): 3857.

18. M. Matsunaga, J. J. Chen, M. Jijiwa, and E. Lim, "The Impact of Diabetes and Osteoarthritis on the Occurrence of Stroke, Acute Myocardial Infarction, and Heart Failure Among Older Adults With Non-Valvular Atrial Fibrillation in Hawaii: A Retrospective Observational Cohort Study," *BMC Public Health* 21, no. 1 (2021): 1183.

19. X. Sun, X. Zhen, X. Hu, et al., "Osteoarthritis in the Middle-Aged and Elderly in China: Prevalence and Influencing Factors," *International Journal of Environmental Research and Public Health* 16, no. 23 (2019): 4701.

20. J. B. Driban, A. C. Stout, J. Duryea, et al., "Coronal Tibial Slope Is Associated With Accelerated Knee Osteoarthritis: Data From the Osteoarthritis Initiative," *BMC Musculoskeletal Disorders* 17 (2016): 299.

21. Y. Wang, Y. Zhang, C. Zhao, W. Cai, Z. Wang, and W. Zhao, "Physical Activity, Sedentary Behavior, and Osteoarthritis: A Two-Sample Mendelian Randomization Analysis," *Iranian Journal of Public Health* 52, no. 10 (2023): 2099–2108.

22. V. Orrù, M. Steri, C. Sidore, et al., "Complex Genetic Signatures in Immune Cells Underlie Autoimmunity and Inform Therapy," *Nature Genetics* 52, no. 10 (2020): 1036–1045.

23. Y. Chen, T. Lu, U. Pettersson-Kymmer, et al., "Genomic Atlas of the Plasma Metabolome Prioritizes Metabolites Implicated in Human Diseases," *Nature Genetics* 55, no. 1 (2023): 44–53.

24. J. Bowden, M. F. Del Greco, C. Minelli, G. Davey Smith, N. A. Sheehan, and J. R. Thompson, "Assessing the Suitability of Summary Data for Two-Sample Mendelian Randomization Analyses Using MR-Egger Regression: The Role of the I^2 Statistic," *International Journal of Epidemiology* 45, no. 6 (2016): 1961–1974.

25. Q. Zhang, C. Sun, X. Liu, C. Zhu, C. Ma, and R. Feng, "Mechanism of Immune Infiltration in Synovial Tissue of Osteoarthritis: A Gene Expression-Based Study," *Journal of Orthopaedic Surgery and Research* 18, no. 1 (2023): 58.

26. Y. Liu, W. Jiang, J. Huang, and L. Zhong, "Bioinformatic Analysis Combined With Immune Infiltration to Explore Osteoarthritis Biomarkers and Drug Prediction," *Medicine (Baltimore)* 103, no. 25 (2024): e38430.

27. M. Teng, J. Wang, X. Su, et al., "Associations Between Immune Cells Signatures and Osteoarthritis: An Integrated Analysis of Bidirectional Mendelian Randomization and Bayesian Colocalization," *Cytokine* 179 (2024): 156633.

28. I. J. Teunissen van Manen, N. J. T. van Kooten, I. Di Ceglie, et al., "Identification of CD64 as a Marker for the Destructive Potential of Synovitis in Osteoarthritis," *Rheumatology (Oxford, England)* 63, no. 4 (2024): 1180–1188.

29. A. J. van Vuuren, J. A. van Roon, V. Walraven, et al., "CD64-Directed Immunotoxin Inhibits Arthritis in a Novel CD64 Transgenic Rat Model," *Journal of Immunology* 176, no. 10 (2006): 5833–5838.

30. M. Alahdal, H. Zhang, R. Huang, et al., "Potential Efficacy of Dendritic Cell Immunomodulation in the Treatment of Osteoarthritis," *Rheumatology (Oxford, England)* 60, no. 2 (2021): 507–517.

31. Z. Liao, X. Han, Y. Wang, et al., "Differential Metabolites in Osteoarthritis: A Systematic Review and Meta-Analysis," *Nutrients* 15, no. 19 (2023): 4191.

32. E. Sasaki, H. Yamamoto, T. Asari, et al., "Metabolomics With Severity of Radiographic Knee Osteoarthritis and Early Phase Synovitis in Middle-Aged Women From the Iwaki Health Promotion Project: A Cross-Sectional Study," *Arthritis Research & Therapy* 24, no. 1 (2022): 145.

33. Q. Fu, X. Yuan, W. Wang, et al., "Causal Association of Genetically Determined Plasma Metabolites With Osteoarthritis: A Two-Sample Mendelian Randomization Study," *Frontiers in Medicine* 11 (2024): 1396746.

34. N. Akhtar, M. J. Miller, and T. M. Haqqi, "Effect of a Herbal-Leucine Mix on the IL-1β-Induced Cartilage Degradation and Inflammatory Gene Expression in Human Chondrocytes," *BMC Complementary and Alternative Medicine* 11 (2011): 66.

35. M. S. Kim, K. Y. Wu, V. Auyeung, Q. Chen, P. A. Gruppuso, and C. Phornphutkul, "Leucine Restriction Inhibits Chondrocyte Proliferation and Differentiation Through Mechanisms Both Dependent and Independent of mTOR Signaling," *American Journal of Physiology. Endocrinology and Metabolism* 296, no. 6 (2009): E1374–E1382.

36. J. Moon, K. H. Cho, J. Jhun, et al., "Small Heterodimer Partner-Interacting Leucine Zipper Protein Suppresses Pain and Cartilage

Destruction in an Osteoarthritis Model by Modulating the AMPK/STAT3 Signaling Pathway," *Arthritis Research & Therapy* 26, no. 1 (2024): 199.

37. N. Tanaka, T. Tashiro, Y. Katsuragawa, M. Sawabe, H. Furukawa, and N. Fukui, "Expression of Minor Cartilage Collagens and Small Leucine Rich Proteoglycans May Be Relatively Reduced in Osteoarthritic Cartilage," *BMC Musculoskeletal Disorders* 20, no. 1 (2019): 232.

38. S. Satis, "The Role of Amıno Acıds in Knee Osteoarthrıtıs: Amıno Acıds in Knee Osteoarthrıtıs," *International Journal of Current Medical and Biological Sciences* 3, no. 2 (2023): 130–137.

39. S. J. Park, C. H. Nam, H. S. Ahn, and T. Kim, "The Efficacy and Safety of Leucine-Enriched Essential Amino Acids in Knee Osteoarthritis Patients: A Randomized Controlled Trial," *Medicine (Baltimore)* 103, no. 19 (2024): e38168.

Supporting Information

Additional supporting information can be found online in the Supporting Information section. **Figure S1:** Forest plot of the MR analysis of immune cells and osteoarthritis. **Figure S2:** Scatter plot of the MR analysis of immune cells and osteoarthritis. **Figure S3:** Funnel plot of the MR analysis of immune cells and osteoarthritis. **Figure S4:** Leave-one-out plot of the MR analysis of immune cells and osteoarthritis. **Figure S5:** Forest plot of the MR analysis of metabolites and osteoarthritis. **Figure S6:** Scatter plot of the MR analysis of metabolites and osteoarthritis. **Figure S7:** Funnel plot of the MR analysis of metabolites and osteoarthritis. **Figure S8:** Leave-one-out plot of the MR analysis of metabolites and osteoarthritis. **Table S1:** MR results in the MR analysis of immune cells and osteoarthritis. **Table S2:** Pleiotropy test in the MR analysis of immune cells and osteoarthritis. **Table S3:** Heterogeneity test in the MR analysis of immune cells and osteoarthritis. **Table S4:** Reverse MR results in the MR analysis of immune cells and osteoarthritis. **Table S5:** MR analysis of metabolites and osteoarthritis. **Table S6:** Pleiotropy test in the MR analysis of metabolites and osteoarthritis. **Table S7:** Heterogeneity test in the MR analysis of metabolites and osteoarthritis. **Table S8:** Results of the direct and mediated effects.

International Journal of Rheumatic Diseases

WILEY

International Journal of Rheumatic Diseases

LETTER TO THE EDITOR

Performance of the Southend Giant Cell Arteritis Probability Score in a Single-Centre New Zealand Fast-Track Pathway

Amy Okamura-Kho[1] | Julia Martin[1] | Nicola Dalbeth[2] | Ravi Suppiah[1]

[1]Department of Rheumatology, Te Toka Tumai – Health New Zealand, Auckland, New Zealand | [2]Department of Medicine, Faculty of Medical and Health Sciences, University of Auckland, Auckland, New Zealand

Correspondence: Amy Okamura-Kho (amycyokamurakho@gmail.com)

Received: 28 July 2025 | **Revised:** 11 January 2026 | **Accepted:** 22 January 2026

Dear Editor,

Fast-track pathways (FTPs) for giant cell arteritis (GCA) aid timely diagnosis and prevention of complications such as vision loss and stroke [1–4], however, patient selection remains a challenge. The Southend GCA probability score (GCAPS) shows promise as a tool to identify low-risk patients who may not require urgent specialist assessment or imaging [5–8]. We analyzed the outcomes of our GCA FTP in Auckland New Zealand, including the performance of the GCAPS in a different population and healthcare system to where it has previously been validated.

We included 137 patients assessed in the Te Toka Tumai Auckland Rheumatology FTP for suspected GCA between January 2021 and July 2024. Data on demographic and clinical characteristics, timepoints through the pathway, investigations, treatment and final diagnosis were collected. Diagnostic confirmation was based on ultrasound (US), temporal artery biopsy (TAB), and/or clinical decision to treat. In our GCA clinic, two rheumatologists (RS, JM) with expertise in US conduct assessments using a GE Logic P9 R4 machine equipped with an L10-22-RS linear probe for cranial arteries and an L4-12t-RS linear probe for extracranial arteries. GCAPS was calculated retrospectively from clinical notes. ROC analysis was performed to evaluate GCAPS performance in predicting final GCA diagnosis.

Of the 137 patients included, 101 (74%) were female and the mean (SD) age was 78 (6.4) years old. European ethnicity made up 75%, 4% each were Māori and Pacific peoples, and the remaining were Asian (15%), Middle Eastern (1%), and African (1%). A final diagnosis of GCA was made in 61 patients (45%), and 76 (55%) were classified as not GCA. The most common alternative diagnoses were primary headache disorder (35 patients, 26%), mechanical causes including osteoarthritis, cervical spondylosis, and temporomandibular dysfunction (11 patients, 8%), and infections including sinusitis, viral, and dental infections (11 patients, 8%). Nine patients (7%) were evaluated as having polymyalgia rheumatica.

Glucocorticoid (GC) therapy was initiated at referral in 127 (93%). Mean time to specialist assessment was 9.6 days. Twenty-two (16%) were assessed within 72 h, 62 (45%) were assessed within 1 week, 113 (82%) within 2 weeks, and 129 (94%) within 3 weeks. All but two patients referred to the FTP had US or TAB or both, as part of the FTP assessment. One patient had a CT head demonstrating an alternative pathology (an intracranial space occupying lesion) after referral and prior to GCA clinic attendance, while another had a CT vascular angiogram confirming extracranial (large vessel) GCA. Most (125 patients, 92%) underwent US, 24 (18%) underwent TAB, and 13 (10%) underwent both diagnostic procedures during their assessment. Of the GCA group, 8 (13%) were diagnosed despite negative imaging/biopsy, based on clinical history and taking into account glucocorticoid exposure. Notably, 5 of these had delayed imaging (> 3 weeks post-GC start), underscoring the limitations of delayed assessment on test performance. In an exploratory analysis of US sensitivity in relation to GC exposure, we calculated a sensitivity of 92% when performed within 3 weeks ($n = 117$), as compared to 50% beyond 3 weeks ($n = 8$).

GCAPS had strong discriminatory performance with an area under the curve (AUC) of 0.91 (95% CI: 0.86–0.96) as shown in

Figure 1. Using a binary cut-off of ≥9, GCAPS demonstrated 100% sensitivity and 22% specificity. Of the 137 patients included, 56 patients (41%) were categorized as high risk, 64 (47%) as intermediate, and 17 (12%) as low risk. GCA prevalence was 86% in the high-risk group, 20% in the intermediate-risk group, and 0% in the low-risk group, indicating a negative predictive value of 100% in the low-risk group (95% CI: 80.4%–100%). Several GCAPS components (Table 1) were significantly associated with GCA, including polymyalgia, fever, weight loss, scalp tenderness, cranial/limb claudication, and elevated CRP.

Our analysis highlights the ongoing challenges in the timely assessment and management of GCA, even with a FTP in place. Despite GC therapy being initiated in most cases at the time of referral, delays in assessment remain a significant concern. The mean time from referral to initial assessment was 9 days, with fewer than half of the referred patients being seen within 1 week. Only 16% met the international recommendations of within 72 h [3]. In our FTP, the availability of US-trained rheumatologists or sonographers remains the main limitation to timely assessment. These delays increase the risk of diagnostic uncertainty, particularly when imaging findings are equivocal or negative due to prolonged GC exposure, underscoring the need for strategies to further streamline the FTP.

This work provides the first validation of the GCAPS in New Zealand. Our findings confirm its high sensitivity, especially in excluding GCA among low-risk patients. This suggests GCAPS could safely reduce unnecessary urgent assessments and imaging in this subgroup—an important consideration for resource-constrained systems, such as in New Zealand where assessment of acute conditions such as GCA are limited to public hospitals. Specifically, all patients with low risk GCAPS ($n = 17$, 12%) underwent an US only, identifying an area where resource allocation can be modified with the routine application of GCAPS to our FTP.

Compared to other cohorts [5–10] in which 15%–34% of referred patients are diagnosed with GCA, our 45% rate likely reflects pre-referral triage by a rheumatologist and also likely contributed

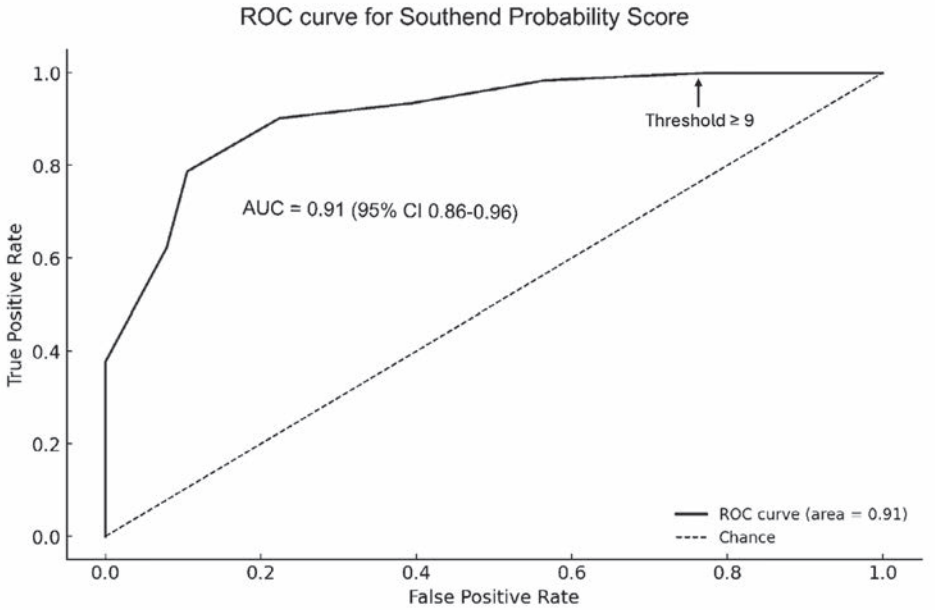

Diagnostic performance of different GCA probability score binary cut-off values

GCAPS cut off*	Total Cases	GCA	Not GCA	Sensitivity	Specificity	PPV	NPV	Accuracy
≥8	125	61	64	100%	16%	49%	100%	53%
≥9	120	61	59	100%	22%	51%	100%	57%
≥10	103	60	43	98%	43%	58%	97%	68%
≥11	87	57	30	93%	61%	66%	92%	75%
≥12	72	55	17	90%	78%	76%	91%	83%
≥13	56	48	8	79%	89%	86%	84%	85%
≥14	44	38	6	62%	92%	86%	75%	79%
≥15	23	23	0	38%	100%	100%	67%	72%
≥16	16	16	0	26%	100%	100%	63%	67%

*GCAPS cut-off of 8 means a score of 8 is considered test positive and a score of <8 test negative.

FIGURE 1 | Receiver operating characteristic curve and binary cut-off values for GCA probability score in predicting final diagnosis of GCA. AUC, area under the curve; GCA, giant cell arteritis; ROC, receiver operating characteristic.

TABLE 1 | GCAPS components in patients with and without GCA.

	All ($n=137$)		GCA ($n=61$)		Not GCA ($n=76$)		
	n	**%**	***n***	**%**	***n***	**%**	***p****
Female	101	74%	45	74%	56	74%	1
Age							
< 50 years (%)	1	1%	0	0%	1	1%	0.205
50–60 years (%)	12	9%	2	3%	10	13%	
61–65 years (%)	22	16%	9	15%	13	17%	
> 65 years (%)	102	74%	50	82%	52	68%	
CRP							
0–5	30	22%	1	2%	29	38%	< 0.001
6–10	9	7%	3	5%	6	8%	0.345
11–25	21	15%	6	10%	15	20%	0.196
> 25	71	52%	49	80%	22	29%	< 0.001
Symptoms							
Duration of symptoms							
< 6 weeks	105	77%	47	77%	58	76%	0.400
6–12 weeks	14	10%	9	15%	5	7%	
12–24 weeks	10	7%	4	7%	6	8%	
> 24 weeks	1	1%	0	0%	1	1%	
Headache	115	84%	48	79%	67	88%	0.205
Polymyalgia	44	32%	28	46%	16	21%	0.004
Fever	17	12%	12	20%	5	7%	0.040
Weight loss	19	14%	14	23%	5	7%	0.012
Visual symptoms							
Blurred	35	26%	17	28%	18	24%	0.718
Diplopia	9	7%	4	7%	5	7%	1.000
Amaurosis	4	3%	3	5%	1	1%	0.463
Cranial or limb claudication	26	19%	22	36%	4	5%	< 0.001
Scalp tenderness	62	45%	38	62%	24	32%	0.001
Signs							
AION, CRAO, Field loss, RAPD	2	1%	2	3%	0	0%	0.382
Temporal artery abnormality							
Tenderness	54	39%	28	46%	26	34%	0.224
Thickening	8	6%	5	8%	3	4%	0.492
Loss of palpable pulse	1	1%	0	0%	1	1%	1.000
Extracranial abnormality							
Thickening	1	1%	1	2%	0	0%	0.912
Bruit	0	0%	0	0%	0	0%	1.000
Loss of palpable pulse	0	0%	0	0%	0	0%	1.000
Cranial nerve palsy	2	1%	1	2%	1	1%	1.000

Abbreviations: AION, anterior ischaemic optic neuropathy; CRAO, central retinal artery occlusion; RAPD, relative afferent pupillary defect.
*Multiple comparison correction applied.

to our slightly higher test performance (AUC). Furthermore, in our analysis, the GCAPS was retrospectively calculated with no missing data, demonstrating that GCAPS parameters are already part of the routine initial assessment of suspected GCA without the need for further additional testing or information to be obtained, supporting its practicality.

A strength of this analysis was that confirmatory testing was universal in patients referred to our FTP, as was the documentation of final diagnosis, without missing data. However, despite the completeness of GCAPS component data, the retrospective design with GCAPS calculated from clinical records was a possible source of information bias whereby elements of the GCAPS were likely to impact the final clinical GCA diagnosis. A further limitation is the lack of a gold standard for GCA diagnosis.

In conclusion, this analysis supports GCAPS as a reliable, practical tool for excluding GCA in low-risk patients, thereby optimizing the allocation of limited rheumatology resources. By validating the GCAPS in a New Zealand context, we provide robust evidence supporting its integration into fast-track pathways, enhancing the efficiency of triaging for suspected GCA cases. However, persistent delays in assessment and the need for confirmatory testing in intermediate- and high-risk groups highlight ongoing challenges in resource management and the complexities of real-world GCA diagnosis. Addressing these gaps is critical to improving outcomes for patients and advancing the utility of streamlined evidence-based pathways in rheumatologic care.

Author Contributions

A.O. developed the protocol, performed data acquisition, performed the statistical analysis, and wrote the manuscript. J.M. contributed to data acquisition and revised the manuscript critically for important intellectual content. N.D. revised the manuscript critically for important intellectual content. R.S. developed the original idea, contributed to data acquisition and interpretation. All authors (A.O., J.M., N.D., and R.S.) read and approved the final manuscript.

Funding

The authors have nothing to report.

Ethics Statement

The Research Review Committee Te Toka Tumai Auckland reviewed and approved the project (A+ 10272). This work was considered audit and further ethics approval was not required.

Consent

Written informed consent for participation was not required in accordance with national legislation and institutional requirements.

Conflicts of Interest

The authors declare no conflicts of interest.

Data Availability Statement

The data that support the findings of this study are available from the corresponding author upon reasonable request.

Amy Okamura-Kho
Julia Martin
Nicola Dalbeth
Ravi Suppiah

References

1. P. Patil, M. Williams, W. Maw, et al., "Fast Track Pathway Reduces Sight Loss in Giant Cell Arteritis: Results of a Longitudinal Observational Cohort Study," *Clinical and Experimental Rheumatology* 33, no. 2 Suppl 89 (2015): S-103-6, https://pubmed.ncbi.nlm.nih.gov/26016758/.

2. A. Diamantopoulos, G. Haugeberg, A. Lindland, and G. Myklebust, "The Fast-Track Ultrasound Clinic for Early Diagnosis of Giant Cell Arteritis Significantly Reduces Permanent Visual Impairment: Towards a More Effective Strategy to Improve Clinical Outcome in Giant Cell Arteritis?," *Rheumatology (Oxford, England)* 55, no. 1 (2016): 66–70, https://pubmed.ncbi.nlm.nih.gov/26286743/.

3. C. Dejaco, S. Ramiro, M. Bond, et al., "EULAR Recommendations for the Use of Imaging in Large Vessel Vasculitis in Clinical Practice: 2023 Update," *Annals of the Rheumatic Diseases* 83, no. 6 (2024): 741–751, https://pubmed.ncbi.nlm.nih.gov/37550004/.

4. S. Mackie, C. Dejaco, S. Appenzeller, et al., "British Society for Rheumatology Guideline on Diagnosis and Treatment of Giant Cell Arteritis," *Rheumatology (Oxford, England)* 59, no. 3 (2020): e1–e23, https://pubmed.ncbi.nlm.nih.gov/31970405/.

5. A. R. Melville, K. Donaldson, J. Dale, and A. Ciechomska, "Validation of the Southend Giant Cell Arteritis Probability Score in a Scottish Single-Centre Fast-Track Pathway," *Rheumatology Advances in Practice* 6, no. 1 (2021): rkab102.

6. L. M. Neuman, M. Van Nieuwland, M. Vermeer, D. Boumans, E. M. Colin, and C. Alves, "External Validation of the Giant Cell Arteritis Probability Score in The Netherlands," *Clinical and Experimental Rheumatology* 40, no. 4 (2021): 787–792, https://www.clinexprheumatol.org/abstract.asp?a=17283.

7. M. Mathake, J. Murdoch, J. L. DeSousa, A. Taylor, and H. Keen, "Performance of the Southend Pre-Test Probability Score (PTPS) for Giant Cell Arteritis in a Fast-Track Clinic in Western Australia," *Rheumatology Advances in Practice* 6, no. 2 (2022): rkac055.

8. J. Carroll, F. Griffith, C. Fox, and M. Khurshid, "P207 External Validation of the Southend Giant Cell Arteritis Pre-Test Probability Score in a Dorset Fast-Track Clinic," cited January 3, 2025, https://doi.org/10.1093/rheumatology/kead104.

9. F. Laskou, F. Coath, S. Mackie, S. Banerjee, T. Aung, and B. Dasgupta, "A Probability Score to Aid the Diagnosis of Suspected Giant Cell Arteritis," *Clinical and Experimental Rheumatology* 37, no. Suppl 117(2) (2019): 104–108, https://pubmed.ncbi.nlm.nih.gov/30767870/.

10. A. Sebastian, A. Tomelleri, A. Kayani, D. Prieto-Pena, C. Ranasinghe, and B. Dasgupta, "Probability-Based Algorithm Using Ultrasound and Additional Tests for Suspected GCA in a Fast-Track Clinic," *RMD Open* 6, no. 3 (2020): e001297.

International Journal of Rheumatic Diseases

WILEY

International Journal of Rheumatic Diseases

EDITORIAL

Large Language Models in Rheumatology: Prospects and Challenges for the Clinician

Po-Cheng Shih[1,2] | James Cheng Chung Wei[1,3,4]

[1]Institute of Medicine, Chung Shan Medical University, Taichung, Taiwan | [2]Division of Allergy, Immunology and Rheumatology, Department of Internal Medicine, Changhua Christian Hospital, Changhua, Taiwan | [3]Department of Allergy, Immunology and Rheumatology, Chung Shan Medical University Hospital, Taichung, Taiwan | [4]Graduate Institute of Integrated Medicine, China Medical University, Taichung, Taiwan

Correspondence: James Cheng Chung Wei (jccwei@gmail.com)

Received: 12 June 2025 | **Revised:** 7 January 2026 | **Accepted:** 27 January 2026

Artificial intelligence (AI) is rapidly evolving and reshaping everyday life for everyone, including healthcare. The general-purpose models, such as the GPT series, Claude, Gemini, Grok, and others, have demonstrated remarkable capabilities in the solution of medical problems and presenting opportunities and challenges for medical research and clinical practice [1]. Rheumatology, characterized by complex chronic diseases, benefits a lot from rapid advances in LLMs, but must also carefully manage the associated risks.

1 | Advancing Rheumatology With Large Language Models: From Clinical Practice to Drug Discovery

AI, within the past few years, particularly machine learning (ML), large language models, and natural language processing (NLP), have demonstrated utility in rheumatology [2]. In rheumatology research, various LLMs are able to assist rheumatologists in daily medical tasks, including imaging analysis, disease classification, literature review, data analysis, language editing, and video generation, covering nearly all aspects of their daily work [3]. LLMs are now capable of more complicated tasks in clinical practice, including:

- Optimizing Clinical Workflows: By automating tasks such as chart summaries, discharge notes, referral letters, and assisting in drafting research protocols and manuscripts, LLMs significantly reduce administrative burdens for clinicians.
- Accessing and Reviewing knowledge with less effort: LLMs have the ability in rapid analysis and summarization of vast quantities of medical literature, enabling researchers and clinicians to keep pace with exponentially growing information. medical content, these models provide new knowledge through interactive engagement.
- Assisting Clinical Decision-Making: AIs could analyze clinical notes, imaging, and laboratory data to provide suggestions ranging from differential diagnosis to management options. Studies have evaluated the performance of LLMs in handling rheumatologic and immunologic cases, showing potential, especially when integrating multimodal information [4]. TImproving Clinician-Patient Communication and Patient Education: LLMs are able to generate adequate patient education materials and address frequently asked patient questions to better assist decision-making [5].
- Practical interactive applications: Previously, chatbots primarily were developed for general patient education [6]. However, with advanced LLMs such as Claude, clinicians can now create practical, interactive applications tailored to healthcare professionals or patients, even without coding expertise.
- Image analysis: Consequently, the field of medical imaging AI is relatively more mature compared to other medical applications of LLMs [7]. Even without fine-tuning, these models maintain a certain degree of accuracy. Given the rapid advancements, clinicians must closely follow these updates.

Include applications in Table 1.

2 | Challenges and Limitations in Clinical Application of AI

Despite rapid and extensive resource investment in AI research, significant limitations persist. First, a primary

TABLE 1 | Current applications of LLM in rheumatology.

Application area	Specific examples	Potential benefits
Clinical Decision Support	Analyzing lab data, images, and symptoms to aid differential diagnosis; suggesting treatment options.	Support for complicated cases to reach differential diagnosis and treatment decision within shorter period
Research & Literature Review	Rapid summary of latest research; organizing literature data; analyzing large datasets for trends; assisting research proposal adjustment	Rapid knowledge acquisition; discovery of new research avenues; improved research efficiency
Documentation & Administration	Revision of chart summaries; drafting referral letters or insurance documents; extracting key information from unstructured notes (NLP)	Reduced administrative burden; improved document quality and consistency
Patient Communication & Education	Generating personalized educational materials; answering common patient questions; analyzing sentiment in PROs; Produce short video for patients to enhance compliance	Enhanced patient engagement and self-management; improved physician-patient communication; improve the adherence of patients
Image Analysis (Multimodal)	Combining imaging with textual information for diagnostic analysis; with fine tuning, image analysis is able to provide suggestion in clinical decision	Improved efficiency & potential accuracy in image interpretation.
Drug Development & Clinical Trials	Predicting drug response with simulation; optimizing clinical trial design; analyzing trial data	Accelerated drug development pipeline; potential for more precise therapies

concern for general use remains the validation of AI accuracy. AI hallucination has yet to be fully resolved within current training paradigms, although numerous approaches to solve this issue have already been proposed. Second, the various training datasets lead to data bias, potentially exacerbating health inequities. Third, cloud-based deployment raises significant concerns regarding patient privacy and data security. Conversely, running AI locally is often constrained by limited computing power on personal devices, thereby further restricting its practical application. Fourth, even with current reasoning models, the internal cognitive mechanisms remain inadequately understood. Therefore, these concerns must be carefully considered when applying AI to clinical scenarios.

3 | Empowering Rheumatologists: Guiding the Ethical and Effective Use of AI

In the face of this transformative technology, the role of the rheumatology community is crucial.

1. Never Stop Learning: Familiarize with the fundamental principles, capabilities, and limitations of state-of-the-art AI.
2. Critical Thinking: Reconfirm the LLM-generated outputs, integrating them with clinical experience and evidence-based medicine for final judgment.
3. Engaging in Research and Development: Collaborating with AI experts to train, validate, and study AI applications tailored to rheumatology needs
4. Guiding Ethical Norms: Actively participating in the development of ethical guidelines and best practice standards for using LLMs within rheumatology
5. Promotion in AI use with Education and Training: Organizing workshops, seminars, and training programs to ensure more rheumatologists are well-prepared for the widespread adoption of AI, thereby preventing the risk of becoming disconnected from emerging advancements.
6. Shared Decision Making: Actively involving patients in discussions regarding the implementation of AI, addressing their concerns, enhancing transparency, and ensuring that AI tools are genuinely patient-centered.
7. Promoting Multidisciplinary Collaboration: Facilitating collaboration among clinicians, data scientists, ethicists, and policymakers, ensuring balanced, inclusive, and holistic approaches to AI adoption.
8. Following Rapid Growth in Computational Power: the community must significantly enhance its learning efforts to accelerate advancements in healthcare beyond the traditionally slower pace of growth.

4 | Conclusion

LLMs offer significant promise as tools for rheumatology, with potential improvement of clinical practice, medical research, and personal life, but several challenges remain. To effectively utilize these technologies, their differences in ability, accuracy, adherence to the highest ethical standards, and flexibility to continuous learning need to be carefully evaluated.

Author Contributions

Po-Cheng Shih wrote the manuscript. James Cheng Chung Wei supervise and edit the manuscript. All authors are responsible for the final version of the manuscript.

Acknowledgments

Use of AI in revising draft.

Disclosure

The views expressed in this article represent those of the authors and do not necessarily reflect the official position of the institutions with which they are affiliated.

Conflicts of Interest

Dr. James Wei is the Editor-in-Chief of IJRD and a co-author of this article. They were excluded from editorial decision-making related to the acceptance and publication of this article. Editorial decision-making was handled independently by other editors to minimize bias. The other authors declare no conflicts of interest.

Data Availability Statement

The data that support the findings of this study are available from the corresponding author upon reasonable request.

References

1. A. J. Thirunavukarasu, D. S. J. Ting, K. Elangovan, L. Gutierrez, T. F. Tan, and D. S. W. Ting, "Large Language Models in Medicine," *Nature Medicine* 29, no. 8 (2023): 1930–1940.

2. A. Zo'ubi, "Review of 2024 Publications on the Applications of Artificial Intelligence in Rheumatology," *Clinical Rheumatology* 44 (2025): 1427–1438.

3. J. M. Sequí-Sabater and D. Benavent, "Artificial Intelligence in Rheumatology Research: What Is It Good for?," *RMD Open* 11, no. 1 (2025): e004309.

4. M. Omar, R. Agbareia, E. Klang, and M. E. Naffaa, "Large Language Models in Rheumatologic Diagnosis: A Multimodal Performance Analysis," *Journal of Rheumatology* 52, no. 2 (2025): 187–188.

5. F. Busch, L. Hoffmann, C. Rueger, et al., "Current Applications and Challenges in Large Language Models for Patient Care: A Systematic Review," *Communications Medicine* 5, no. 1 (2025): 26.

6. P. G. Gondode, R. Singh, S. Mehta, S. Singh, S. Kumar, and S. S. Nayak, "Artificial Intelligence Chatbots Versus Traditional Medical Resources for Patient Education on "Labor Epidurals": An Evaluation of Accuracy, Emotional Tone, and Readability," *International Journal of Obstetric Anesthesia* 61 (2025): 104302.

7. P. Rajpurkar and M. P. Lungren, "The Current and Future State of AI Interpretation of Medical Images," *New England Journal of Medicine* 388, no. 21 (2023): 1981–1990.

International Journal of Rheumatic Diseases

WILEY

International Journal of Rheumatic Diseases

LETTER TO THE EDITOR

A Case With Concurrent Monoclonal Gammopathy, Thrombocytopenia, and Antiphospholipid Antibodies

Zhan Su[1] | Jie Xu[2] | Hui Yan[3]

[1]Department of Hematology, The Affiliated Hospital of Qingdao University, Qingdao, China | [2]Center of Hematology, Peking University People's Hospital Qingdao, Qingdao, China | [3]Medical Clinic, The Affiliated Hospital of Qingdao University, Qingdao, China

Correspondence: Zhan Su (suwubz@qdu.edu.cn) | Hui Yan (qdfyyan@163.com)

Received: 11 July 2025 | **Revised:** 10 January 2026 | **Accepted:** 15 January 2026

Keywords: antiphospholipid antibody | monoclonal gammopathy | thrombocytopenia

Dear Editor,

Monoclonal gammopathy of undetermined significance (MGUS) is defined by the detection of monoclonal protein (M-protein) in the serum without meeting the diagnostic criteria for other lymphoid or plasma cell neoplasms. MGUS can be associated with various autoimmune phenomena, including cytopenia and the production of autoantibodies. Antiphospholipid antibodies (aPL) are a group of autoantibodies directed against phospholipid-protein complexes. Although persistent aPL positivity is a hallmark of antiphospholipid syndrome (APS), it can also be found in other conditions or in asymptomatic individuals. The prevalence of aPL is significantly higher in patients with MGUS than in the general population [1]. The coexistence of MGUS with thrombocytopenia and aPL positivity presents a considerable clinical challenge, as it necessitates balancing the risks of bleeding and thrombosis. Here, we report a rare case of concurrent MGUS, refractory thrombocytopenia, and aPL positivity.

An 82-year-old woman was admitted with a 1-month history of epistaxis and gingival bleeding, followed by 5 days of hematemesis. She had been diagnosed with immune thrombocytopenia over a decade earlier, with her platelet count once dropping to 1×10^9/L. After 6 months of glucocorticoid treatment, her platelets peaked at 50×10^9/L, but she subsequently discontinued therapy and relied on herbal medicine without routine blood monitoring. Over the next 10 years, she experienced intermittent epistaxis. One month before admission, she developed spontaneous limb purpura, recurrent epistaxis, and gingival bleeding. A local hospital recorded a platelet count of 5×10^9/L, yet she continued herbal treatment. Five days prior to admission, she vomited blood once, accompanied by dizziness, fatigue, and melena. Laboratory tests revealed leukocytosis (12.42×10^9/L) with neutrophilia (11.55×10^9/L), anemia (hemoglobin 99 g/L), and thrombocytopenia (55×10^9/L post-transfusion). Immunological testing showed positive antinuclear antibodies (homogeneous pattern 1:320, speckled patterns 1:100), anticentromere antibody positivity, and elevated antiphospholipid antibodies (anti-cardiolipin IgG + M + A 25.70 AU/mL, IgG 27.00 GPL-U/mL; anti-β2 glycoprotein I IgG 28.10 AU/mL). Testing for lupus anticoagulant was not performed. The aPL positivity was confirmed on repeat testing 12 weeks later. Immunofixation electrophoresis detected a faint IgG-λ band. Bone marrow aspiration, biopsy, and flow cytometry were unremarkable, confirming MGUS. She received methylprednisolone (40 mg/day, 10 days), IV immunoglobulin (15 g/day, 3 days), somatostatin, and esomeprazole. Although her bleeding resolved, her platelets remained low. The patient declined further therapy and was discharged.

Studies indicate a significantly higher incidence of aPL in MGUS patients than in healthy controls, with diversity in both antibody isotypes (IgG, IgM, and IgA) and phospholipid specificity (e.g., cardiolipin, phosphatidylserine, and phosphatidylinositol) [1]. For instance, Stern et al. reported elevated IgG anti-phosphatidylinositol in 32% and IgM anti-phosphatidylserine in 45% of MGUS samples [1]. This suggests the M-protein itself may possess aPL activity or that there is a pathophysiological link between MGUS and aPL production. However, aPL positivity in MGUS patients does not invariably lead to thrombotic events, and its clinical significance may differ from classical APS [1, 2].

The pathogenesis of MGUS-related thrombocytopenia (MGRT) remains incompletely understood. One proposed mechanism

is that the M-protein acts as an autoantibody targeting platelet membrane antigens (e.g., GPIIb/IIIa), mediating immune platelet destruction similar to classic immune thrombocytopenia (ITP) [3]. Another, non-immune mechanism involves physical adsorption of the M-protein onto the platelet surface, altering its properties and leading to premature clearance by the mononuclear-phagocyte system, primarily in the spleen [4]. The scenario is more complex when the M-protein also exhibits aPL activity, as in our case. It has been speculated that such paraproteins might interact with phospholipid components or membrane proteins on platelets, directly causing platelet destruction or dysfunction and thus contributing to thrombocytopenia [2, 5]. Our patient did not experience thrombosis, and therefore evidence for a direct prothrombotic role of the M-protein is lacking. The prolonged and severe thrombocytopenia in the absence of thrombotic history highlights the heterogeneity of this condition, where bleeding, rather than thrombosis, becomes the primary clinical concern.

Our patient responded poorly to glucocorticoids. For patients with MGRT, treatment strategies targeting the underlying clonal plasma cell or B-cell disorder may be considered, as addressing the source of the paraprotein could more effectively alleviate the thrombocytopenia. Management becomes particularly cautious when aPL co-exists. In the absence of thrombosis, routine anticoagulation is generally not recommended to avoid increasing bleeding risk [2]. Our patient did not receive anticoagulation due to gastrointestinal bleeding. Thrombopoietin receptor agonists (TPO-RAs) have also been suggested as a potential option for MGRT in the literature [3], although they were not used in this case. For refractory patients, rituximab (particularly for IgM-type MGUS) or therapies targeting the clonal cells (e.g., proteasome inhibitors, and immunomodulatory agents) may be considered [3, 4]. The treatment strategy must be individualized, carefully weighing the bleeding risk against the burden of the clonal disease.

In summary, we describe a complex case of concurrent MGUS, refractory thrombocytopenia, and aPL positivity. This case presented with bleeding, contrary to typical APS. For such patients, treatment requires balancing the control of bleeding risk against the management of the underlying clonal disorder, and more research is needed to define optimal management strategies.

Author Contributions

Hui Yan and Zhan Su designed the study. Zhan Su and Jie Xu collected the clinical information and wrote the manuscript. All authors read and approved the final manuscript.

Funding

The authors have nothing to report.

Consent

Informed consent was obtained from the patient.

Conflicts of Interest

The authors declare no conflicts of interest.

Data Availability Statement

Data sharing is not applicable to this article as no datasets were generated or analyzed during the current study.

Zhan Su
Jie Xu
Hui Yan

References

1. J. J. Stern, R. H. Ng, D. A. Triplett, and J. A. McIntyre, "Incidence of Antiphospholipid Antibodies in Patients With Monoclonal Gammopathy of Undetermined Significance," *American Journal of Clinical Pathology* 101, no. 4 (1994): 471–474, https://doi.org/10.1093/ajcp/101.4.471.

2. W. Ryżewska, M. Zarzycka, M. Witkowski, M. Witkowska, and T. Robak, "Management of Patient With Immune Thrombocytopenia With Antiphospholipid Syndrome and Monoclonal Gammopathy of Undetermined Significance," *OncoReview* 11 (2021): 106–111, https://doi.org/10.24292/01.OR.124301021.

3. Z. Su, X. Liu, and X. Yu, "Monoclonal Gammopathy-Related Thrombocytopenia: Case Report and Literature Review," *International Journal of Rheumatic Diseases* 27, no. 12 (2024): e15388, https://doi.org/10.1111/1756-185X.15388.

4. D. Rossi, L. D. Paoli, S. Franceschetti, et al., "Prevalence and Clinical Characteristics of Immune Thrombocytopenic Purpura in a Cohort of Monoclonal Gammopathy of Uncertain Significance," *British Journal of Haematology* 138, no. 2 (2007): 249–252, https://doi.org/10.1111/j.1365-2141.2007.06633.x.

5. R. Naka, H. Kaneko, O. Nagata, et al., "Refractory Immune Thrombocytopenic Purpura Associated With IgM Monoclonal Gammopathy of Undetermined Significance: Successful Treatment With Tirabrutinib Plus Conventional Therapies," *eJHaem* 3, no. 2 (2022): 513–516, https://doi.org/10.1002/jha2.423.

International Journal of Rheumatic Diseases

WILEY

International Journal of Rheumatic Diseases

EDITORIAL

Perspectives on a Large Language Models-Generated Referral Summary for Rheumatology Co-Management

Shiuan-Tzuen Su[1,2] | Wei-Chih Shen[3,4] | Shih-Chun Kuo[2,5] | Hung-Ke Lin[6]

[1]Department of Surgery, Chung Shan Medical University Hospital, Taichung, Taiwan | [2]School of Medicine, Chung Shan Medical University, Taichung, Taiwan | [3]Artificial Intelligence Center, Chung Shan Medical University Hospital, Taichung, Taiwan | [4]Department of Medical Informatics, Chung Shan Medical University, Taichung, Taiwan | [5]Department of Medical Imaging, Chung Shan Medical University Hospital, Taichung, Taiwan | [6]Department of Rheumatology, Show Chwan Memorial Hospital, Changhua, Taiwan

Correspondence: Shih-Chun Kuo (serso.tw@gmail.com) | Hung-Ke Lin (ke6465@gmail.com)

Received: 25 December 2025 | **Revised:** 25 December 2025 | **Accepted:** 28 January 2026

1 | Clinical Importance of Complete Referral Information in Rheumatology, Technological Advances and Knowledge Gap

Rheumatologic diagnosis is complex, requiring detailed history, examination findings, serologic markers, and advanced imaging, such as magnetic resonance imaging (MRI). In chronic inflammatory rheumatic diseases, such as axial spondyloarthritis (axSpA) and rheumatoid arthritis (RA), early diagnosis within the so-called "window of opportunity" was crucial to optimizing long-term functional outcomes, underscoring the necessity for high-quality referral documentation to support efficient care pathways [1].

2 | Large Language Models-Generated Referral Summaries in Rheumatology Might Significantly Improve Information Completeness and Writing Efficiency

Large language models (LLMs) could analyze unstructured clinical text alongside structured data for early rheumatic disease detection, enabling faster referrals. By identifying patterns in general practitioner (GP) records, they could support timely recognition and greater efficiency. Evidence from other specialties showed artificial intelligence (AI)-assisted documentation could reduce preparation time while maintaining accuracy and improving clinician satisfaction. Veen et al. reported that LLMs might surpass experts in summarization, might reduce documentation burden and clinician workload, and improve care, warranting further prospective validation [2]. Table 1 summarizes current applications of large language models in clinical note generation.

Cross-institutional referrals required exchanging sensitive electronic medical record (EMR) data across heterogeneous systems, and integrating generative AI amplifies privacy and security risks, including unauthorized access, re-identification, and model-driven data leakage. Encrypted transfer, strict access control, auditability, and institutional governance were essential to ensure compliant AI-enabled workflows. At the same time, current evidence showed that LLMs could enhance diagnostic pathways by accurately interpreting patient narratives, accelerating recognition of inflammatory diseases, improving documentation, and supporting task shifting. Embedded within hybrid care models, LLMs enabled scalable education and multimodal data processing, helping reduce diagnostic delays and strengthen patient-centered rheumatology care when properly validated and regulated [7]. Effective prompt engineering was also essential for generating accurate LLMs summaries. Suboptimal prompts often lead to superficial or incorrect outputs, whereas precise phrasing and clear context enable models to produce focused, reliable results [8].

3 | Humans Must Review Model Outputs to Avoid Hallucinations

Although LLMs could automate rheumatology referral summaries, hallucinated or inaccurate content remains a major risk,

TABLE 1 | Overview of current applications of large language models in clinical note generation.

Author (year)	Participants	Study period	Study location	Key findings	Study design	Level of evidence
Williams et al. 2025 [3]	100 inpatient hospital medicine encounters	2019–2022	University of California, San Francisco	GPT-4 Turbo–generated narratives contained more errors but had low harmfulness.	Cross-sectional	Level IV
Song et al. 2025 [4]	592 representative cases	September 1, 2022–August 31, 2023	2400-bed tertiary care hospital, Seoul, Korea	LLM assistant reduced writing time for ED discharge notes	Retrospective	Level II
Small et al. 2025 [5]	100 general medicine admissions	December 2023	New York University Langone Health	LLM-generated summaries more complete, concise, cohesive	Retrospective	Level II
Hartman et al. 2023 [6]	6600 neurology inpatient admissions	2010–2020	New York-Presbyterian/ Weill Cornell Medical Center	Automated summaries comparable to physician narratives	Retrospective	Level II

Abbreviations: ED, emergency department; LLM, large language model.

often masked by confident language [9]. Such errors might misrepresent disease activity and delay care, making expert oversight essential for alignment with clinical guidelines.

If an LLMs mistakenly "hallucinated" a positive antinuclear antibody (ANA) result or an elevated rheumatoid factor (RF) value in a referral document, the triage pathway may be distorted. Patients without autoimmune disease could be prioritized as urgent rheumatology cases, diverting limited clinic capacity from those with true inflammatory arthritis or connective tissue disease. Unnecessary anxiety, extensive workups, and inappropriate immunosuppressive therapy might follow, while genuinely high-risk patients experience delayed assessment and irreversible joint or organ damage. Although AI can generate substantial analyses, it could not replace important thinking. Clinicians must guide data selection, model development, and validation to ensure safe use.

4 | Comparison Between Discriminative AI and Generative AI and Their Clinical Applications

AI in rheumatology could be broadly categorized into discriminative and generative paradigms. Discriminative models learned P(y|x), enabling accurate classification and outcome prediction from clinical variables. These models had supported early RA detection through serologic and imaging features, predicted treatment response in systemic lupus erythematosus (SLE), and enabled clinically meaningful axSpA phenotype mapping that informed risk stratification and linked phenotypic patterns to radiographic progression.

In SLE, discriminative AI models played a valuable role not only in forecasting treatment response but also in early screening. By analyzing structured serologic markers, complement levels, renal parameters, and longitudinal clinical features, these systems could spot patients who may not respond well to treatment before serious organ damage develops. Early identification supports timelier referrals, personalized monitoring, ultimately improving outcomes and conserving limited rheumatology resources.

Generative AI focused on joint probability P(x,y) to produce synthetic data and might support patient education, training, office management, research, and clinical practice. They could make custom handouts, act as virtual tutors, and automate tasks, such as scheduling and triage. In research, they might accelerate literature reviews and hypothesis generation, though risks of inaccuracies remain. Clinically, they could simplify note writing and support problem-solving [9].

Example of a task prompt used to generate structured rheumatology referral summaries included as follows: patient age/sex, chief complaint, symptom duration, relevant joints, functional impact, exam findings, confirmed laboratories (RF, ANA, Erythrocyte Sedimentation Rate/C-Reactive Protein), medications, comorbidities, imaging, and urgency. Keep the summary concise ($\leq$150 words) and suitable for specialist triage.

Discriminative AI supported diagnosis and outcome prediction, whereas generative AI assisted documentation and

communication. Hybrid systems might enhance rheumatology care by combining accuracy and efficiency, but generative outputs risk errors and require careful clinician oversight.

5 | Electronic Medical Record Integration, Multilingual and Clinical Decision Support

Integrating LLM-based referral summarization into EMR systems was essential for wider rheumatology adoption. Such integration enabled automated data extraction, real-time standardized summaries, and identification of missing details, easing documentation while supporting better diagnoses. Future progress must address linguistic and cultural diversity through multilingual, cross-national training to enhance generalizability and collaboration in rare diseases.

Before submission, the referring physician would review and validate the LLM-generated summary, confirm supporting data, and list a few preliminary differential diagnoses. The structured referral would then be forwarded to the rheumatologist, who applies specialist expertise to establish the definitive diagnosis, determine disease severity, and recommend an appropriate treatment and follow-up plan.

LLM-based summarization and decision support could streamline rheumatology workflows by clarifying diagnoses, referral urgency, and initial management. Combined with AI tools that improve early detection, predict progression, and personalize therapy, demonstrated in knee osteoarthritis [10], these technologies enhanced imaging interpretation and shared decision-making, moving rheumatic care toward a patient-centered future.

6 | Conclusion

LLMs have the potential to significantly enhance rheumatology referral quality by improving documentation completeness and efficiency. Current evidence was indirect; future prospective rheumatology-specific LLMs studies remain essential. Combining discriminative and generative AI models could optimize diagnosis and workflow, but real-world validation and careful integration into existing systems were necessary for maximizing their clinical impact. Multilingual capabilities and clinical decision support integration would further enhance their applicability in global rheumatology practice.

Author Contributions

S.-T.S., W.-C.S., S.-C.K., and H.-K.L. had full access to the study data and verified the underlying study data. S.-T.S. led the conception, and W.-C.S. led the data collection and data analysis. S.-T.S., W.-C.S., and S.-C.K. wrote the original draft of this paper. S.-T.S., W.-C.S., S.-C.K., and H.-K.L. contributed to the conception and writing with review and editing of this paper. All authors were involved in study design, data analysis, interpretation, and report writing, and had final responsibility for the decision to submit for publication.

Acknowledgments

The authors have nothing to report.

Funding

The authors have nothing to report.

Conflicts of Interest

The authors declare no conflicts of interest.

Data Availability Statement

Data sharing is not applicable to this article as no datasets were generated or analyzed during the current study.

References

1. J. S. Smolen, D. Aletaha, and I. B. McInnes, "Rheumatoid Arthritis," *Lancet* 388, no. 10055 (2016): 2023–2038, https://doi.org/10.1016/S0140-6736(16)30173-8.

2. D. V. Veen, C. V. Uden, L. Blankemeier, et al., "Adapted Large Language Models Can Outperform Medical Experts in Clinical Text Summarization," *Nature Medicine* 30 (2024): 1134–1142.

3. C. Y. K. Williams, C. R. Subramanian, S. S. Ali, et al., "Physician- and Large Language Model–Generated Hospital Discharge Summaries," *JAMA Internal Medicine* 185, no. 7 (2025): 1–8, https://doi.org/10.1001/jamainternmed.2025.0821.

4. J. Song, J. Park, J. H. Kim, J. W. Song, and S. C. You, "Large Language Model Assistant for Emergency Department Discharge Documentation," *JAMA Network Open* 8, no. 10 (2025): e2538427, https://doi.org/10.1001/jamanetworkopen.2025.38427.

5. W. R. Small, L. O'Donnell, J. Austrian, et al., "Evaluating Hospital Course Summarization by an Electronic Health Record–Based Large Language Model," *JAMA Network Open* 8, no. 8 (2025): e2526339, https://doi.org/10.1001/jamanetworkopen.2025.26339.

6. V. C. Hartman, S. S. Bapat, M. G. Weiner, B. B. Navi, E. T. Sholle, and T. R. Campion Jr, "A Method to Automate the Discharge Summary Hospital Course for Neurology Patients," *Journal of the American Medical Informatics Association* 30, no. 12 (2023): 1995–2003, https://doi.org/10.1093/jamia/ocad177.

7. F. Lechner, J. Knitza, P. Kremer, et al., "Harnessing Large Language Models for Rheumatic Disease Diagnosis: Advancing Hybrid Care and Task Shifting," *International Journal of Rheumatic Diseases* 28, no. 2 (2025): e70124.

8. V. Venerito, D. Lalwani, S. D. Vescovo, et al., "Prompt Engineering: The Next Big Skill in Rheumatology Research," *International Journal of Rheumatic Diseases* 27, no. 5 (2024): e15157.

9. J. Kantor, "ChatGPT, Large Language Models, and Artificial Intelligence in Medicine and Healthcare: A Primer for Clinicians and Researchers," *JAAD International* 13 (2023): 168.

10. C. W. Chen, J. L. H. Shi, Y. H. Lee, and J. C. C. Wei, "Outlook of Future AI-Supported All-Around Rheumatic Disease Management: An Example of Knee Osteoarthritis," *International Journal of Rheumatic Diseases* 28 (2025): e70309, https://doi.org/10.1111/1756-185X.70309.

International Journal of Rheumatic Diseases

WILEY

International Journal of Rheumatic Diseases

ORIGINAL ARTICLE

Impact of Hydroxychloroquine on Mortality and Cardiovascular Outcomes in Systemic Sclerosis: A Retrospective Cohort Study

Bal K. Subedi[1] | Naveen Gautam[2] | Rafal Ali[3] | Irene J. Tan[3]

[1]Internal Medicine, Jefferson Einstein Montgomery Hospital, East Norriton, Pennsylvania, USA | [2]General Medicine, Gulmi Durbar Basic Hospital, Gulmi, Nepal | [3]Rheumatology, Jefferson Einstein Philadelphia Hospital, Philadelphia, Pennsylvania, USA

Correspondence: Bal K. Subedi (bal.subedi@jefferson.edu)

Received: 28 April 2025 | **Revised:** 10 November 2025 | **Accepted:** 9 December 2025

ABSTRACT

Objective: Systemic sclerosis (SSc) is a rare autoimmune disease with high mortality, often due to cardiopulmonary complications. Hydroxychloroquine (HCQ), commonly used in other rheumatic diseases, has immunomodulatory and potentially cardioprotective effects, but its role in SSc remains unclear. This study aimed to evaluate the association between HCQ use and the risk of mortality, ischemic heart disease (IHD), and pulmonary hypertension (PH) in a large real-world SSc cohort.

Methods: This retrospective cohort study utilized de-identified electronic medical records from the TriNetX Research network. Adults with an SSc diagnosis (ICD-10-CM: M34) were divided into HCQ users and non-users. After 1:1 propensity score matching for demographics, comorbidities and medications, outcomes including mortality, PH, acute myocardial infarction (MI), cerebral infarction, conduction heart disease, and myocarditis were assessed over 5 years. Risk ratios (RR) and Kaplan–Meier hazard ratios were calculated.

Results: Out of 17 395 HCQ users and 58 576 non-users, 15 485 propensity score matched pairs were analyzed. Over 5 years, HCQ users showed higher PH (RR 1.124, 95% CI, 1.052–1.200, $p < 0.001$) but lower mortality (RR 0.719, 95% CI, 0.674–0.767, $p < 0.001$), indicating potential survival benefits. No significant differences were observed for IHD, MI, cerebral infarction, conduction disorders, or myocarditis.

Conclusion: Our research indicated that although patients on HCQ had a higher prevalence of PH, they exhibited lower mortality rates, suggesting a possible survival benefit. Further prospective studies are needed to explore these findings and clarify HCQ's role in SSC management.

1 | Introduction

Systemic sclerosis (SSc) is a rare, chronic autoimmune disease characterized by widespread microvascular damage, immune activation, and progressive fibrosis of the skin and internal organs [1, 2]. It predominantly affects women and carries the highest case-specific mortality among connective tissue diseases [3], largely due to complications like interstitial lung disease (ILD) and pulmonary arterial hypertension (PH) [1, 3, 4]. Other significant manifestations include gastrointestinal, renal, musculoskeletal, and primary cardiac involvement, leading to substantial morbidity [3, 5].

The complex pathophysiology involves endothelial injury, immune dysregulation with characteristic autoantibodies, and fibroblast activation leading to excessive matrix deposition [2, 3]. Early vascular changes, potentially triggered by genetic predisposition and environmental factors, lead to abnormal vasoreactivity (like Raynaud's phenomenon, present in > 95% of patients) and microvascular obliteration [2, 3, 5]. This is followed by innate and

adaptive immune activation, involving T cells (especially Th2), B cells, macrophages, and the release of pro-inflammatory and profibrotic cytokines such as Interleukin-6 (IL-6) and Transforming Growth Factor-beta (TGF-β) [2]. Autoantibodies, such as anti-topoisomerase I (Scl-70) and anti-centromere antibodies, are common and associated with specific clinical phenotypes and prognoses [2, 3]. Cardiac involvement stems from similar processes, including microvascular ischemia–reperfusion injury ("cardiac Raynaud's"), inflammation, and patchy myocardial fibrosis, affecting heart function and conduction [5, 6].

Hydroxychloroquine (HCQ), an antimalarial drug with immunomodulatory effects, is standard therapy in systemic lupus erythematosus (SLE) and rheumatoid arthritis (RA) [7]. It also exhibits potentially beneficial pleiotropic effects, including antithrombotic and metabolic actions, suggesting cardiovascular protection in some contexts [6, 7]. However, its role in SSc is unclear, lacking strong evidence for major organ modification, and rare long-term cardiotoxicity is a concern [7–10]. Given the high cardiovascular burden in SSc [4, 6], this study aimed to evaluate the association between HCQ use and the risk of mortality, ischemic heart disease, and pulmonary hypertension (PH) in a large, propensity score-matched real-world SSc cohort.

2 | Materials and Methods

2.1 | Data Source and Study Design

This study utilized de-identified electronic medical record (EMR) data accessed through the TriNetX Research network, a global federated health research platform which facilitates clinical and translational research by partnering with healthcare organizations (HCOs) and provides billions of clinical facts on more than 275 million patients. The platform is ISO 27001:2013 certified and HIPAA compliant as it provides self-service access to de-identified electronic health record data and follows GDPR regulations. At the time of analysis (December 31, 2024), the network included data from 104 HCOs, primarily located in the United States. We conducted a retrospective cohort study comparing outcomes between SSc patients treated with HCQ and those not treated with HCQ. The study protocol was generated using the TriNetX analytics platform and institutional review board approval was not required due to the use of aggregated, de-identified patient data (as per de-identification standard defined in Section §164.514(b)(1) of the HIPAA Privacy Rule).

2.2 | Cohort Selection

Two patient cohorts were defined based on criteria applied to the TriNetX Research network database. Cohort 1 (HCQ users) included patients aged 18 years or older with diagnosis code for SSc (ICD-10-CM: M34) and medication record for HCQ (RxNorm: 5521) on or after the date of their SSc diagnosis (ICD-10-CM: M34). Cohort 2 (HCQ non-users) included patients aged 18 years or older with diagnosis code for SSc (ICD-10-CM: M34) who did not have any medication record for HCQ (RxNorm: 5521).

The index event for each patient was defined as the date of the first qualifying event meeting the cohort criteria. For cohort 1, the index date was defined as the date of the first HCQ prescription that occurred after the first SSc diagnosis, to ensure HCQ exposure followed the SSc diagnosis. For Cohort 2, the index date was the first date of the SSc diagnosis. Only index events occurring within the last 5 years from the analysis date were included.

2.3 | Propensity Score Estimation and Matching

To account for baseline differences between patients receiving HCQ and those who did not, propensity score matching (PSM) was performed on all available patient characteristics. The propensity score was estimated using a logistic regression model that predicted the likelihood of HCQ use based on covariates measured at the index date. The covariates included demographic factors such as age at index, race, ethnicity, and sex; clinical diagnoses including diabetes mellitus, hypertensive diseases, hyperlipidemia, chronic kidney disease (CKD), tobacco use, overweight and obesity, and other secondary PH; and medication exposures including methotrexate, sulfasalazine, azathioprine, angiotensin-converting enzyme inhibitors, angiotensin receptor blockers, aspirin, statins, mycophenolate mofetil, rituximab, prednisone, and methylprednisolone. Matching was conducted using the nearest neighbor algorithm without replacement, and no caliper width was specified. Balance between cohorts was assessed using standardized mean differences, with an absolute value less than 0.10 considered acceptable. After matching,15 485 patients receiving HCQ were matched to an equal number of non-users, and all covariates achieved standardized mean differences below 0.10. Pre- and post-match standardized mean differences are presented in (Table S1), and the corresponding propensity score density plot is shown in (Figure S1). Data on SSc subtype, serologic profile, and disease duration were unavailable in this database, including SSc subtype (limited/diffuse), disease duration, key serological profiles (e.g., anti-Scl-70, anti-centromere antibodies), and baseline diagnosis of ILD. The absence of these critical indicators may contribute to residual confounding, as these factors strongly influence both prognosis and treatment decisions.

2.4 | Outcome of Interest

The primary outcomes of interest were assessed within a time window starting 1 day after the index date and ending 1825 days (5 years) after the index date. Outcomes were identified using relevant ICD-10-CM codes or specific demographic flags within the EMR data. The specific outcomes analyzed were IHD (ICD-10 I20-I25), Acute Myocardial Infarction (Acute MI) (ICD-10 I21), Cerebral Infarction (ICD-10 I63), Conduction Heart Disease (ICD-10 I45), Myocarditis (ICD-10 I51.4), Mortality (Deceased status flag), and PH (ICD-10 I27.2). For the risk and survival analyses of each outcome, patients who had a record of the specific outcome prior to the index event were excluded from the analysis for that specific outcome to ensure the cohort was at risk.

2.5 | Statistical Analysis

All analyses were performed on the propensity score-matched cohorts. Baseline characteristics were summarized using means and standard deviations (SD) for continuous variables and counts and percentages for categorical variables. Differences between groups post-matching were assessed using *p*-values from *t*-tests or chi-squared tests as appropriate, alongside standardized differences. Data on HCQ dosage, cumulative dose, and medication adherence or duration were not available in the database. Therefore, our analysis defines exposure as at least one prescription and could not distinguish between short-term and long-term use.

For each outcome, the following analyses were conducted. Risk analysis involved calculating the proportion of patients experiencing the outcome within the 5 year window for each cohort. Risk ratio (RR) with 95% confidence interval (CI) comparing Cohort 1 (HCQ Users) to Cohort 2 (HCQ non-users) were calculated. Survival analysis utilized Kaplan–Meier survival curves to estimate the probability of remaining free from the outcome over the 5-year time window. Patients were censored at the date of their last recorded activity in the database if they did not experience the outcome during follow-up. The log-rank test was used to compare survival distributions between the two cohorts. Furthermore, a Cox proportional hazards model was constructed on the matched cohort to calculate the hazard ratio (HR) and 95% CI for each outcome. All analyses were performed using the TriNetX analytics platform. A p-value < 0.05 was considered statistically significant.

3 | Results

This analysis compared outcomes between patients with SSc treated with HCQ (Cohort 1: SCC on HCQ) and those not treated with HCQ (Cohort 2: SCC without HCQ) using data from the TriNetX Research network, encompassing 104 HCOs.

3.1 | Cohort Characteristics and Propensity Score Matching

Initially, Cohort 1 included 17 395 patients and Cohort 2 included 58 576 patients. Propensity score matching was performed to balance baseline characteristics between the two groups. The characteristics used for matching included demographics (age at index, race, sex, ethnicity) and diagnoses/medications such as diabetes mellitus, hypertensive diseases, hyperlipidemia, CKD, tobacco use, obesity, methotrexate use, various antihypertensives (losartan, lisinopril, etc.), aspirin, statins (atorvastatin, rosuvastatin, etc.), mycophenolate mofetil, and rituximab.

After PSM, each cohort consisted of 15 485 patients. The matching process successfully balanced most baseline characteristics between the cohorts, as indicated by the standardized differences and *p*-values. Notably, characteristics like age at index, race (White, Black or African American, Asian), ethnicity (Hispanic or Latino), diagnoses (CKD, Tobacco use, Overweight/obesity), and use of most medications (methotrexate, sulfasalazine, azathioprine, most antihypertensives, statins, mycophenolate mofetil, rituximab) showed small, standardized differences and non-significant or borderline *p*-values post-matching (Table 1). After matching, standardized mean differences for all covariates were less than 0.10, indicating adequate balance between groups. Some minor differences remained post-matching for variables like sex (Female/Male), diabetes mellitus, hypertensive diseases, hyperlipidemia, aspirin use, and atorvastatin use, although the standardized differences were generally small (≤ 0.042). A figure depicting the propensity score density functions before and after matching was also generated, visually demonstrating the improved balance after matching (Figure 1).

3.2 | Outcome Analyses (Post-Matching)

Outcome analyses were performed on the propensity score-matched cohorts. The time window for analysis started 1 day after the index event and ended 1825 days (5 years) after the index event. Patients with the outcome prior to the time window were excluded from the respective risk and survival analyses for specific outcomes. The detailed results for each outcome analysis are presented in (Table 2).

For Ischemic Heart Diseases, after excluding patients with prior events, the risk analysis showed a higher risk in the HCQ group (10.2% vs. 9.6%; RR 1.058, 95% CI, [0.983, 1.138], $p = 0.124$) but the difference was not statistically significant.

Similarly, for Acute MI, after exclusions, the risk analysis revealed no significant difference in risk between the HCQ group (3.0%) and the non-HCQ group (3.2%; RR 0.935, 95% CI, [0.823, 1.062], $p = 0.298$).

For Cerebral Infarction, following exclusions, both groups had a similar incidence, the risk analysis indicated no significant difference in risk (2.1% in both groups; RR 0.986, 95% CI, [0.846, 1.149], $p = 0.854$).

Analysis of Conduction Heart Disease, after exclusions, showed no significant difference in risk (3.1% in HCQ user vs. 3.2% in non HCQ group; RR 0.955, 95% CI, [0.842, 1.083], $p = 0.469$).

For Myocarditis, after exclusions, the risk analysis found no significant difference in the very low risk (0.3% in both groups, RR 1.128 95% CI, [0.762, 1.670], $p = 0.546$).

Analysis of Mortality revealed a significant difference after exclusions. The risk analysis showed a significantly lower risk of death in the HCQ group (9.0%) compared to the non-HCQ group (12.5%; RR 0.719, 95% CI, [0.674, 0.767], $p < 0.001$). The Kaplan–Meier survival analysis strongly confirmed this finding, showing a significant difference in survival distributions between the two groups (Log-Rank $p < 0.001$) (Figure 2). Furthermore, a Cox proportional hazards model demonstrated a significantly lower hazard of death in the HCQ group (HR 0.641, 95% CI, 0.599–0.687, $p = 0.015$).

Finally, for PH, after excluding patients with prior events, the risk analysis indicated a statistically significant higher risk in

TABLE 1 | Baseline characteristics of systemic sclerosis patients after propensity score matching.

Characteristic	Cohort 1 (HCQ Users) ($N=15485$)	Cohort 2 (Non-users) ($N=15485$)	p	Std. diff.
Demographics				
Age at ndex (years), Mean ± SD	54.0 ± 15.3	54.5 ± 16.3	0.003	0.033
Female, *n* (%)	13 612 (87.9)	13 411 (86.6)	0.001	0.039
Male, *n* (%)	1629 (10.5)	1818 (11.7)	0.001	0.039
Race				
White, *n* (%)	9079 (58.6)	9158 (59.1)	0.362	0.010
Black or African American, *n* (%)	2166 (14.0)	2048 (13.2)	0.051	0.022
Asian, *n* (%)	1199 (7.7)	1279 (8.3)	0.094	0.019
Hispanic or Latino, *n* (%)	1446 (9.3)	1473 (9.5)	0.600	0.006
Diagnoses (comorbidities)				
Diabetes mellitus, *n* (%)	1671 (10.8)	1810 (11.7)	0.012	0.028
Hypertensive diseases, *n* (%)	5086 (32.8)	5424 (35.0)	< 0.001	0.046
Hyperlipidemia, unspecified, *n* (%)	2697 (17.4)	2941 (19.0)	< 0.001	0.041
Chronic kidney disease (CKD), *n* (%)	1325 (8.6)	1345 (8.7)	0.686	0.005
Tobacco use, *n* (%)	301 (1.9)	320 (2.1)	0.441	0.009
Overweight and obesity, *n* (%)	1901 (12.3)	2069 (13.4)	0.004	0.032
Other secondary pulmonary hypertension, *n* (%)	1991 (12.9)	2017 (13.0)	0.660	0.005
Medications				
Methotrexate, *n* (%)	1412 (9.1)	1312 (8.5)	0.045	0.023
Sulfasalazine, *n* (%)	144 (0.9)	111 (0.7)	0.038	0.024
Azathioprine, *n* (%)	606 (3.9)	545 (3.5)	0.067	0.021
Losartan, *n* (%)	1136 (7.3)	1230 (7.9)	0.044	0.023
Lisinopril, *n* (%)	1670 (10.8)	1746 (11.3)	0.168	0.016
Valsartan, *n* (%)	470 (3.0)	480 (3.1)	0.742	0.004
Captopril, *n* (%)	126 (0.8)	125 (0.8)	0.949	0.001
Ramipril, *n* (%)	69 (0.4)	73 (0.5)	0.737	0.004
Enalapril, *n* (%)	221 (1.4)	227 (1.5)	0.775	0.003
Irbesartan, *n* (%)	96 (0.6)	101 (0.7)	0.721	0.004
Azilsartan, *n* (%)	10 (0.1)	10 (0.1%)	1.0	< 0.01
Olmesartan, *n* (%)	144 (0.9)	151 (1.0)	0.682	0.005
Telmisartan, *n* (%)	59 (0.4)	61 (0.4)	0.855	0.002
Aspirin, *n* (%)	3151 (20.3)	3386 (21.9)	0.001	0.037
Atorvastatin, *n* (%)	1637 (10.6)	1825 (11.8)	0.001	0.039
Rosuvastatin, *n* (%)	610 (3.9)	659 (4.3)	0.160	0.016
Lovastatin, *n* (%)	105 (0.7)	128 (0.8)	0.130	0.017
Simvastatin, *n* (%)	746 (4.8)	812 (5.2)	0.086	0.020

(Continues)

TABLE 1 | (Continued)

Characteristic	Cohort 1 (HCQ Users) ($N=15485$)	Cohort 2 (Non-users) ($N=15485$)	p	Std. diff.
Fluvastatin, *n* (%)	13 (0.1)	11 (0.1)	0.683	0.005
Mycophenolate mofetil, *n* (%)	1668 (10.8)	1648 (10.6)	0.713	0.004
Rituximab, *n* (%)	246 (1.6)	232 (1.5)	0.519	0.007
Prednisone, *n* (%)	5053 (32.6)	5375 (34.7)	<0.001	0.044
Methylprednisone, *n* (%)	2878 (18.6)	3086 (19.9)	0.003	0.034

Abbreviations: HCQ, Hydroxychloroquine; SD, Standard Deviation; Std. Diff., Standardized Difference. Data presented as Mean ± SD or *n* (%).

the HCQ group (12.9%) compared to the non-HCQ group (11.5%; RR 1.124, 95% CI, [1.052, 1.200], $p<0.001$).

4 | Discussion

This large, propensity score-matched cohort study utilizing the TriNetX real-world database investigated the association between HCQ use and major outcomes in patients with SSc. Our primary findings indicate that after adjusting for numerous baseline demographic and clinical characteristics, HCQ use was associated with a statistically significant reduction in all-cause mortality over a 5-year follow-up period. However, paradoxically, HCQ use was also associated with a significantly increased risk of developing IHD and PH, based on risk analyses. No significant associations were found for acute MI, cerebral infarction, conduction heart disease, or myocarditis.

The observed reduction in mortality associated with HCQ use aligns with findings from at least one previously published retrospective SSc cohort study [9], although that study examined mortality determinants without focusing specifically on HCQ's effect on different causes of death. In SLE, HCQ is well-established to improve survival [7]. The potential mechanisms underlying a survival benefit in SSc remain speculative but could relate to HCQ's broad immunomodulatory effects, potentially attenuating systemic inflammation or specific disease processes not captured in our measured outcomes [7]. For instance, HCQ might influence factors identified as independent mortality predictors in SSc, such as elevated C-reactive protein (CRP) [4], via its anti-inflammatory actions [7]. Alternatively, its known pleiotropic effects, such as antithrombotic properties [6, 7], could be beneficial in a prothrombotic disease like SSc, or metabolic benefits might play a role [7]. This finding is particularly relevant given the high mortality burden in SSc, often linked to cardiopulmonary complications like ILD and PH [1, 3, 4]. While newer therapies like mesenchymal stem cell transplantation (MSCT) also show promise for improving survival in severe SSc [11], the potential benefit of a widely available drug like HCQ warrants further investigation. However, our study, being observational, cannot definitively prove causality, and residual confounding may still exist despite PSM [12].

The findings regarding increased risk of IHD and PH associated with HCQ use in our SSc cohort are unexpected and differ from the cardioprotective effects generally attributed to HCQ in other rheumatic diseases like SLE and Sjögren's syndrome [6, 7]. SSc itself confers a high risk of various cardiovascular complications, including primary cardiac involvement (myocardial fibrosis, microvascular disease, conduction abnormalities), PAH, and potentially accelerated macrovascular atherosclerosis [3–6]. The increased risk might reflect residual confounding by indication, where HCQ might be preferentially used in patients with subtle, unmeasured characteristics associated with higher cardiovascular risk, despite matching on measured confounders [12]. Alternatively, the underlying pathophysiology of SSc might alter the drug's effects. For instance, HCQ's impact on endothelial function or myocardial processes could differ in the context of SSc-specific vasculopathy (intimal proliferation, capillary loss) and fibrosis [2, 3, 5]. Significantly, one recent large database study found that medium-to-long-term HCQ use was associated with a higher risk of pulmonary vascular disease (PVD) in patients with ILD [13]. Given that ILD is a common and severe manifestation of SSc [1, 3], this finding by Yeh et al. [13] lends credence to our observation regarding PH risk, suggesting HCQ might have complex or even detrimental effects on the pulmonary vasculature in certain chronic inflammatory lung contexts, potentially related to drug adherence, dosage, or interaction with viral triggers as hypothesized by the authors [13]. This contrasts starkly with a small pilot study abstract suggesting HCQ might improve markers of endothelial injury (E-selectin, VCAM-1, ET-1) and nailfold videocapillaroscopy scores in SSc over 3 months [14]. This discrepancy highlights potentially differential short-term versus long-term effects, or that these biomarkers may not accurately reflect clinical risk for IHD or PH development. The lack of association with conduction disease or myocarditis in our study, despite these being known cardiac issues in SSc [3, 5], further complicates the interpretation of the IHD/PH findings.

Concerns regarding HCQ cardiotoxicity, though rare, typically involve cardiomyopathy or conduction system abnormalities arising after prolonged use (often > 10 years) and high cumulative doses, or in acute overdose settings [7, 10]. These classic manifestations, often identified via ECG changes or biopsy findings of lysosomal disruption [7], differ from the IHD and PH outcomes assessed in our study. Fram et al.'s systematic review pre-COVID-19 emphasized the rarity of cardiac events with appropriate HCQ use, finding most cases linked to cumulative doses exceeding 1 400 000 mg [10]. While our study lacked data on HCQ dosage and duration, it is unlikely that the observed increased risk of IHD/PH represents typical HCQ-induced cardiomyopathy or conduction block, especially

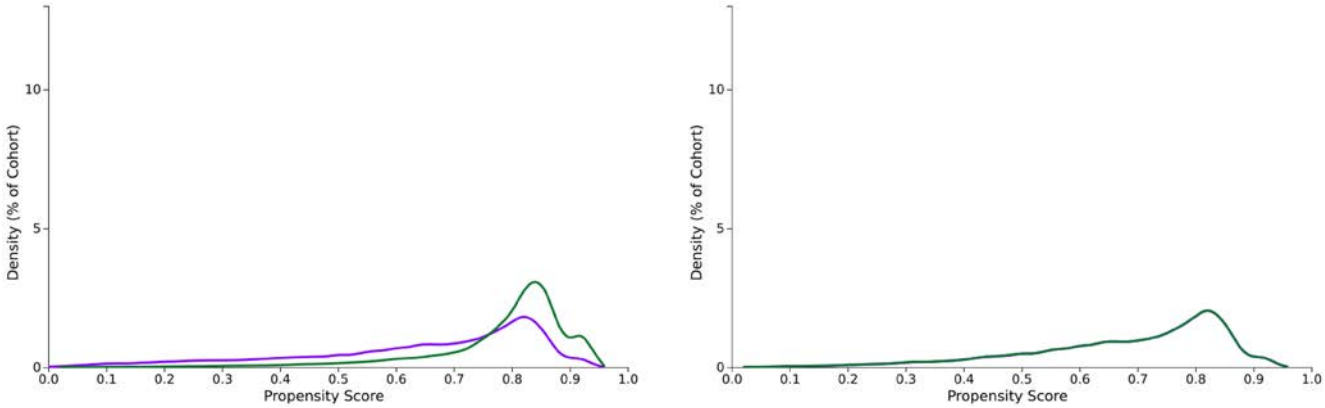

FIGURE 1 | Propensity score distribution plot (showing distributions before and after matching); (cohort 1—purple, cohort 2—green).

TABLE 2 | Comparison of clinical outcomes over 5 years between HCQ users and non-users in systemic sclerosis after propensity score matching.

Outcomes[a,b]	HCQ users (*N* = 15485)	HCQ non-users (*N* = 15485)	RR (95% CI)	*p*
Mortality (*n*, %)	1393 (9.01%)	1936 (12.54%)	0.719 (0.674, 0.767)	< 0.001
Pulmonary hypertension (*n*, %)	1686 (12.9%)	1464 (11.48%)	1.124 (1.052, 1.200)	< 0.001
Ischemic heart disease (*n*, %)	1376 (10.17%)	1281 (9.6%)	1.058 (0.985, 1.138)	0.124
Acute myocardial infarction (*n*, %)	446 (2.9%)	473 (3.16%)	0.935 (0.823, 1.062)	0.298
Cerebral infarction (*n*, %)	318 (2.10%)	322 (2.1%)	0.986 (0.846, 1.149)	0.854
Conduction heart disease (*n*, %)	460 (3.05%)	478 (3.19%)	0.955 (0.842, 1.083)	0.469
Myocarditis (*n*, %)	53 (0.30%)	47 (0.30%)	1.128 (0.762, 1.670)	0.546

Abbreviations: HCQ: Hydroxychloroquine, MACE: Major Cardiovascular Events, *N*: total number of patients in the cohort, *n*: Number of patients affected by the outcome, RR: Relative Risk, 95% CI: 95% Confidence Interval.
[a]Propensity matching balanced cohorts according to demographic variables, laboratory results, associated comorbidities, and use of medications at baseline.
[b]Patients who had outcome before time window were excluded from each cohort.

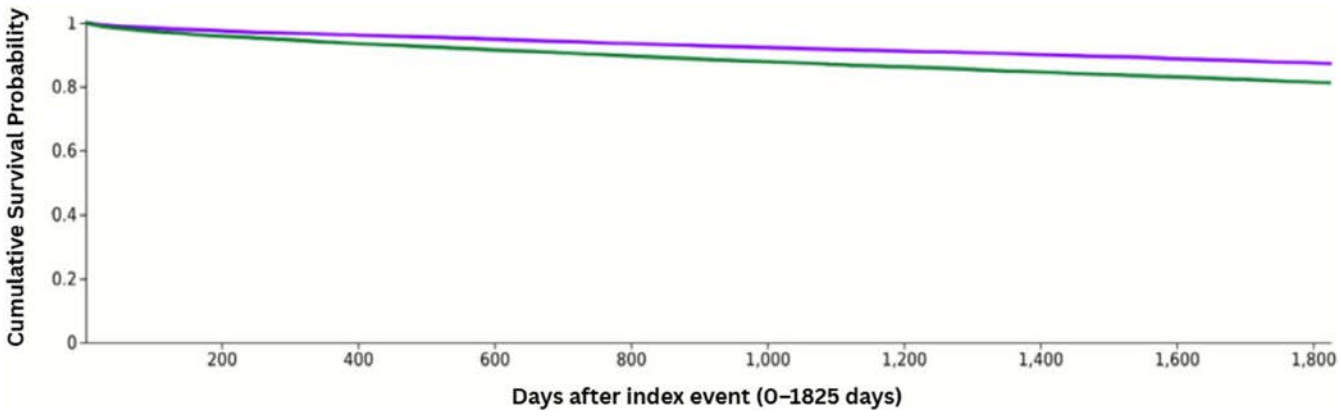

FIGURE 2 | Kaplan–Meier survival curve for mortality; (cohort 1—purple, cohort 2—green).

given the 5-year timeframe. However, whether HCQ could subtly exacerbate underlying SSc-related myocardial ischemia (potentially through effects on microvasculature [5] or pulmonary vascular remodeling through mechanisms distinct from its classic toxicity profile) remains speculative. Furthermore, the limited proven efficacy of HCQ for major SSc manifestations, as reflected in recent EULAR guidelines [8] and the lack of effect on functional outcomes (HAQ-DI, CHFS) in the large EUSTAR cohort [9], must be weighed against any potential risks.

This study utilized a large TriNetX sample with PSM to reduce confounding, but several limitations warrant consideration. Residual confounding from unmeasured SSc-specific prognostic indicators persists, including disease subtype (limited/diffuse), disease duration, serological profiles (anti-RNA polymerase III associated with SRC risk [3]), baseline ILD presence/severity, lifestyle factors, and HCQ dosage, duration, adherence, and treatment initiation/discontinuation reasons. Confounding by indication is a major concern, as HCQ may be preferentially prescribed to milder disease patients with inherently better

prognosis, potentially exaggerating observed survival benefit [12]. Despite PSM achieving SMDs < 0.1, statistically significant differences remained for sex, hypertension, hyperlipidemia, and prednisone use; these were not included as covariates in final survival models and may represent residual confounding sources. ICD-10 code reliance introduces misclassification bias: PH (I27.2) does not distinguish SSc-associated PAH from ILD-associated PH (distinct pathophysiologies potentially responding differently to HCQ), and IHD codes (I20-I25) cannot separate atherosclerotic disease from SSc-specific microvascular impairment or primary SSc cardiac involvement such as patchy fibrosis [3, 5]. HCQ exposure definition lacks dosage, adherence, and cumulative duration data, preventing differentiation between continuous long-term users and short-term trials, which may dilute true treatment effects. The database does not specify missing value rates or handling methods, precluding selection bias assessment from complete case analysis. The analysis did not account for competing risks (e.g., death from ILD before PH development), potentially overestimating outcomes like PH. The 5-year timeframe may miss longer-term effects or toxicity [10]. Inability to perform subgroup analyses based on key SSc phenotypes (limited vs. diffuse cutaneous SSc, anti-Scl-70 vs. anti-centromere antibodies) prevents determination of whether observed associations—lower mortality and higher PH risk—are consistent across all SSc populations or driven by specific unmeasured subgroups. The observational design precludes causal inference, and contrasting mortality vs. IHD/PH findings underscore the complexity of evaluating drug effects in heterogeneous diseases like SSc using observational data [12].

5 | Conclusion

This large propensity score-matched analysis of real-world data suggests a complex and potentially paradoxical association between HCQ use and outcomes in SSc. While HCQ was associated with significantly lower 5 year mortality, it was also unexpectedly associated with an increased risk of PH diagnoses. These findings highlight the need for cautious interpretation, mandate further investigation ideally including prospective studies with detailed data collection or potentially targeted RCTs.

Author Contributions

The author takes full responsibility for this article.

Conflicts of Interest

No financial grants were received for this project. Otherwise, the authors have no conflicts of interest to disclose.

Data Availability Statement

As per TriNetX data sharing regulations and/or guidelines.

References

1. A. Bergamasco, N. Hartmann, L. Wallace, and P. Verpillat, "Epidemiology of Systemic Sclerosis and Systemic Sclerosis-Associated Interstitial Lung Disease," *Clinical Epidemiology* 11 (2019): 257–273.

2. A. H. Rosendahl, K. Schönborn, and T. Krieg, "Pathophysiology of Systemic Sclerosis (Scleroderma)," *Kaohsiung Journal of Medical Sciences* 38 (2022): 187–195.

3. R. Adigun, A. Goyal, and A. Hariz, "Systemic Sclerosis (Scleroderma)," in *StatPearls [Internet]* (StatPearls Publishing, 2024).

4. S. D. Chaves, T. Porel, D. Adoue, et al., "THU0362 Predictors of Mortality in Systemic Sclerosis [Abstract]," *Annals of the Rheumatic Diseases* 79 (2020): 412–413.

5. C. Bruni and L. Ross, "Cardiac Involvement in Systemic Sclerosis: Getting to The Heart of The Matter [Review]," *Best Practice & Research. Clinical Rheumatology* 35 (2021): 101668.

6. P. Mani, D. Gonzalez, S. Chatterjee, and M. D. Faulx, "Cardiovascular Complications of Systemic Sclerosis: What to Look for," *Cleveland Clinic Journal of Medicine* 86 (2019): 685–695.

7. E. Haładyj, M. Sikora, A. Felis-Giemza, and M. Olesińska, "Antimalarials–are They Effective and Safe in Rheumatic Diseases?," *Reumatologia* 56 (2018): 164–173.

8. F. Del Galdo, A. Lescoat, P. G. Conaghan, et al., "EULAR Recommendations for the Treatment of Systemic Sclerosis: 2023 update," *Annals of the Rheumatic Diseases* 84 (2025): 29–40.

9. S. Bellando-Randone, H. Wilhalme, C. Bruni, et al., The Effect of Hydroxychloroquine on Activities of Daily Living and Hand Function in Systemic Sclerosis: Results From an Analysis of the EUSTAR Cohort.

10. G. Fram, D. D. Wang, K. Malette, et al., "Cardiac Complications Attributed to Hydroxychloroquine: A Systematic Review of the Literature pre-COVID-19," *Current Cardiology Reviews* 17 (2021): 319–327.

11. W. Yuan, M. Liu, D. Yang, et al., "Improvement in Long-Term Survival With Mesenchymal Stem Cell Transplantation in Systemic Sclerosis Patients: A Propensity Score-Matched Cohort Study," *Stem Cell Research & Therapy* 16 (2025): 128.

12. E. J. Boyko, "Observational Research—Opportunities and Limitations," *Journal of Diabetic Complications* 27 (2013): 642–648.

13. J. J. Yeh, S. H. Syue, Y. F. Sun, et al., "Hydroxychloroquine on the Pulmonary Vascular Diseases in Interstitial Lung Disease: Immunologic Effects, and Virus Interplay," *Biomedicine* 10 (2022): 1290.

14. F. Basta, R. Irace, A. Borgia, et al., "FRI0312 Hydroxychloroquine Significantly Reduces Serum Markers of Endothelial Injury and Nemo Videocapillaroscopy Score in Systemic Sclerosis: a 3-Months Prospective Observational Study [Abstract]," *Annals of the Rheumatic Diseases* 78 (2019): 837–838.

Supporting Information

Additional supporting information can be found online in the Supporting Information section. **Figure S1:** Covariate balance before and after propensity score matching. This plot displays the absolute SMD for baseline characteristics across three categories: Demographics, diagnosis, and medication. Red solid circles represent the imbalance between HCQ users and non-users prior to matching (pre-matching). Blue open circles represent the balance achieved after 1:1 propensity score matching (post-matching). As shown, all covariates achieved an SMD of < 0.10 after matching, indicating adequate balance between the two study cohorts. **Table S1:** Propensity score matching balance metrics.

International Journal of Rheumatic Diseases

WILEY

International Journal of Rheumatic Diseases

EDITORIAL

Clinical Recommendations of the Qazaq College of Rheumatology for the Diagnosis and Treatment of Rheumatoid Arthritis: 2025 National Initiative

Galymzhan Togizbayev[1] | Aigul Turtayeva[2] | Gulzhan Gabdullina[3] | Zharkynay Akhmetova[4] | Bibikhan Eraliyeva[3]

[1]JSC "Research Institute of Cardiology and Internal Diseases", Almaty, Kazakhstan | [2]South Kazakhstan Medical Academy, Shymkent, Kazakhstan | [3]Asfendiyarov Kazakh National Medical University, Almaty, Kazakhstan | [4]City Rheumatology Center, Almaty, Kazakhstan

Correspondence: Galymzhan Togizbayev (g.togizbayev@gmail.com)

Received: 8 January 2026 | **Revised:** 8 January 2026 | **Accepted:** 28 January 2026

Rheumatoid arthritis (RA) remains a major cause of disability and reduced quality of life worldwide [1], with notable differences in disease management across regions. In Kazakhstan, the increasing burden of RA [2] and the need for harmonized care have led to the development of the country's first comprehensive national clinical recommendations for the diagnosis and treatment of RA under the leadership of the Qazaq College of Rheumatology (QCR) in 2025.

While international guidelines from the European Alliance of Associations for Rheumatology (EULAR) [3], the American College of Rheumatology (ACR) [4], and the British Society for Rheumatology (BSR) provide robust frameworks for RA management, their implementation often requires regional adaptation. Kazakhstan presents several unique epidemiological and healthcare system considerations, including:

- A higher prevalence of latent tuberculosis and viral hepatitis;
- A substantial burden of comorbidities such as osteoporosis and cardiovascular disease;
- Variability in access to biologic and targeted synthetic DMARDs;
- Pregnancy-related considerations due to the younger age at RA onset in many patients.

The QCR 2025 recommendations were developed by a national expert panel integrating international evidence with local epidemiological data and clinical experience from rheumatology centers across the country. The recommendations are aligned with the 2022 EULAR and 2021 ACR guidelines while addressing clinical priorities specific to Kazakhstan.

Key components of the 2025 QCR recommendations include:

- A standardized diagnostic framework based on clinical assessment, serological markers (RF, anti-CCP, anti-MCV), and imaging;
- Prioritization of early initiation of csDMARD therapy (with methotrexate as the anchor drug), followed by bDMARDs or tsDMARDs in cases of inadequate response;
- Integration of IL-6 inhibitors (tocilizumab, olokizumab [5], levilimab [6]) into treatment algorithms for patients with an inadequate response to csDMARDs or with poor prognostic factors;
- Individualized management strategies for RA patients with comorbid conditions such as interstitial lung disease, heart failure, and viral hepatitis;
- A tailored approach to pregnancy planning and management based on EULAR points to consider;
- Rigorous screening and prophylaxis for latent tuberculosis infection among patients initiating biologic therapy.

Consistent with EULAR and ACR principles, the QCR recommendations emphasize treat-to-target strategies, regular monitoring of disease activity (DAS28), and shared decision-making between clinicians and patients. At the same time, the initiative highlights issues of particular relevance to Kazakhstan and other countries in Central Asia.

For example, the management of latent tuberculosis infection (LTBI) remains critical in a country with an intermediate TB burden. The new recommendations outline clear screening and prophylactic treatment pathways developed in collaboration with infectious disease specialists. Likewise, viral hepatitis B and C, prevalent in the region, are addressed with guidance on safe use of csDMARDs, bDMARDs, and tsDMARDs in affected patients.

In pregnant patients, the recommendations adapt EULAR guidance to local practice, supporting the use of sulfasalazine, glucocorticoids, and selected TNF inhibitors during pregnancy and lactation, while strictly avoiding teratogenic agents such as methotrexate and leflunomide.

The QCR guidelines also encourage integration of RA management into Kazakhstan's national digital health strategy, including expansion of national RA registries to collect real-world data and improve health system planning [7]. This experience of adapting international recommendations to local conditions may provide a useful model for other countries in Central Asia, Eastern Europe, and low- and middle-income regions.

Looking ahead, the Qazaq College of Rheumatology is committed to:

- Continuous evaluation and updating of the national RA recommendations;
- Expansion of RA registries and real-world data initiatives;
- Strengthening patient-centered care through education and shared decision-making;
- Enhancing regional collaboration to advance evidence-based rheumatology.

The development of national clinical recommendations represents an important milestone in improving the quality of RA care in Kazakhstan and contributes to global efforts to ensure equitable access to evidence-based rheumatologic treatment for all patients.

Author Contributions

G.T.: conceptualization, writing – project administration, original draft preparation, review and editing. A.T.: methodology, literature search, writing. G.G.: data curation, formal analysis. Z.A.: visualization, validation, clinical expertise. B.E.: evidence verification and pharmacological expertise.

Acknowledgments

The authors have nothing to report.

Funding

The authors have nothing to report.

Conflicts of Interest

The authors declare no conflicts of interest.

Data Availability Statement

No new data were generated or analyzed for this article. Data sharing is not applicable.

References

1. J. S. Smolen, D. Aletaha, and I. B. McInnes, "Rheumatoid Arthritis," *Lancet* 388, no. 10055 (2016): 2023–2038.

2. GBD 2021 Rheumatoid Arthritis Collaborators, "Global, Regional, and National Burden of Rheumatoid Arthritis, 1990–2020, and Projections to 2050: A Systematic Analysis of the Global Burden of Disease Study 2021," *Lancet Rheumatology* 5, no. 10 (2023): e594–e610.

3. J. S. Smolen, R. B. M. Landewé, S. A. Bergstra, et al., "EULAR Recommendations for the Management of RA: 2022 Update," *Annals of the Rheumatic Diseases* 82, no. 1 (2023): 3–18.

4. L. Fraenkel, J. M. Bathon, B. R. England, et al., "2021 ACR Guideline for Treatment of RA," *Arthritis and Rheumatology* 73, no. 7 (2021): 1108–1123.

5. G. Togizbayev, E. Y. Polishchuk, E. S. Filatova, et al., "Olokizumab Effect on Chronic Pain in RA: PROLOGUE Study," *International Journal of Rheumatic Diseases* 27, no. 10 (2024): e15320.

6. A. I. Zagrebneva, E. N. Simonova, Y. A. Gavrikova, and G. A. Togizbayev, "High Efficacy and Retention Rate of Levilimab in Real-Life RA Practice," *Rheumatology Science and Practice* 63, no. 1 (2025): 70–78.

7. G. Togizbayev, I. Shametekov, D. Maksot, et al., "Biologic Therapy in Rheumatology: Analysis of Multidisciplinary Teams in Kazakhstan," *International Journal of Rheumatic Diseases* 28, no. 6 (2025): e70304.

International Journal of Rheumatic Diseases

WILEY

International Journal of Rheumatic Diseases

ORIGINAL ARTICLE

Neutrophil Extracellular Traps Induce PANoptosis and Inflammatory Responses in Fibroblast-Like Synoviocytes of Rheumatoid Arthritis

Xing Zhang[1] | Shaoqing Yang[2] | Jun Li[1] | Jing Mao[1] | Jianhui Ma[3] | Haili Shen[4]

[1]The Second Hospital and Clinical Medical School, Lanzhou University, Lanzhou, Gansu, China | [2]Ultrasound Medical Center, the Second Hospital and Clinical Medical School, Lanzhou University, Lanzhou, Gansu, China | [3]Department of Rheumatism and Immunology, Affiliated Hospital of Gansu Medical College (Ping Liang People's Hospital), Pingliang, Gansu, China | [4]Department of Rheumatology, the Second Hospital and Clinical Medical School, Lanzhou University, Lanzhou, Gansu, China

Correspondence: Haili Shen (shenhl@lzu.edu.cn)

Received: 19 July 2025 | **Revised:** 26 August 2025 | **Accepted:** 14 October 2025

Funding: This study was funded by the Science and Technology Program of Gansu Province (No. 23JRRA1510), the Science and Technology Program of Lanzhou (No. 2024-3-77), and the Gansu Province Health Industry Scientific Research Project (No. GSWSKY2024-01).

Keywords: AIM2 | NETs | PANoptosis | rheumatoid arthritis

ABSTRACT

Introduction: Neutrophil extracellular traps (NETs) significantly contribute to rheumatoid arthritis (RA) pathogenesis, though their exact mechanisms remain unclear. In this research, we explored how NETs influence RA development through the PANoptosis core molecule AIM2.

Methods: Enzyme-linked immunosorbent assay and Quant-iT Pico Green measured AIM2 and cell-free DNA (cfDNA) levels in synovial fluid. Immunohistochemistry examined the levels of AIM2 in synovial tissues. In vitro, the CCK-8 assay evaluated cell proliferation. Western blot detected the expression changes of AIM2, PANoptosis-related proteins, and NF-κB pathway-related proteins. Real-time quantitative PCR measured mRNA levels of IL-1β, IL-18, and IL-6. Immunofluorescence quantified AIM2, Caspase-8, GSDMD, and p-MLKL fluorescence intensity and cfDNA/AIM2 co-localization. An AIM2-silenced cell model was established to examine changes in the AIM2, PANoptosis-related proteins, and NF-κB pathway-related proteins (Western blot), fluorescence intensity (IF), inflammatory cytokine transcription (RT-qPCR), and RA-FLS migration (scratch and transwell assays).

Results: Our results showed an increase in AIM2 expression in RA synovial fluid and tissues, which correlates with both cfDNA high levels and clinical disease activity scores. In vitro, in RA fibroblast-like synoviocytes (RA-FLSs), NETs elevated AIM2 and PANoptosis-related protein levels, activated the NF-κB signaling pathway, and enhanced the release of inflammatory cytokines. Treatment with DNase1 and AIM2 silencing resulted in lower levels of PANoptosis proteins and AIM2, inhibited NF-κB signaling, and decreased cytokine production.

Conclusion: This is the first time exploring the pathogenic mechanism of NETs-induced PANoptosis in RA, and targeting AIM2 may represent a potential new therapeutic approach for RA.

1 | Introduction

RA is a chronic systemic autoimmune disease that significantly impacts patients' health and quality of life, with its pathogenic mechanisms remaining incompletely understood [1]. Although current treatment options have significantly improved clinical outcomes in RA patients, treatment non-response rates persist at 5.5% [2] to 27.5% [3], indicating a failure to meet clinical needs. This phenomenon highlights the urgent need to investigate novel mechanisms of RA pathogenesis.

Neutrophils serve as pivotal effector cells during the inflammatory phase of RA [4]. Upon external stimulation, these cells undergo nuclear membrane rupture, releasing NETs. Beyond their established role in innate immunity against pathogens, NETs significantly contribute to autoimmune pathogenesis [5, 6]. NETs are a double-edged sword: The right amount of NETs can reduce inflammation, but excessive release or insufficient clearance can easily lead to an inflammatory imbalance and damage normal cells or tissues. Evidence indicates that aberrant NETs accumulation triggers various programmed cell death (PCD) pathways, including pyroptosis and necroptosis [7, 8]. PANoptosis, a recently identified PCD pathway [9], integrates molecular features of pyroptosis, apoptosis, and necroptosis through sophisticated cross-regulation mechanisms [10]. PANoptosis is involved in multiple systemic disorders, including infectious diseases [11], malignancies [12], neurodegenerative conditions [13], and autoimmune disorders [14]. Notably, recent studies have established connections between NETs and PANoptosis induction [15, 16]. Current research predominantly focuses on individual PCD pathways in NETs-mediated RA pathogenesis [7, 17], while the crosstalk between different PCD modalities in RA development remains largely unexplored. Elucidating these mechanisms will deepen our understanding of RA pathophysiology.

AIM2, a member of the IFN-inducible pyrin and HIN domain (PYHIN) protein family, functions as a cytosolic DNA sensor. AIM2 binds to double-stranded DNA (dsDNA) in a sequence-independent manner [18], mediating inflammatory responses and immune defense mechanisms. As a major component of NETs, DNA acts as a damage-associated molecular pattern (DAMP) that can be recognized by various cellular DNA sensors, including Toll-like receptor 9 (TLR9), cyclic GMP-AMP synthase (cGAS) [19], retinoic acid-inducible gene I (RIG-I), and AIM2. CfDNA has been demonstrated to participate in the progression of RA [20, 21]. AIM2 contributes to multiple pathological processes in RA [22]. Recent studies indicate that cfDNA can induce hepatocyte PANoptosis through AIM2 activation [23]. Furthermore, cytosolic DNA accumulation may represent a crucial factor in AIM2-mediated RA pathogenesis [24]. Given that the precise molecular mechanisms of NETs in RA remain incompletely understood, the DNA-AIM2 signaling axis may constitute a critical pathogenic link in NETs-mediated RA development.

This study investigates novel mechanisms of NETs-induced RA-FLSs damage. For the first time, we demonstrate that AIM2 regulates NETs-mediated PANoptosis in RA-FLSs and promotes the release of inflammatory cytokines through the AIM2/NF-κB signaling pathway. These findings offer an innovative therapeutic target for RA.

2 | Materials and Methods

2.1 | Clinical Data

Joint fluid samples from RA patients ($n = 29$) and other non-RA arthritis patients (Non-RA, $n = 30$; included patients with OA, $n = 21$; primary Gout, $n = 5$; Traumatic arthritis, $n = 4$) were collected by those who attended the Department of Rheumatology and Immunology at the Second Hospital of Lanzhou University between October 2023 and June 2024. RA patients were included according to the new diagnostic criteria jointly introduced by the American College of Rheumatology (ACR) and the European League Against Rheumatism (EULAR) in 2010. Inclusion criteria: patients with a definite diagnosis of RA with knee joint cavity effusion, aged 18 years or older. Exclusion criteria: suffering from other rheumatic diseases, severe infections, other autoimmune diseases, acute inflammation, fever, thyroid disease, diabetes mellitus, neoplasms, pregnancy, and severe liver and kidney diseases.

Human synovial tissues were obtained from patients with RA who underwent total knee arthroplasty at the Department of Orthopedics of the Second Hospital of Lanzhou University ($n = 5$) or from trauma controls (TC) who underwent traumatic knee surgery after a car accident ($n = 5$). The study protocol was approved by the Ethics Committee of the Second Hospital and Clinical Medical School (No. 2024A-147), and all participants provided written informed consent.

2.2 | Reagents and Antibodies

Primary antibodies used in this experiment: anti-AIM2 (20590-1-AP, Proteintech, China), anti-caspase 8 (13423-1-AP, Proteintech, China), anti-c.Caspase 8 (#8592, Cell Signaling Technology, USA), anti-GSDMD-NT (ab215203, Abcam, USA), anti-BAX (20590–1-AP, Proteintech, China), anti-BCL-2 (12789-1-AP, Proteintech, China), anti-MLKL (66675-1-I, Proteintech, China), anti-p-MLKL (#18640, Cell Signaling Technology, USA), anti-p65 (ab32536, Abcam, USA), anti-p-p65 (ab31624, Abcam, USA), anti-p-IκBα (ab133462, Abcam, USA), anti-GAPDH (60004-1Ig, Proteintech, China).

2.3 | Enzyme-Linked Immunosorbent Assay (ELISA)

The level of AIM2 (Yutong, Jiangsu, China) in synovial fluid was detected using ELISA assay kits according to the manufacturer's instructions.

2.4 | Isolation of Neutrophils and Induction of NETs

Neutrophils were obtained from healthy human peripheral blood by density gradient centrifugation. The lower leukocyte

layer was collected. The collected cells were subsequently suspended in RPMI-1640 medium (Gibco, NY, USA). The plates were treated with 100 nM Phorbol 12-myristate 13-acetate (PMA, Selleck, China) for 4 h. After removing the culture medium, the NETs attached to the bottom were eluted with Ca^{2+}/Mg^{2+}-free PBS. Centrifuge to collect the supernatant. NETs supernatants were mixed with Pico Green (Invitrogen, USA) and fluorescence was measured (Ex/Em = 480/520 nm) using a microplate reader (Thermo Fisher Scientific, USA). Finally, the concentration of NETs was determined using a standard curve that had been established.

2.5 | Microscopic Detection of NETs Production

Isolated and purified neutrophils were suspended in 96-well plates (5×10^3/well), where one group was stimulated with 100 nM PMA and the other without any stimulation, and co-incubated for 4 h at 37°C and 5% CO_2. SYTOX Green (Invitrogen, USA) was added at 5 μM and stained for 10 min, protected from light. Nets' generation and distribution were directly observed under a fluorescence microscope.

2.6 | Cell Line Culture

RA-FLSs were purchased from Jennio Biologicals (Guangzhou, China). Cells were cultured at 37°C and 5% CO_2 in a humidified environment with complete medium with DMEM (Gibco, NY, USA), 10% FBS, and 1% penicillin–streptomycin solution. Subsequent experiments were performed using 3rd–10th generation RA-FLSs.

2.7 | Small Interfering RNA (siRNA) Transfection

AIM2 siRNA (si-AIM2) and the corresponding negative control siRNA (si-NC) were constructed by Gemma Biotechnology (Shanghai, China) with the following sequences: AIM2 siRNA: 5′-GCAAGCAGGAGAUGUUUCATT-3′, siRNA control: 5′-UGAAACAUCUCCUGCUUUGCTT-3′. AIM2 was silenced by siRNA according to the manufacturer's instructions, and the efficiency of AIM2 silencing was detected by qRT-PCR and WB. When the RA-FLS growth density reached 50%–60%, the siRNA (si-AIM2 and si-NC), Buffer, and siRNA mate plus were mixed according to the manufacturer's instructions. We continued the incubation with complete medium with 10% FBS. Experiments were performed 24 or 48 h after transfection.

2.8 | Hematoxylin Eosin (H&E) Staining

Fresh human synovial tissue was fixed with 4% paraformaldehyde, dehydrated, and embedded in paraffin, then sectioned into 4-μm-thick slices. The paraffin sections were baked, dewaxed, and hydrated, and then sequentially stained with hematoxylin and eosin dyes. Finally, the sections were dehydrated with alcohol, then clarified with xylene, and subsequently sealed with neutral resin. They were then observed under a microscope (Olympus, Japan).

2.9 | Immunohistochemical (IHC) Staining

First, paraffin sections were dewaxed and rehydrated, and sodium citrate buffer was heated in a microwave to retrieve the antigen. Then, the sections were washed, incubated overnight with the anti-AIM2 primary antibody, and then incubated at room temperature for 10 min after the addition of the secondary antibody. Finally, the sections were examined using DAB chromogenic examination, stained with hematoxylin, dehydrated with a graded series of alcohols, and sealed with neutral resin. They were then visualized under a microscope (Olympus, Japan).

2.10 | Cell Counting Kit 8 (CCK8) Assay

RA-FLSs (5×10^3/well) were inoculated into 96-well plates. The following day, stimuli of varying conditions were added to the wells, and the cells were further incubated for 24 h. Subsequently, 10 μL of CCK8 reagent (Biosharp, Guangzhou, China) was added to each well. The absorbance of each well was measured at 450 nm to calculate cell viability.

2.11 | Western Blot (WB) Analysis

Samples were collected, and samples were extracted by centrifugation using RIPA lysis buffer (Solarbio, Beijing, China), which contains protease inhibitors and phosphatase inhibitors. The BCA assay kit (Solarbio, Beijing, China) was used to determine the concentration of extracted proteins. Proteins were then separated by SDS-PAGE and transferred to PVDF membranes. After 5% skim milk was incubated for 1 h at room temperature, the PVDF membranes were incubated with the primary antibody overnight at 4°C. The secondary antibody was then incubated for 1 h. Finally, the bands were visualized with the ECL kit and quantified using ImageJ software.

2.12 | Quantitative Real-Time Polymerase Chain Reaction (qRT-PCR) Assays

Total RNA of RA-FLSs was extracted using Trizol reagent (AgBio, Hunan, China). Reverse transcription and elimination of genomic DNA were performed by the Prime Script RT kit with gDNA Eraser (Takara Bio Inc. Japan). Subsequently, the synthesized cDNA was used as a template for qRT-PCR and amplified on Bio-Rad CFX96 (Bio-Rad Inc. USA) using the TB green Premixed Ex Taq II Kit (Takara Bio, Japan). The relative expression of each target gene was normalized against β-actin, using the $2^{-\Delta\Delta Cq}$ method for calculation. The primers used for cDNA amplification were as follows (forward and reverse): IL-1β, 5′-CCGACCACCACTACAGCAAGG-3′ and 5′-GGGCAGGGAACCAGCATCTTC-3′; IL-6, 5′-GCCTTCGGTCCAGTTGCCTTC-3′ and 5′-GTTCTGAAGAGGTGAGTGGCTGTC-3′; IL-18, 5′-TGACCAAGGAAATCGGCCTC-3′ and 5′-CCATACCTCTAGGCTGGCTA-3′; AIM2 siRNA: 5′-GCAAGCAGGAGAUGUUUCATT-3′ and 5′-CTTGGGTCTCAAACGTGAAGG-3′. β-Actin, 5′-ACCCTGAAGTACCCCATCGAG-3′ and 5′-AGCACAGCCTGGATAGCAAC-3′.

2.13 | High-Content Cell Imaging

RA-FLSs (5×10^3/well) were inoculated into 96-well high-content staining plates. The next day, 500 ng/mL NETs were added to the experimental wells, and an equal volume of 10% complete medium was added to the control group. Pre-staining was performed by adding SYTOX Green (green) and Hochest (blue) for 20 min. Visualized in non-confocal mode using a 63× (N.A. 1.15) objective on a PerkinElmer Opera High Intensity Imaging System. Images were analyzed using the PerkinElmer Opera system for image analysis.

2.14 | Immunofluorescence (IF)

The cell-crawling slices were placed, and RA-FLSs (4×10^4/well) were inoculated in 24-well plates overnight and then subjected to different treatments. Cells were fixed with 4% paraformaldehyde for 10 min. Then, it was closed with 2% BSA for 30 min at room temperature. Cells were incubated with the antibodies to Caspase 8, GSDMD, AIM2, SYTOX Green, or p-MLKL at 4°C overnight. The cells were incubated with a fluorescent secondary antibody at room temperature for 1 h. Cells were incubated with DAPI for 15 min, and then dropwise added with anti-quencher. The images were observed by an inverted fluorescence microscope (Olympus, Japan).

2.15 | Wound Healing Assay

RA-FLSs (4×10^5/well) were grown in 6-well plates. The next day, the cells were treated in different ways. The cellular monolayer was scratched using sterile 200-μL pipette tips. Then, the cells were treated with NETs for 24 h. ImageJ software was used to observe the gaps at 0 and 24 h after scratching and calculate the area of the scratched area.

2.16 | Migration Experiments

AIM2-silenced and non-silenced AIM2 RA-FLS (1.5×10^4/well) were resuspended in serum-free DMEM medium and grown in the upper compartment of a Transwell (Corning, New York, USA). In the experimental group, 200 μL of a 500 ng/mL NETs and serum-free DMEM mixture was added, whereas the control group received serum-free DMEM only. The lower chamber was filled with 800 μL of DMEM containing 20% FBS. After 24 h of incubation at 37°C, cells were fixed, stained with 1% crystal violet/methanol solution, observed under the microscope (Olympus, Japan), and counted with ImageJ.

2.17 | Statistical Analysis

GraphPad Prism 10.0 was used for statistical analysis, and data are expressed as mean ± standard deviation (SD). An independent samples *t*-test was used to compare the two groups. One-way analysis of variance (ANOVA) with Tukey's multiple comparisons test was used for multiple group comparisons. We performed Bartlett's test/Brown-Forsythe test to confirm homogeneity of variances across comparison groups. Correlation analysis was performed using Spearman's rank correlation method. $p<0.05$ was regarded as a significant difference. Each experiment was repeated more than three times.

3 | Results

3.1 | The Expression of AIM2 and cfDNA Was Up-Regulated in Synovial Fluid and Synovial Tissues of RA Patients

To investigate AIM2 and cfDNA expression in RA, we compared synovial fluid samples from the RA group ($n=29$) and the non-RA group ($n=30$) using ELISA and Pico Green assay. The RA group exhibited significantly higher AIM2 and levels ($p<0.001$, Figure 1A). Pico Green assay [25] revealed elevated cfDNA in RA synovial fluid ($p<0.0001$, Figure 1B, Table S1). Spearman correlation analysis demonstrated a positive association between AIM2 and cfDNA levels in synovial fluid ($r=0.4126$, $p=0.0032$; Figure 1C). Further analysis of clinical significance found that synovial fluid AIM2 levels correlated with disease activity (DAS28-ESR; $r=0.4673$, $p=0.0220$; Figure 1D), suggesting its involvement in RA progression. We further examined synovial tissues from 5 RA patients and 5 TC patients. H&E analysis showed RA synovium exhibited marked synovial hyperplasia and inflammatory infiltration compared to TC samples (Figure 1G). Immunohistochemistry and WB confirmed significantly higher AIM2 expression in RA synovium (Figure 1E–G). These findings indicate that AIM2 level is associated with synovial proliferation and inflammation.

3.2 | NETs Stimulation Upregulates AIM2 Expression in RA-FLSs

SYTOX Green staining confirmed successful NETs formation induced by PMA (Figure 2A). CCK-8 assays demonstrated that 500 ng/mL NETs significantly reduced RA-FLS viability (Figure 2B). Combined with previous research findings [7, 26, 27], subsequent experiments were performed at this concentration. Following 24-h stimulation with 500 ng/mL NETs, WB analysis revealed markedly increased AIM2 protein expression in RA-FLSs (Figure 2C,D). Immunofluorescence verified enhanced AIM2 fluorescence intensity in NETs-treated groups compared to controls (Figure 2E). These findings collectively indicate that NETs stimulation upregulates AIM2 expression in RA-FLSs.

3.3 | NETs Induce PANoptosis in RA-FLSs In Vitro

Given the established role of NETs in inducing cellular damage across various disease models, we hypothesized that NETs might similarly cause cellular injury or death in RA-FLSs. We found that after 24 h of treatment in RA-FLS with 500 ng/mL NETs, Bax, cleavage Caspase 8 (c.Caspase8), GSDMD-FL, and its N-terminal fragment (GSDMD-NT) were increased, while the expression of BCL-2 was down-regulated. At the same time, the ratio of phosphorylated mixed series protein kinase-like domains (p-MLKL) to total MLKL was also increased (Figure 3A–F). IF staining further confirmed

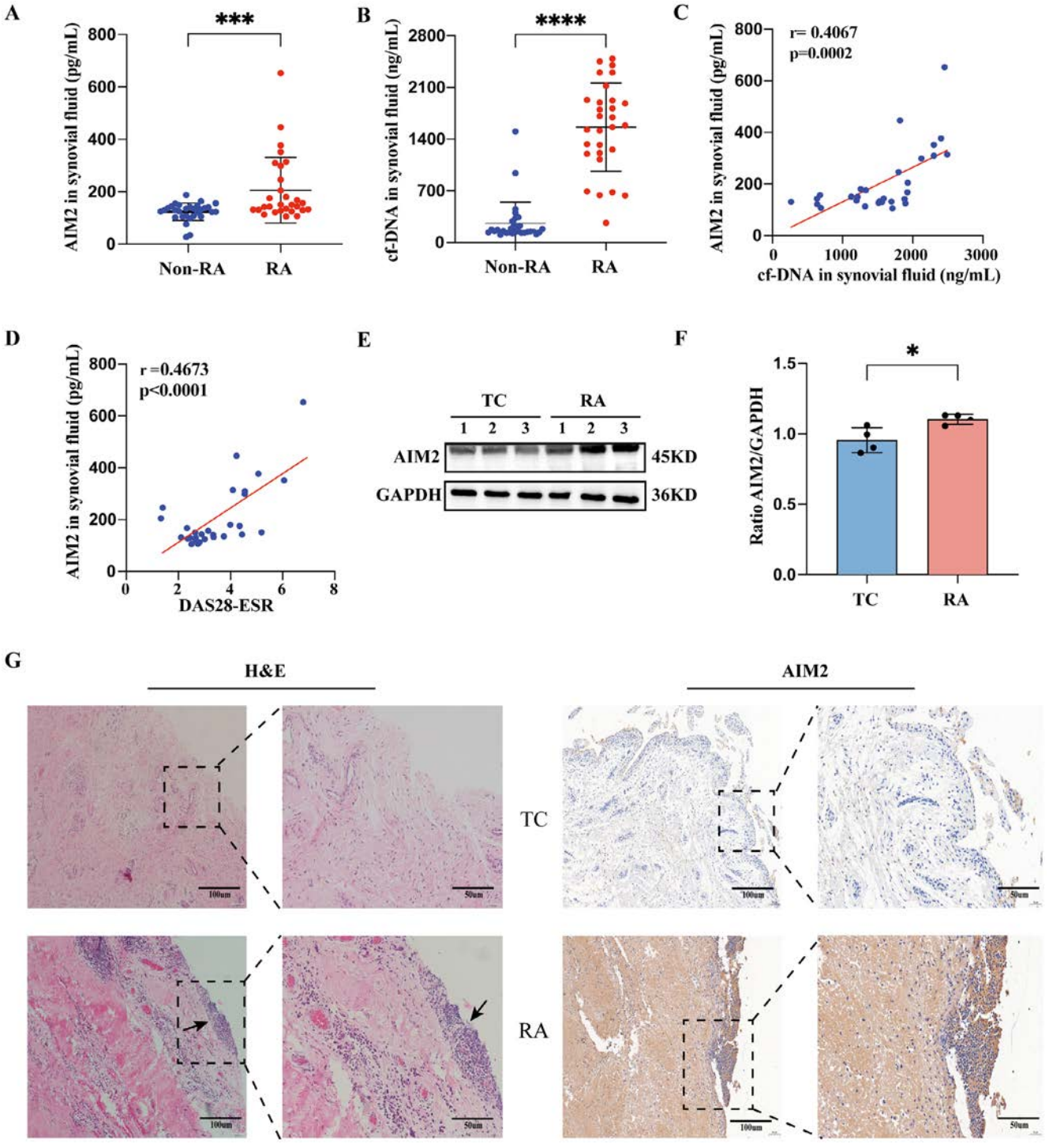

FIGURE 1 | The expression characteristics and clinical correlations of AIM2 and cfDNA in the synovial fluid and tissues of RA patients are investigated. (A, B) Compared to the Non-RA group ($n = 30$), the RA group ($n = 29$) showed significantly elevated levels of AIM2 and cfDNA in synovial fluid. (C) AIM2 level in RA synovial fluid was correlated with cfDNA expression. (D) AIM2 level in RA synovial fluid was correlated with DAS28-ESR scores. (E, F) The protein expression of AIM2 in synovium tissues from RA ($n = 3$) patients and TC ($n = 3$) patients was detected by WB analysis, along with their quantitative results. (GAPDH as a loading control). (G) Representative H&E staining images of AIM2 in the synovial tissues of RA patients and TC patients ($n = 5$; dashed boxes indicate magnified regions; scale bars = 100/50 μm). RA tissues exhibited marked synovial hyperplasia and inflammatory cell infiltration, whereas TC tissues showed no significant synovial thickening or inflammation. Representative IHC staining images of AIM2 in the synovial tissues of RA patients and TC patients ($n = 5$; dashed boxes indicate magnified regions; scale bars = 100/50 μm). DAS28-ESR, Disease Activity Score in 28 joints based on erythrocyte sedimentation rate. Each experiment is replicated at least three times independently. *$p < 0.05$, ***$p < 0.001$, and ****$p < 0.0001$.

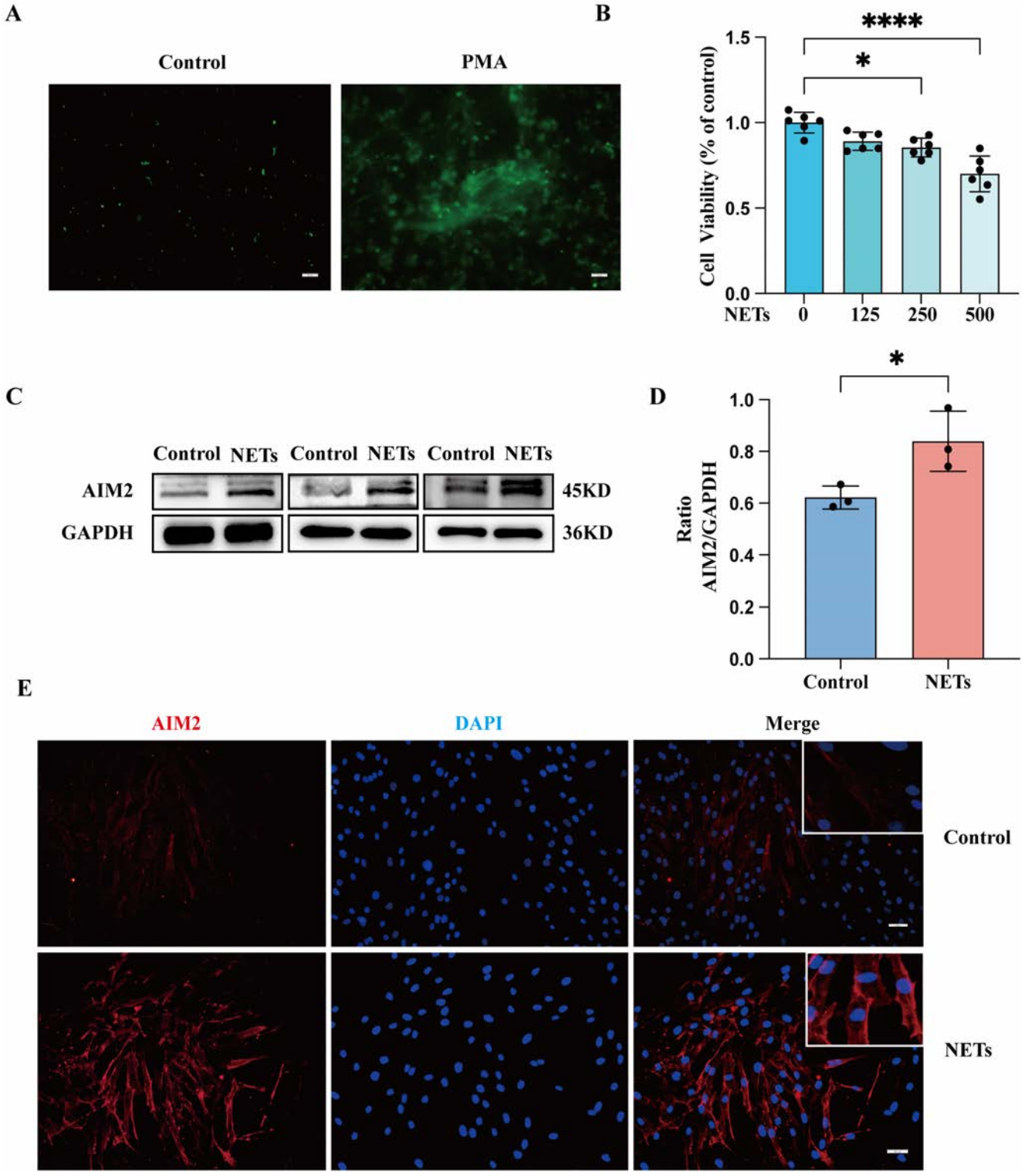

FIGURE 2 | The effects of NETs stimulation on AIM2 expression in RA-FLSs were investigated. (A) SYTOX Green staining demonstrated successful induction of NETs by PMA (scale bar = 100 μm, magnification: ×20). (B) Cell viability was assessed by CCK-8 assay after 24-h treatment with varying NETs concentrations (0, 125, 250, 500 ng/mL). Data are analyzed by one-way ANOVA with Tukey's multiple comparisons test, FB = 17.97. The *p* value of Bartlett's test is 0.3612. (C, D) The protein expression of AIM2 in RA-FLSs following 24-h stimulation with 500 ng/mL NETs was detected by WB analysis, along with their quantitative results (GAPDH served as a loading control). (E) Representative Immunofluorescence staining images of AIM2 by RA-FLSs treated with NETs (scale bar = 100 μm, magnification: ×20). Each experiment is replicated at least three times independently. $^{*}p < 0.05$, $^{****}p < 0.0001$.

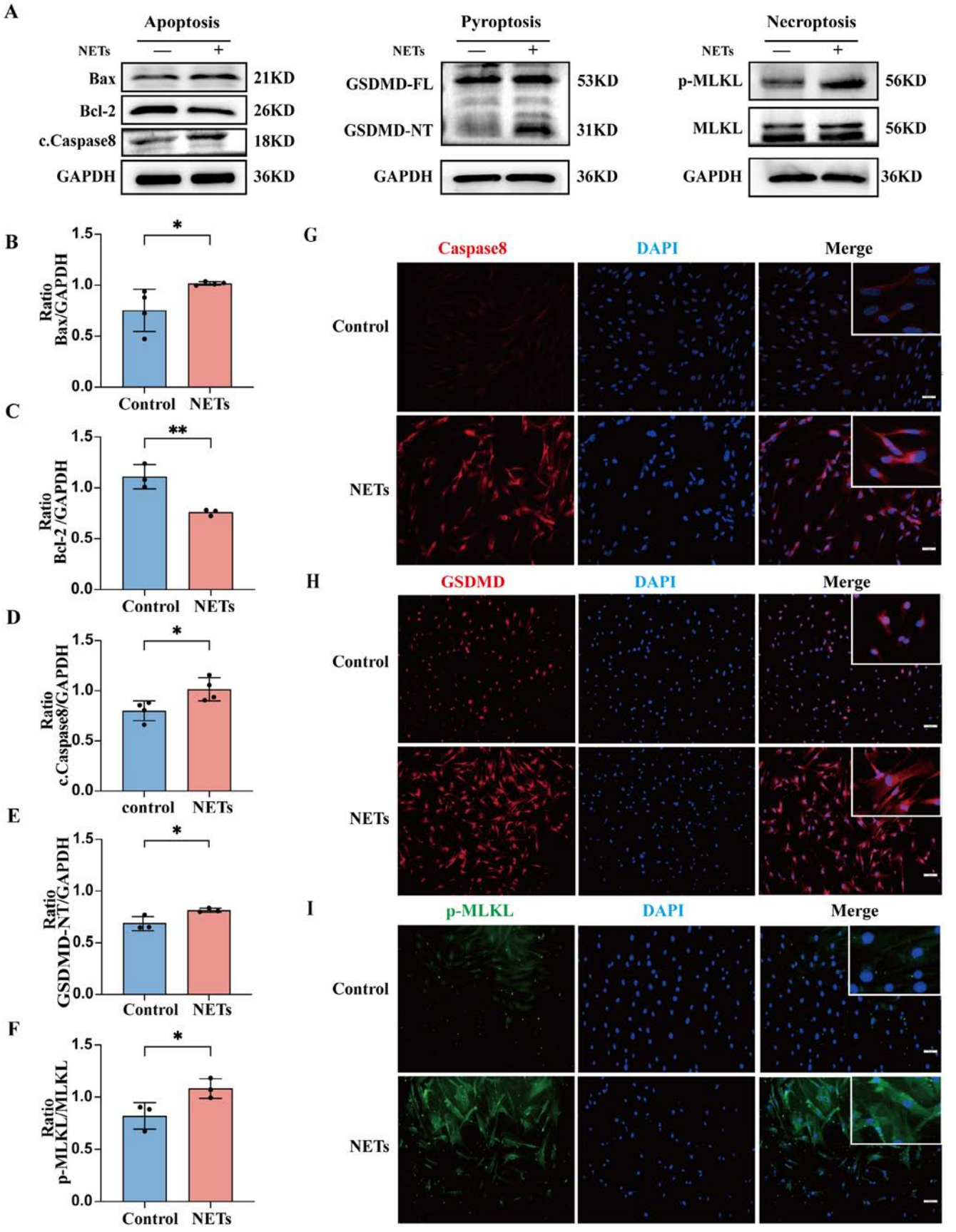

FIGURE 3 | 500 ng/mL NETs induce PANoptosis in RA-FLSs. (A–F) The expression changes of PANoptosis-related proteins were detected by WB analysis, along with their quantitative results (GAPDH served as a loading control, and total MLKL was used as a reference for p-MLKL). (G–I) Immunofluorescence representative images of Caspase-8, GSDMD, and p-MLKL in differently treated RA-FLSs (scale bar = 100 μm; magnification: ×20). Each experiment is replicated at least three times independently. $^{*}p < 0.05$, $^{**}p < 0.01$.

enhanced fluorescence intensity of Caspase8, GSDMD, and p-MLKL in the NETs-treated group compared to controls (Figure 3G–I). Experimental results found that NETs could induce PANoptosis of RA-FLSs in vitro.

3.4 | NETs Activate AIM2 to Induce PANoptosis in RA-FLSs

To investigate whether cfDNA activates AIM2 to induce PANoptosis in RA-FLSs, we used DNase I as a DNA scavenger for reverse validation [28]. CCK8 assays demonstrated that the 50 U/mL DNase1 + 500 ng/mL NETs treatment group significantly increased OD values compared to the control group (0 U/mL DNase1 + 500 ng/mL NETs) (Figure 4A), indicating reduced cell death and partial restoration of viability. WB analysis revealed that the 50 U/mL DNase1 + 500 ng/mL NETs treatment group significantly altered PANoptosis-related protein expression profiles, characterized by decreased levels of Bax, cleaved Caspase8, GSDMD-FL, GSDMD-NT, MLKL, and p-MLKL, along with increased BCL-2 expression (Figure 4B–H,J). It confirmed that DNase1 reverses NETs-induced PANoptosis. To further elucidate the regulatory role of AIM2 in NETs-mediated PANoptosis, we found that the expression of AIM2 was downregulated in the 50 U/mL DNase1 + 500 ng/mL NETs treatment group (Figure 4I,K). Using SYTOX Green-labeled NETs DNA components, high-content live-cell imaging showed progressive accumulation of extracellular cfDNA and an increase in intracellular fluorescence intensity, indicating RA-FLSs internalized cfDNA (Figure 4M). What's more, internalized cfDNA co-localized with AIM2 in RA-FLSs (Figure 4L). These findings demonstrate cfDNA-mediated AIM2 activation as a key mechanism in NETs-induced RA-FLSs PANoptosis.

3.5 | Silencing AIM2 Inhibits PANoptosis of RA-FLSs

To determine whether AIM2 serves as a critical mediator of NET-induced PANoptosis in RA-FLSs, we performed gene silencing using AIM2-specific siRNA. QRT-PCR and WB confirmed efficient AIM2 knockdown (Figure 5A–C). WB results revealed significant downregulation in the expression levels of AIM2 and PANoptosis-related proteins in the si-AIM2 + NETs group compared to the si-NC + NETs group (Figure 5D–J). Immunofluorescence staining further validated these findings, showing reduced fluorescence intensity of AIM2, Caspase-8, GSDMD, and p-MLKL in the si-AIM2 + NETs group compared with the si-NC + NETs group (Figure 5K–N). These results suggest that AIM2 silencing reverses NETs-induced PANoptosis in RA-FLSs.

3.6 | AIM2 Exacerbates RA Inflammation via the NF-κB Pathway

PANoptosis is accompanied by the release of various inflammatory cytokines [29, 30]. Our qRT-PCR analysis revealed that NET stimulation significantly upregulated the expression of IL-1β, IL-18, and IL-6 in RA-FLSs compared to si-NC, with particularly marked increases in IL-1β and IL-18. AIM2 silencing significantly inhibited this cytokine release (Figure 6K–M). To investigate whether cytokine release occurs through the AIM2/NF-κB pathway, we examined p65, p-p65, and p-IκBα by WB and found that NETs stimulation significantly increased the expression of these pathway components (Figure 6A–C). AIM2 knockdown effectively suppressed their activation (Figure 6D–F). These findings demonstrate that AIM2 serves as a key regulator of cytokine release in RA-FLSs, with NF-κB acting as the downstream mediator of the inflammatory pathway. Wound healing and Transwell migration assays demonstrated that NETs significantly enhanced RA-FLS migration compared to si-NC controls, an effect that was inhibited by AIM2 silencing (Figure 6G–J). In conclusion, NETs may induce the inflammatory response of RA-FLS through the AIM2/NF-κB pathway, and NETs can enhance the migration ability of RA-FLSs after activating AIM2.

4 | Discussion

The precise pathogenic mechanisms underlying RA remain incompletely understood. This experiment is the first attempt to explore the relationship between NETs and PANoptosis in RA. Our findings demonstrate that NETs can induce PANoptosis in RA-FLSs through AIM2 activation, while simultaneously enhancing their migratory capacity. This process is accompanied by NF-κB pathway activation, which exacerbates synovial tissue inflammation. These discoveries broaden our understanding of NETs' role in RA pathogenesis.

Current research on NETs in RA has primarily focused on serological aspects. However, NETs mainly mediate RA progression through interactions with cells in the synovial microenvironment, particularly with RA-FLSs. There is limited research on this mechanism. Combined with the literature and experimental results, we found that although the cfDNA levels of OA and Gout patients were higher than those of healthy people [27, 31], they were still significantly lower than those of RA patients. The important role of cfDNA in RA is highlighted. Accumulation of cytosolic dsDNA can trigger RA-FLS-mediated inflammatory responses, potentially through AIM2 inflammasome activation [32]. Our findings observed an elevated AIM2 level in RA synovial fluid and tissues [22], which correlates with both disease activity and cfDNA concentration. Our results also found that AIM2 levels in synovial fluid correlated with both disease activity and cfDNA concentrations. Through western blot and immunofluorescence assays, we confirmed that NETs upregulate AIM2 expression in RA-FLSs in vitro. These results suggest that both AIM2 and cfDNA are involved in the progression of RA; however, the mechanisms by which they promote the development of RA still need to be further explored.

NETs and PANoptosis play crucial roles in the pathogenesis of RA. Current research predominantly focuses on investigating the association between NETs and unitary cell death [17, 26, 33]. However, merely inhibiting a single cell death may allow cells to escape death through compensatory pathways, and organisms readily develop resistance to monotherapeutic death regulators. Our findings represent a paradigm shift in understanding NET-driven pathology: rather than activating isolated death pathways, NETs trigger a synergistic PANoptotic response in

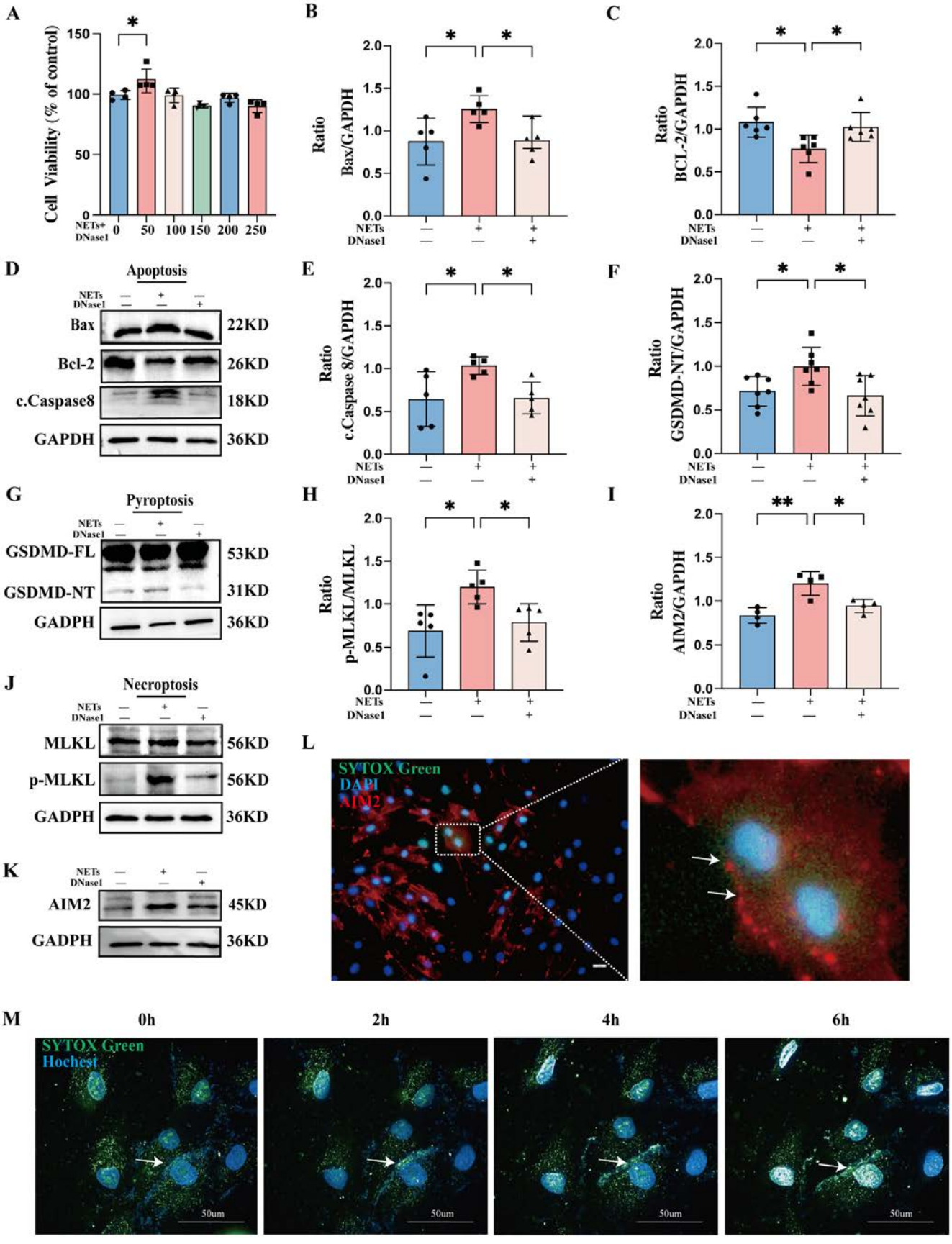

FIGURE 4 | Legend on next page.

FIGURE 4 | CfDNA activates AIM2 to promote NET-induced PANoptosis in RA-FLSs. (A) Cell viability of RA-FLSs treated with 500 ng/mL NETs and varying concentrations of DNase 1 for 24 h was assessed by CCK-8 assay. Data are analyzed by one-way ANOVA with Tukey's multiple comparisons test, FA = 8.491. The *p* value of Bartlett's test is 0.1606. (B–H, J) 500 ng/mL NETs and 50 U/mL DNase 1 were premixed for 30 min and incubated with RA-FLSs for 24 h. The expression changes of PANoptosis-related proteins were detected by WB analysis, along with their quantitative results (GAPDH as a loading control; total MLKL as a reference for p-MLKL). Data are analyzed by one-way ANOVA with Tukey's multiple comparisons test, FB = 5.108, FC = 5.837, FE = 5.050, FF = 5.323, FH = 6.238. The *p* value of Bartlett's test: PB = 0.5520, PC = 0.9822, PE = 0.1234, PF = 0.7657, PH = 0.9691. (I, K) The expression change of AIM2 proteins was detected by WB analysis, along with their quantitative results (GAPDH as a loading control). Data are analyzed by one-way ANOVA with Tukey's multiple comparisons test, FI = 13.21. The *p* value of Bartlett's test is 0.3612. (L) Fluorescence microscopy images of colocalization of NETs and AIM2 to RA-FLSs. SYTOX Green-labeled cfDNA (green) was incubated with RA-FLSs for 8 h, with AIM2 (red) and nuclei (DAPI, blue) staining (scale bar = 100 μm, magnification: ×20). (M) The internalization of cfDNA (green) by RA-FLS was shown by high-content dynamic imaging. Hoechst dye is used to stain the nucleus (blue) (scale bar = 50 μm, magnification: ×63). All experiments were independently repeated at least three times. *$p < 0.05$, **$p < 0.01$, ***$p < 0.01$.

RA. Targeting PANoptosis components could simultaneously achieve multi-point blockade. It makes it difficult for cells to achieve complete escape through single gene mutations or repressive proteins, resulting in a reduced incidence of drug resistance. Thus, it provides a broader range of therapeutic effects compared to inhibiting a single pathway. Studies demonstrate that targeting key PANoptosis molecules mitigates tissue damage [34]. Recent work shows that NETs can induce PANoptosis in cells [16, 23]. Studies have also found that AIM2 is involved in the PANoptosis and inflammatory responses of cells [30, 35]. In this experiment, upon stimulation of RA-FLSs with NETs, both WB and immunofluorescence detection revealed an increased expression level of PANoptosis-related proteins. However, the expression of these proteins was inhibited when DNase1 was used to degrade cfDNA within NETs or when AIM2 was silenced. High-content cell imaging analysis and immunofluorescence colocalization results further confirmed that cfDNA induces PANoptosis by activating AIM2. Collectively, these results indicate that AIM2 is a key target regulating NETs-induced PANoptosis in RA-FLSs.

NETs exacerbate the inflammatory response in RA-FLSs through the AIM2/NF-κB pathway. Our previous studies have demonstrated that NETs enhance the proliferation, migration, and invasive capacity of RA-FLSs, while inducing the release of inflammatory cytokines through NF-κB pathway activation. Activated AIM2 inflammasomes promote IL-1β and IL-18 secretion [36]. Studies have shown that AIM2 can initiate the NF-κB signaling pathway through multiple mediators, including caspase-1, IL-1β/IL-18 [37], mitochondrial DNA (mtDNA)/Reactive oxygen species [38], and caspase activation and recruitment domain (CARD)/receptor-interacting protein 2 [39]. It is involved in inflammatory responses in a variety of diseases, including RA [40–42]. PANoptosis is frequently accompanied by massive cytokine release, potentially triggering cytokine storms and establishing a pro-inflammatory feedback loop [11, 43], which may involve dysregulation of neutrophils, $CD8^+$ T cells, regulatory memory B cells, and macrophages [44]. Furthermore, upon the induction of PANoptosis, substantial amounts of DAMPs are released, including mtDNA, ATP, and high mobility group box 1 (HMGB1) [7]. These molecules engage TLR9 [23], P2X1 [45], and TLR4 [46] pathways on neutrophils, thereby lowering the threshold for NADPH-oxidase-dependent NET formation. Establishing the pro-inflammatory feedback loop that progressively amplifies inflammatory responses. However, whether PANoptosis in RA induces similarly robust inflammatory responses requires further validation. Our experimental findings demonstrate that NETs activate AIM2 to promote robust release of inflammatory cytokines, through the NF-κB pathway. AIM2 silencing significantly reduced NF-κB pathway activity and markedly decreased cytokine secretion. Consequently, inhibiting AIM2 activity may disrupt this vicious cycle, thereby preventing the systemic accumulation of inflammation. Furthermore, AIM2 exhibits functional roles in abnormal proliferation, migration, and cytokine secretion. We observed that NETs enhance the migratory capacity of RA-FLSs, while AIM2 silencing effectively suppresses these pathological behaviors. The results demonstrate that NETs stimulation induces PANoptosis in RA-FLSs and enhances their migratory capacity.

Emerging pharmacological studies support targeting AIM2 for the control of inflammation. For instance, Ginsenoside Rg1 alleviates AIM2-mediated myocarditis [47] or Inhibition of the AIM2/NLRC4/IRF1 signaling pathway reduces cardiac inflammation and hypertrophy in diabetic mice [48]. Compared to conventional RA targets (e.g., TNF-α), AIM2 operates upstream in inflammatory cascades. Its DNA-sensing mechanism offers

FIGURE 5 | AIM2 silencing inhibits NETs-induced PANoptosis in RA-FLSs. Experimental design: Cells were transfected with either si-NC or si-AIM2 for 24 or 48 h, followed by treatment with 500 ng/mL NETs for 24 h before subsequent assays. (A, B) The AIM2 knockdown efficiency was detected by WB analysis, along with their quantitative results. Data are analyzed by one-way ANOVA with Tukey's multiple comparisons test, FB = 6.654. The *p* value of Bartlett's test is 0.7841. (C) The reduction of AIM2 mRNA level was validated by qRT-PCR. Data are analyzed by one-way ANOVA with Tukey's multiple comparisons test, FC = 19.19. The *p* value of the Brown-Forsythe test is 0.3406. (D–J) The expressions of AIM2 and PANoptosis-related proteins were detected by WB analysis, along with their quantitative results (GAPDH as loading control; total MLKL as reference for p-MLKL). Data are analyzed by one-way ANOVA with Tukey's multiple comparisons test, FD = 5.732, FE = 5.527, FG = 12.11, FH = 8.149, FI = 4.712, FJ = 4.845. The *p* value of Bartlett's test: PD = 0.3082, PE = 0.2596, PG = 0.3678, PH = 0.0850, PI = 0.4810, PJ = 0.8436. (K–N) Representative immunofluorescence staining images of Caspase8, GSDMD, p-MLKL, and AIM2 in different groups (scale bar = 100 μm; magnification: ×20). All experiments were independently repeated at least three times. *$p < 0.05$, **$p < 0.01$, and ***$p < 0.001$.

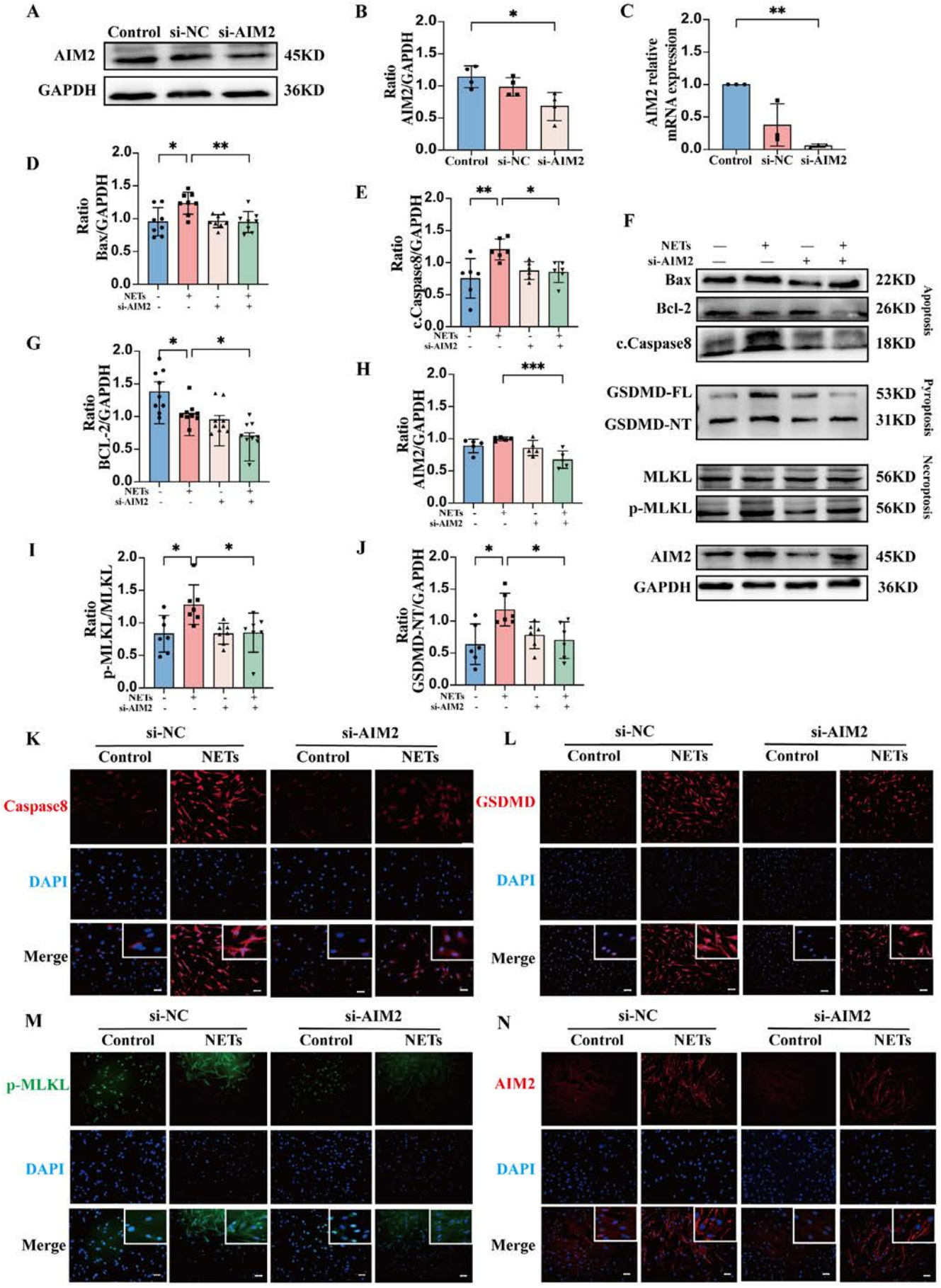

FIGURE 5 | Legend on previous page.

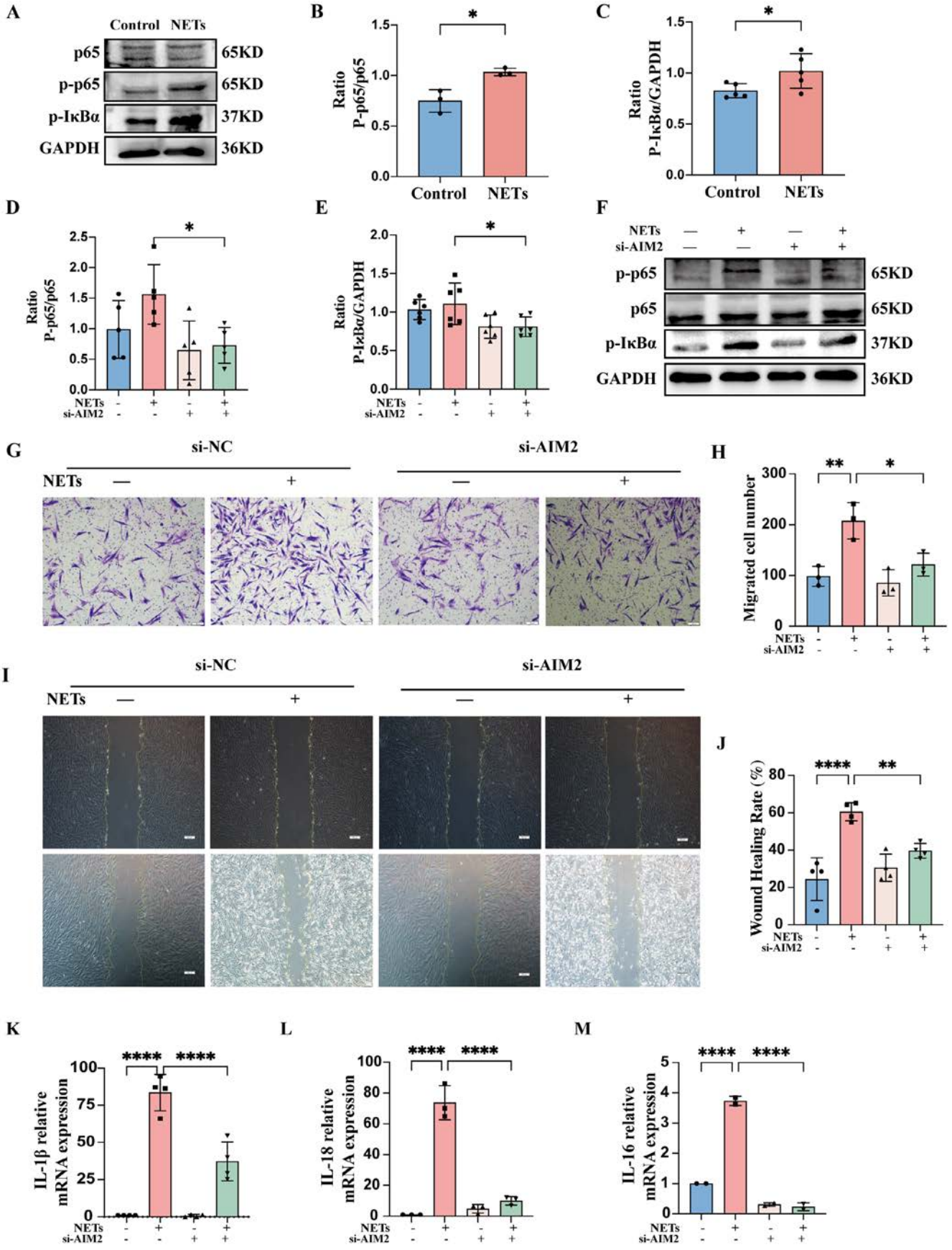

FIGURE 6 | Legend on next page.

FIGURE 6 | The effects of AIM2 gene silencing on the migration ability of RA-FLS and the release of NF-κB-mediated inflammatory cytokines were investigated. (A–C) The expressions of p65, p-p65, and p-IκBα in response to NETs stimulation under non-silencing conditions were detected by WB analysis, along with their quantitative results (GAPDH as a reference for p-IκBα; total p65 as a reference for p-p65). (D–F) The expressions of p65, p-p65, and p-IκBα in different groups were detected by WB analysis, along with their quantitative results (GAPDH as reference for p-IκBα; total p65 as reference for p-p65). Data are analyzed by one-way ANOVA with Tukey's multiple comparisons test, FD = 4.388, FE = 4.360. The *p* value of Bartlett's test: PD = 0.7748, PE = 0.2714. (G, H) Cell migration was assessed by Transwell assay (scale bar = 100 μm). Data are analyzed by one-way ANOVA with Tukey's multiple comparisons test, FH = 12.81. The *p* value of the Brown-Forsythe test is 0.8992. (I, J) Representative images and wound healing rates in different groups were assessed using a wound healing assay (scale bar = 500 μm). Data are analyzed by one-way ANOVA with Tukey's multiple comparisons test, FJ = 17.78. The *p* value of Bartlett's test is 0.3180. (K–M) The mRNA expression of IL-1β, IL-18, and IL-16 was detected by qRT-PCR. Data are analyzed by one-way ANOVA with Tukey's multiple comparisons test, FK = 76.65, FL = 102.8, FM = 495.1. The *p* value of the Brown-Forsythe test: PK = 0.0849, PL = 0.2998. All experiments were independently repeated at least three times. *$p < 0.05$, **$p < 0.01$, ***$p < 0.001$, and ****$p < 0.0001$.

precise regulatory potential. It can also inhibit IL-1β- and IL-18-mediated pyroptosis and suppresses the cGAS-STING-NF-κB signaling cascade, thereby enabling simultaneous intervention across multiple inflammatory axes [49]. Moreover, in inflammatory bowel disease patients exhibiting inadequate response to anti-TNF-α therapy, AIM2 can be used as a potential therapeutic target for ineffective treatment of TNF-α [50]. However, AIM2-targeted therapy still faces two challenges. First, AIM2 plays a crucial role in maintaining barrier homeostasis by detecting pathogenic or damaged DNA and initiating appropriate immune responses. AIM2 deficiency may disrupt barrier homeostasis and increase the incidence of opportunistic infections by affecting DNA-sensing pathways [51]. Second, potential off-target effects could interfere with AIM2's non-inflammasome functions. Therefore, its therapeutic efficacy and safety profile in autoimmune diseases remain subject to rigorous validation.

In conclusion, NETs can induce PANoptosis in RA-FLSs by activating AIM2, while simultaneously exacerbating inflammatory responses through the activation of the NF-κB pathway. Targeted inhibition of AIM2 can effectively block PANoptosis and the burst release of inflammatory factors, thereby breaking the pathological cycle between the release of inflammatory factors and the intensification of the inflammatory state.

5 | Limitations and Perspectives

This study has two limitations: firstly, due to the challenges in collecting fresh synovial fluid and tissue samples, our analysis was based on a relatively small sample size, which may limit the generalizability of our findings and reduce statistical power. Future studies will employ larger-scale, multi-center investigations to expand sample sizes, thereby enhancing the reliability of our conclusions. Secondly, the current understanding of PANoptosis mechanisms remains in the exploratory phase, with new molecules and pathways being continually discovered. Our study only investigated AIM2 in inducing PANoptosis in RA-FLSs, while other pathways may also contribute to this process. Subsequent investigations will further elucidate the additional molecular mechanisms underlying NETs-induced PANoptosis in RA-FLSs, with the objective of more comprehensively establishing the role of AIM2 or other potential molecules as critical regulators in this PCD pathway.

Author Contributions

Xing Zhang: original draft, project administration, data curation. **Shaoqing Yang:** original draft, formal analysis. **Jun Li:** original draft, methodology, formal analysis. **Jing Mao:** original draft, investigation. **Jianhui Ma:** methodology, formal analysis. **Haili Shen:** review and editing, formal analysis.

Acknowledgments

We are very grateful to all the patients and staff who generously participated in this study.

Ethics Statement

The studies involving human participants were reviewed and approved by the Medical Ethics Committee of Lanzhou University Second Hospital (protocol no. 2024A-147) in accordance with the Declaration of Helsinki. All experimental procedures strictly comply with the regulations formulated by the Ethics Committee of the Second Hospital of Lanzhou University.

Consent

The patients/participants provided their written informed consent to participate in this study.

Conflicts of Interest

The authors declare no conflicts of interest.

Data Availability Statement

The data that support the findings of this study are available on request from the corresponding author. The data are not publicly available due to privacy or ethical restrictions.

References

1. E. M. Gravallese and G. S. Firestein, "Rheumatoid Arthritis—Common Origins, Divergent Mechanisms," *New England Journal of Medicine* 388, no. 6 (2023): 529–542.

2. L. Leon, A. Madrid-Garcia, P. Lopez-Viejo, et al., "Difficult-to-Treat Rheumatoid Arthritis (D2T RA): Clinical Issues at Early Stages of Disease," *RMD Open* 9, no. 1 (2023): e002842.

3. R. Garcia-Salinas, E. Sanchez-Prado, J. Mareco, et al., "Difficult to Treat Rheumatoid Arthritis in a Comprehensive Evaluation Program: Frequency According to Different Objective Evaluations," *Rheumatology International* 43, no. 10 (2023): 1821–1828.

4. R. Grieshaber-Bouyer, T. Exner, N. S. Hackert, et al., "Ageing and Interferon Gamma Response Drive the Phenotype of Neutrophils in the Inflamed Joint," *Annals of the Rheumatic Diseases* 81, no. 6 (2022): 805–814.

5. Y. M. Ji, T. Li, Y. H. Qin, et al., "Neutrophil Extracellular Traps (NETs) in Sterile Inflammatory Diseases," *Journal of Inflammation Research* 18 (2025): 7989–8004.

6. F. Yin, H. Hong, Y. Wang, et al., "Mechanistic Insights Into NETs-Induced Osteogenesis Inhibition in BMSCs of Rheumatoid Arthritis," *Bone* 198 (2025): 117533.

7. J. Mao, M. Tan, J. Li, et al., "Neutrophil Extracellular Traps Induce Pyroptosis of Rheumatoid Arthritis Fibroblast-Like Synoviocytes via the NF-κB/Caspase 3/GSDME Pathway," *Inflammation* 47, no. 3 (2024): 921–938.

8. H. Zhang, Z. Wang, J. Li, et al., "Inhibition of MMP9 Ameliorates Neutrophil Extracellular Traps-Mediated Necroptosis Through Regulation of Impaired Autophagy in Severe Acute Pancreatitis," *International Immunopharmacology* 162 (2025): 115109.

9. R. K. S. Malireddi, R. E. Tweedell, and T. D. Kanneganti, "PANoptosis Components, Regulation, and Implications," *Aging (Albany NY)* 12, no. 12 (2020): 11163–11164.

10. P. Zhu, Z. R. Ke, J. X. Chen, S. J. Li, T. L. Ma, and X. L. Fan, "Advances in Mechanism and Regulation of PANoptosis: Prospects in Disease Treatment," *Frontiers in Immunology* 14 (2023): 1120034.

11. D. E. Place, S. Lee, and T. D. Kanneganti, "PANoptosis in Microbial Infection," *Current Opinion in Microbiology* 59 (2021): 42–49.

12. M. Yao, L. Miao, X. Wang, and Y. Han, "Targeting Programmed Cell Death Pathways in Gastric Cancer: A Focus on Pyroptosis, Apoptosis, Necroptosis and PANoptosis," *Gene* 960 (2025): 149546.

13. D. Shi, Y. Bai, R. Long, et al., "Neuronal LAMP2A-Mediated Reduction of Adenylyl Cyclases Induces Acute Neurodegenerative Responses and Neuroinflammation After Ischemic Stroke," *Cell Death and Differentiation* 32, no. 2 (2025): 337–352.

14. K. Liu, M. Wang, D. Li, et al., "PANoptosis in Autoimmune Diseases Interplay Between Apoptosis, Necrosis, and Pyroptosis," *Frontiers in Immunology* 15 (2024): 1502855.

15. Y. Messaoud-Nacer, E. Culerier, S. Rose, et al., "STING Agonist diABZI Induces PANoptosis and DNA Mediated Acute Respiratory Distress Syndrome (ARDS)," *Cell Death & Disease* 13, no. 3 (2022): 269.

16. S. Zhuang, F. Li, L. Wang, et al., "Neutrophil Extracellular Trap-Derived Double-Stranded RNA Aggravates PANoptosis in Renal Ischemia Reperfusion Injury," *Cell Communication and Signaling: CCS* 23, no. 1 (2025): 140.

17. P. Liu, H. Liu, Y. Sang, et al., "Triptolide Regulates Neutrophil Function Through the Hippo Signaling Pathway to Alleviate Rheumatoid Arthritis Disease Progression," *Journal of Translational Autoimmunity* 8 (2024): 100242.

18. S. Zeng, Z. Zhou, Y. Li, D. Wu, Q. Xiao, and H. Peng, "The Dual Roles of Human PYHIN Family Proteins in Cancer: Mechanisms and Therapeutic Implications," *Frontiers in Immunology* 16 (2025): 1576674.

19. V. Kumar, "The Trinity of cGAS, TLR9, and ALRs Guardians of the Cellular Galaxy Against Host-Derived Self-DNA," *Frontiers in Immunology* 11 (2020): 624597.

20. W. D. Luo, Y. P. Wang, J. Lv, et al., "Age-Related Self-DNA Accumulation May Accelerate Arthritis in Rats and in Human Rheumatoid Arthritis," *Nature Communications* 14, no. 1 (2023): 4394.

21. H. Moness, R. A. Ibrahim, S. A. Soliman, A. S. M. Abdel-Naiem, S. M. Hafez, and N. M. Abdullah, "Association of Cell-Free DNA, MicroRNA 21, and Micro-RNA 146a Levels With Rheumatoid Arthritis Activity," *Molecular Biology Reports* 52, no. 1 (2025): 200.

22. Y. Chen, Q. Fujuan, E. Chen, et al., "Expression of AIM2 in Rheumatoid Arthritis and Its Role on Fibroblast-Like Synoviocytes," *Mediators of Inflammation* 2020 (2020): 1693730.

23. F. L. Zeng, Y. Zhang, Z. H. Wang, et al., "Neutrophil Extracellular Traps Promote Acetaminophen-Induced Acute Liver Injury in Mice via AIM2," *Acta Pharmacologica Sinica* 45, no. 8 (2024): 1660–1672.

24. J. Wang, R. Li, H. Lin, et al., "Accumulation of Cytosolic dsDNA Contributes to Fibroblast-Like Synoviocytes-Mediated Rheumatoid Arthritis Synovial Inflammation," *International Immunopharmacology* 76 (2019): 105791.

25. H. Li, Q. Yuan, W. Sun, et al., "Investigating the Mechanism of Tongfeng Qingxiao Formula for Improving Gouty Arthritis Based on the Neutrophil Extracellular Trapping Network," *Journal of Ethnopharmacology* 341 (2025): 119304.

26. H. X. Sha, Y. B. Liu, Y. L. Qiu, et al., "Neutrophil Extracellular Traps Trigger Alveolar Epithelial Cell Necroptosis Through the cGAS-STING Pathway During Acute Lung Injury in Mice," *International Journal of Biological Sciences* 20, no. 12 (2024): 4713–4730.

27. C. Dong, Y. Liu, C. Sun, et al., "Identification of Specific Joint-Inflammatogenic Cell-Free DNA Molecules From Synovial Fluids of Patients With Rheumatoid Arthritis," *Frontiers in Immunology* 11 (2020): 662.

28. S. Zalghout and K. Martinod, "Therapeutic Potential of DNases in Immunothrombosis: Promising Succor or Uncertain Future?," *Journal of Thrombosis and Haemostasis* 23, no. 3 (2025): 760–778.

29. B. Sundaram, N. Pandian, R. Mall, et al., "NLRP12-PANoptosome Activates PANoptosis and Pathology in Response to Heme and PAMPs," *Cell* 186, no. 13 (2023): 2783–2801.e20.

30. J. Xie, Q. Fu, L. Qin, et al., "Ochratoxin A Induces Lung Cell PANoptosis Through Activation of the AIM 2 Inflammasome," *International Immunopharmacology* 150 (2025): 114184.

31. D. Vedder, M. Gerritsen, B. Duvvuri, R. F. van Vollenhoven, M. T. Nurmohamed, and C. Lood, "Neutrophil Activation Identifies Patients With Active Polyarticular Gout," *Arthritis Research & Therapy* 22, no. 1 (2020): 148.

32. C. Xu, W. Jing, C. Liu, et al., "Cytoplasmic DNA and AIM2 Inflammasome in RA: Where They Come From and Where They Go?," *Frontiers in Immunology* 15 (2024): 1343325.

33. R. Zhang, Y. Tan, D. Jiang, et al., "Anoikis and NETosis in Colorectal Cancer Liver Metastasis: The Relationship and Perspectives," *Biochimica Et Biophysica Acta. Reviews on Cancer* 1880, no. 5 (2025): 189401.

34. R. Karki and T. D. Kanneganti, "Innate Immunity, Cytokine Storm, and Inflammatory Cell Death in COVID-19," *Journal of Translational Medicine* 20, no. 1 (2022): 542.

35. J. Guo, S. Meng, J. Zhang, N. Wang, and F. Guo, "Zn(2+) Regulates Mitochondrial DNA Efflux to Inhibit AIM2-Mediated ZBP1-PANoptosome Pathway and Alleviate Septic Myocardial Injury," *Chemico-Biological Interactions* 417 (2025): 111525.

36. L. Huang, X. Chen, R. Liu, et al., "Targeting Inflammasomes as an Immunotherapeutic Strategy for Cancer," *Journal of Translational Medicine* 23, no. 1 (2025): 634.

37. F. M. Marim, M. M. C. Franco, M. T. R. Gomes, M. C. Miraglia, G. H. Giambartolomei, and S. C. Oliveira, "The Role of NLRP3 and AIM2 in Inflammasome Activation During *Brucella abortus* Infection," *Seminars in Immunopathology* 39, no. 2 (2017): 215–223.

38. B. Zhou, X. Chen, R. Ding, et al., "Biosilica Nanoparticulate Scavengers for the Therapy of Hepatic Ischemia-Reperfusion Injury in Preclinical Models," *Nature Communications* 16, no. 1 (2025): 7650.

39. S. R. Hofmann, L. Girschick, R. Stein, and F. Schulze, "Immune Modulating Effects of Receptor Interacting Protein 2 (RIP2) in

Autoinflammation and Immunity," *Clinical Immunology* 223 (2021): 108648.

40. L. Sui, Y. Xi, S. Zheng, Q. Xiao, and Z. Liu, "The Role of AIM2 in Cancer Development: Inflammasomes and Beyond," *Journal of Cancer* 16, no. 1 (2025): 157–170.

41. X. Sha, H. Ye, X. Wang, et al., "GSDMD Mediated Pyroptosis Induced Inflammation of Graves' Orbitopathy via the NF-κB/AIM2/Caspase-1 Pathway," *Experimental Eye Research* 240 (2024): 109812.

42. H. W. Chiu, H. L. Lee, H. H. Lee, et al., "AIM2 Promotes Irradiation Resistance, Migration Ability and PD-L1 Expression Through STAT1/NF-κB Activation in Oral Squamous Cell Carcinoma," *Journal of Translational Medicine* 22, no. 1 (2024): 13.

43. R. Karki, B. R. Sharma, S. Tuladhar, et al., "Synergism of TNF-α and IFN-γ Triggers Inflammatory Cell Death, Tissue Damage, and Mortality in SARS-CoV-2 Infection and Cytokine Shock Syndromes," *Cell* 184, no. 1 (2021): 149–168.e17.

44. W. Sun, P. Li, M. Wang, et al., "Molecular Characterization of PANoptosis-Related Genes With Features of Immune Dysregulation in Systemic Lupus Erythematosus," *Clinical Immunology* 253 (2023): 109660.

45. P. Alarcón, C. Manosalva, J. Quiroga, et al., "Oleic and Linoleic Acids Induce the Release of Neutrophil Extracellular Traps via Pannexin 1-Dependent ATP Release and P2X1 Receptor Activation," *Frontiers in Veterinary Science* 7 (2020): 260.

46. W. Sun, J. Xu, S. Li, et al., "GLUT1-Mediated HMGB1 O-GlcNAcylation Drives Hyperglycemia-Induced Neutrophil Extracellular Trap Networks Formation via TLR4 Signaling and Exacerbates Fibroblast Inflammation," *Scientific Reports* 15, no. 1 (2025): 18853.

47. X. Xu, Q. Wu, K. Pei, et al., "Ginsenoside Rg1 Reduces Cardiac Inflammation Against Myocardial Ischemia/Reperfusion Injury by Inhibiting Macrophage Polarization," *Journal of Ginseng Research* 48, no. 6 (2024): 570–580.

48. J. P. Wu, C. Wu, Y. J. Ma, J. B. Zhu, L. L. Ma, and F. J. Kong, "AIM2 Deficiency Alleviates Cardiac Inflammation and Hypertrophy in HFD/STZ-Induced Diabetic Mice by Inhibiting the NLRC4/IRF1 Signaling Pathway," *Journal of Cardiovascular Translational Research* 18, no. 1 (2025): 94–109.

49. J. Z. Cui, Z. H. Chew, and L. H. K. Lim, "New Insights Into Nucleic Acid Sensor AIM2: The Potential Benefit in Targeted Therapy for Cancer," *Pharmacological Research* 200 (2024): 107079.

50. X. Gao, C. Wang, X. T. Shen, et al., "Pyroptosis Burden Is Associated With Anti-TNF Treatment Outcome in Inflammatory Bowel Disease: New Insights From Bioinformatics Analysis," *Scientific Reports* 13, no. 1 (2023): 15821.

51. Y. Maruzuru, N. Koyanagi, A. Kato, and Y. Kawaguchi, "Role of the DNA Binding Activity of Herpes Simplex Virus 1 VP22 in Evading AIM2-Dependent Inflammasome Activation Induced by the Virus," *Journal of Virology* 95, no. 5 (2021): e02172-20.

Supporting Information

Additional supporting information can be found online in the Supporting Information section. **Table S1:** apl70452-sup-0001-TableS1.docx.